

**ON THE PATHS OF TRANSITIONS AMONG
DIFFERENT KINDS OF NONLINEAR
OSCILLATIONS IN GLOW DISCHARGE
PLASMA**

by

Sabuj Ghosh

(Enrolment No.-PHYS05201204019)

Saha Institute of Nuclear Physics, Kolkata

*A thesis submitted to the
Board of Studies in Physical Sciences*

*In partial fulfillment of requirements
for the degree of*

DOCTOR OF PHILOSOPHY

of

HOMI BHABHA NATIONAL INSTITUTE

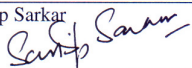
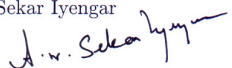


October, 2017

Homi Bhabha National Institute

Recommendations of the Viva Voce Committee

As members of the Viva Voce Committee, we certify that we have read the dissertation prepared by Sabuj Ghosh entitled "On the paths of transitions among different kinds of nonlinear oscillations in glow discharge plasma" and recommend that it may be accepted as fulfilling the thesis requirement for the award of Degree of Doctor of Philosophy.

Chairman - Prof. Alokmay Datta		Date: 9/2/2018
Guide / Convener - Prof. M.S. Janaki		Date: 9/2/2018
Co-guide - (if any)		Date: 9/2/2018
Examiner - Prof. M.S. Santhanam		Date:
Member 1- Prof. Sandip Sarkar		Date: 9/2/2018
Member 2- Prof. A.N. Sekar Iyengar		Date: 9/2/2018

Final approval and acceptance of this thesis is contingent upon the candidate's submission of the final copies of the thesis to HBNI.

I/We hereby certify that I/we have read this thesis prepared under my/our direction and recommend that it may be accepted as fulfilling the thesis requirement.

Date: 9/2/2018

Place: KOLKATA

Co-guide (if applicable)

Guide



STATEMENT BY AUTHOR

This dissertation has been submitted in partial fulfillment of requirements for the doctoral degree at Homi Bhabha National Institute (HBNI) and is deposited in the Library to be made available to borrowers under rules of the HBNI.

Brief quotations from this dissertation are allowable without special permission, provided that accurate acknowledgement of source is made. Requests for permission for extended quotation from or reproduction of this manuscript in whole or in part may be granted by the Competent Authority of HBNI when in his or her judgment the proposed use of the material is in the interests of scholarship. In all other instances, however, permission must be obtained from the author.

Sabuj Ghosh

DECLARATION

I, hereby declare that the investigation presented in the thesis has been carried out by me. The work is original and has not been submitted earlier as a whole or in part for a degree / diploma at this or any other Institution / University.

Sabuj Ghosh

List of Publications arising from this thesis

(Peer reviewed journals)

1. Experimental evidence of intermittent chaos in a glow discharge plasma without external forcing and its numerical modelling.
S. Ghosh, P. K. Shaw, A. N. S. Iyengar, M. S. Janaki, D. Saha, A. M. Wharton, V. Mitra, *Physics of Plasmas* **21**, 032303 (2014).
2. Irregular-regular-irregular mixed mode oscillations in a glow discharge plasma.
S. Ghosh, P. K. Shaw, D. Saha, A. N. S. Iyengar, M. S. Janaki, *Physics of Plasmas* **22**, 052304 (2015).
3. Hysteresis of fluctuation dynamics associated with a fireball in a magnetized glow discharge plasma in a currentless toroidal assembly.
S. Ghosh, P. K. Shaw, D. Saha, A. N. S. Iyengar, M. S. Janaki, *Physics of Plasmas* **23**, 093511 (2017).

Sabuj Ghosh

*Dedicated to “Baba”, “Maa”, “Didi”, “Dada”
and “Mantu”*

Acknowledgements

The research included in this dissertation could not have been performed without the assistance, patience, and support of many individuals. I would like to express my sincere gratitude first to my supervisor Prof. M.S.Janaki for her careful guidance, encouragement and moral support throughout my tenure. Under her guidance, I successfully overcame many difficulties and learned a lot. Also it will be a sin not to mention Prof. A.N.Sekar Iyengar who helped me through my entire Ph.D. life with his expertise, encouragement and scrutiny. It has been a great pleasure and honour to work with them at Saha Institute of Nuclear Physics.

My special words of thankfulness should also acknowledge Prof. R. Pal, Prof. S.Saha and Prof Nikhil Chakrabarti for their fruitful comments and discussions.

This research would not have been possible without the assistance and cooperation of my seniors Subir da, Chandan da, Sudip da, Debu da, Avik da, Abhijit da, Sourav da and Anwesa. I must thank Anwesa individually who motivated me greatly by sharing her knowledge and insights. I also feel very lucky to spend innumerable joyful moments with Satyajit, Pankaj, Debajyoti, Sayanee, Mithun and Subha. I would like to extend my appreciation to Ashok Da, Dipankar Da, Subhasish Da, Monobir Da, Santanu Da, Partha Da and many other colleagues in SINP.

I thank my doctoral committee members in making yearly evaluation of my progress report and giving valuable suggestions.

The five years journey of my doctoral work would not have been easy without my friends. Whenever I needed them, they have always been there, in front of my eyes for last five years, motivating and inspiring every bit of me. I don't want to name a few and offend others; thank you all for making my journey memorable.

I should convey my deepest gratitude to my beloved parents, siblings and wife. Without their love, support and understanding I could never have completed this doctoral degree.

Lastly, I want to express my sincere apologies for my inability to individually acknowledge many others, who might have helped me in the completion of this Ph.D. work one way or another.

SINP, Kolkata
October, 2017

Sabuj Ghosh

Table of Contents

Synopsis	x
List of figures	xvi
1 Introduction	1
1.1 Nonlinear Oscillation	2
1.2 Nonlinear Oscillations in Plasma	3
1.3 Path of transition among different nonlinear oscillations	5
1.4 Motivation	7
1.5 Experimental Inventory	9
1.6 Analysis Techniques	11
1.7 Numerical Modeling	15
1.8 Brief Discussion On Different Plasma Oscillations	16
2 Experimental evidence of intermittent chaos in a glow discharge plasma without external forcing and its numerical modelling.	19
2.1 Introduction	21
2.2 Experimental setup	23
2.3 Experimental results	24
2.3.1 Raw Data	24
2.3.2 Normal Variance of Interpeak Time-Interval	26
2.3.3 Power Spectrum	27
2.3.4 Phase Space Plots	29
2.3.5 Skewness and Kurtosis	30
2.4 Numerical Modelling	31
2.5 Conclusions	38
3 Irregular - regular - irregular mixed mode oscillations in a glow discharge plasma	39
3.1 Introduction	39

3.2	Experimental setup	42
3.3	Results and discussions	43
3.3.1	Floating Potential Fluctuations	44
3.3.2	Power Spectra	45
3.3.3	Phase Space Reconstruction	47
3.3.4	Nonlinear analyses	49
3.4	Numerical Modeling	53
3.5	conclusions	59
4	Hysteresis of fluctuation dynamics associated with a fireball in a magnetized glow discharge plasma in a currentless toroidal assembly	61
4.1	Introduction	62
4.2	Experimental setup	64
4.3	Results and discussions	66
4.4	Statistical behaviour and chaoticity	70
4.5	Conclusions	71
5	Conclusions and Future Plans	84
5.1	Conclusions	84
5.2	Future Plans	87
	Bibliography	89

Synopsis

This doctoral work is a comprehensive and elaborate picture of the transitions of the floating potential fluctuations in a glow discharge plasma system. A more specific description will tell that this work consists of experiments in glow discharge plasma under magnetized and unmagnetized conditions where the floating potential fluctuations were found to exhibit transitions from one kind of nonlinear oscillations to another kind of nonlinear oscillations. These oscillations are of various nature: chaotic oscillation, relaxation oscillation, intermittent oscillations and various kinds of mixed mode ones. The floating potential transits from one kind of oscillation to another kind of oscillation as the control parameter was changed; this control parameter was different for different experiments: discharge voltage, magnetic field and pressure. Variation of statistical as well as nonlinear parameters were observed during these transitions to identify stable and unstable scenarios differently. A few clever guesses have been done using numerical modeling to recreate same kind of transition in the density of the system and it is often seen that a simple forcing, sometimes sinusoidal and noise in others, can actually trigger the system to go through this kind of transition. These kind of transitions gives us an opportunity to explore the behaviour of statistical and nonlinear parameters of the FPFs. To gather these knowledge experiments are performed in Argon plasma in a coaxial symmetry. Glow discharge floating potential fluctuations have shown intermittent chaos while transiting from one kind of relaxation oscillation to another kind of relaxation oscillation. The same system under different condition is shown to exhibit a transition from one kind of irregular mixed mode oscillation to another kind of irregular mixed mode oscillation via compound and regular mixed mode oscillations. These works give us insight on how the statistical parameters, power spectra contributions, phase space scenarios and nonlinear exponents change during various kinds of transitions. Under proper circumstances some of these phases, regular or chaotic, of these transitions may be desirable. For further exploration of applicability the toroidal vessel of SINP tokamak is used to perform experiments with hydrogen glow discharge plasma under the action of

vertical magnetic field. Glow in the plasma sheath has been observed to change type under the action of magnetic field and the system shows a hysteresis. Favorable situations for glow discharge cleaning, plasma material processing can be observed and extracted from this work which is of immense importance now a days. A brief introduction to all these experiments follows.

In plasma systems intermittency has been observed in externally forced glow discharge plasma [1, 2, 3, 4] and in tokamaks [5, 6], the existence of coherent structures in strongly turbulent plasmas in the edge region has been considered to be responsible for the intermittent nature of particle transport.

A more introspective understanding can be gained about intermittency in plasma if the phenomenon is observed as a self excited oscillation and a numerical modeling of the same phenomenon can be provided using an internal element within the system acting as its forcing. Intermittent chaos was observed in a glow discharge plasma as the system evolved from regular type of relaxation oscillations (of larger amplitude) to an irregular type of oscillations (of smaller amplitude) as the discharge voltage was increased. Floating potential fluctuations were analyzed by different statistical and spectral methods. Features like a gradual change in the normal variance of the interpeak time intervals, a dip in the skewness and a hump in the kurtosis with variation in the control parameter have been seen which are strongly indicative of intermittent behavior in the system. Detailed analysis also suggest that the intrinsic noise level in the experiment increases with the increasing discharge voltage. An attempt has been made to model the experimental observations by a second order nonlinear ordinary differential equation derived from the fluid equations for an unmagnetized plasma following Keen and Fletcher's legendary works [7, 8, 9] with Kadji et al's [10] modifications. Though the experiment had no external forcing, it was conjectured that the intrinsic noise in the experiment could be playing a vital role in the dynamics of the system. Hence a constant bias and noise as forcing terms were included in the model. Results from the theoretical model are in close qualitative agreement with the experimental

results.

Another not so well explored and understood complex nonlinear phenomena in the context of transiting nonlinear oscillations in plasmas are the periodic sequences of multi-peaked oscillatory patterns known as mixed mode oscillations. In general oscillations with clearly distinct amplitudes displaying a temporal cycle or pattern can be considered as mixed mode oscillations[11]. Although this was very widely observed in chemical[12, 13] and other systems like neural network[14, 15] and electronic[16] ones; it has not been experimentally examined in plasma systems previously.

Floating potential fluctuations of a glow discharge plasma are found to exhibit different kinds of mixed mode oscillations. Power spectrum analysis reveals that with change in the nature of the mixed mode oscillation (MMO), there occurs a transfer of power between the different harmonics and subharmonics which directly relates to the degree of nonlinearity in the system[17]. Estimates of correlation dimension and the Hurst exponent suggest that these MMOs are of low dimensional nature with an anti persistent character. A basic numerical modeling, similar to the one used previously, also reflects the experimentally found transitions between the different MMOs. In the numerical model it is considered that a mode within the system is acting as an agent of excitation to the system itself. And a few transitions seen experimentally are also qualitatively mimicked by the model while changing either the mode's amplitude or the frequency.

As one can infer from the previously mentioned results that the transitions among different nonlinear oscillations in a plasma system can control the dynamics of it. Therefore in the next experiment nonlinear oscillations of glow discharge plasma in the SINP tokamak vessel was observed in the presence of vertical magnetic field. The dynamics of anode sheath was recorded with a very high speed camera and was correlated with the dynamics of the floating potential fluctuations. Oscillations associated with an anode fireball in a glow discharge plasma in the toroidal vacuum vessel of the SINP tokamak are found to exhibit different kinds of oscillations under the action of vertical magnetic field of different strength.

While increasing the vertical magnetic field the fluctuations have shown transitions as: chaotic oscillation → inverse homoclinic transition → intermittency → chaotic oscillation. However on decreasing the magnetic field the fluctuations are seen to follow: chaotic oscillations → homoclinic transition → chaotic oscillation; that is the intermittent feature is not observed. In other words the nonlinear properties of the floating potential fluctuations undergo a hysteresis under the action of the vertically applied magnetic field. Previously found hysteresis in plasma system mainly considered hysteresis in steady state plasma properties[18, 19, 20] like temperature, current[21] or energy distribution[22]; however the hysteresis in fluctuation dynamics is a fresh phenomenon to scrutinize.

Here, not only the fluctuation dynamics but the fireball dynamics is also found to be closely related to the magnetic field applied; results of visual inspection with a high speed camera are in close agreement with the fluctuations and the fireball dynamics is found to be closely related to the transitions. The statistical properties like skewness, kurtosis and entropy of the fluctuations are also found to exhibit this hysteresis behaviour.

These observations have profound applicability. As plasma is finding its various applications- from material processing to propulsion systems and controlled fusion devices it becomes more and more important to acquire knowledge about its dynamics. Studying the transitions of glow discharge plasma system through different kind of non-linear oscillations enable us to settle the system to a desirable operating conditions. The final segment of our work can provide crucial knowledge for plasma cleaning of tokamak systems under magnetized conditions. Also it gives an window of operation where the cylindrical symmetry in the rotation of the anode fireball can be tuned using external magnetic field; also the same symmetry can be exploited to enhance plasma processing of different materials.

To summarize this doctoral work is a detailed description of different transitions in nonlinear oscillations in glow discharge plasma.

Bibliography

- [1] D. L. Feng, C. X. Yu, J. L. Xie, and W. X. Ding, Phys. Re. E **58**, 3678 (1998).
- [2] D. L. Feng, J. Zheng, W. Huang, and C. X. Yu, Phys. Re. E **54**, 2839 (1996).
- [3] S. Chiriac, D. G. Dimitriu, and M. Sanduloviciu, Phys. Of Plasmas **14**, 072309 (2007).
- [4] Cristina Stan, C.P.Cristescu and D.G. Dimitriu, Phys. Of Plasmas **17**, 042115 (2010).
- [5] J. A. Boedo et al, Phys. Of Plasmas, **10**, 1670 (2003).
- [6] S. K. Saha, and S. Chowdhury, Phys. Of Plasma. **15**, 012305 (2008).
- [7] B.E.Keen, and W.H.W.Fletcher, J. Phys. D: Appl. Phys. **3**, 1868 (1970)
- [8] B.E.Keen, and W.H.W.Fletcher, Plasma Phys. **13**, 419 (1971)
- [9] B.E.Keen, and W.H.W.Fletcher, J. Phys. A: Gen. Phys. **5**, 152 (1972)
- [10] H. G. Enjieu Kadji, B. R. Nana Nbandjo, J. B. Chabi Orou, and P. K. Talla, Phys. Of Plasma **15**, 032308 (2008)
- [11] M. Desroches, J. Guckenheimer B. Krauskopf, C. Kuehn, H. M. Osinga, M. Wechselberger SIAM Review **54**, No. 2, pp. 211288.
- [12] A.M. Zhabotinskii, Dokl. Acad. Nauk. SSSR 157, 392 (1964).
- [13] J.S. Turner, J.C. Roux, W.D. McCormick, and H.L. Swinney, Phys. Lett. **37**, 194 (1980).

- [14] Irina Erchova and David J. McGonigle Chaos **18**, 015115 (2008).
- [15] Martin Krupa, Nikola Popovi, Nancy Kopell, and Horacio G. Rotstein Chaos **18**, 015106 (2008).
- [16] S. Chakraborty, S.K. Dana, Chaos. 20,023107(2010).
- [17] T. M. Flanagan and J. Goree Physics of Plasmas **18**, 013705(2011)
- [18] A. Dinklage, B. Bruhn, H. Testrich, and C. Wilke, Physics of Plasmas 15, 063502 **2008**
- [19] R. Kumar, R. Narayanan, and Awadhesh Prasad, Physics of Plasmas 21, 123501 **2014**
- [20] He Kaifen and A. Salat Plasma Physics and Controlled Fusion, Vol. 31. No. 1 , pp. 123 to 141, **1989**
- [21] R. A. Bosch and R. L. Merlino Contrib. Plasma Phys. 26 **1986** 1, 1-12
- [22] Hyo-Chang Lee and Chin-Wook Chung Scientific Reports 5, 15254 **2015**

List of Figures

2.1	Schematic diagram of the experimental setup(DV- Discharge Voltage, DPO-Digital Phosphorescence Oscilloscope)	23
2.2	Floating potential fluctuations for various DV: a) 628 V b) 636 V c) 638 V d) 640 V e) 642 V f) 645 V g) 648 V h) 651 V i) 655 V j) 660 V k) 670 V l) 674 V	24
2.3	T_{lam} vs V_r	25
2.4	Normal Variance of inter-peak time-interval vs Discharge Voltage	26
2.5	Power spectra of FPF of the raw data shown in fig.2.2	28
2.6	Significant frequencies for different DVs	29
2.7	Phase space plots for various floating potential fluctuations shown in figure 2.2	30
2.8	Skewness and Kurtosis of FPFs for various DVs	31
2.9	Noise level for various floating potential fluctuations shown in figure 2.2	32
2.10	Solutions of theoretical modelling for various A : a) 0.78, b) 0.79, c) 0.80, d) 0.805, e) 0.81, f) 0.815, g) 0.82, h) 0.825, i) 0.83, j) 0.835, k) 0.84, l) 0.845, m) 0.85, n) 0.855, o) 0.86, p) 0.865, q) 0.87, r) 0.875	33
2.11	Normal variance of interpeak time interval of numerical solutions vs A	34
2.12	Power spectra of numerical solutions shown in fig.2.10	34
2.13	Frequencies of Power spectra peaks plotted against A	35
2.14	Phase space plot of numerical solutions	36
2.15	Skewness and Kurtosis of solutions for different values of A	36

2.16	Kurtosis and Skewness of solutions plotted as a function of constant bias and noise amplitude	37
3.1	Schematic diagram of the experimental setup	42
3.2	Floating potential fluctuations for different voltages	45
3.3	Power spectrum of FPFs obtained at different discharge voltages	46
3.4	3D reconstructed phase space diagram for various discharge voltage	48
3.5	Luapunov Exponent for various floating potential fluctuations	50
3.6	Hurst exponent and Correlation dimension for various floating potential fluctuations	51
3.7	Maximas found in different time series while solving eqn. 3.4 with $\omega = 0.19$ and changing A	55
3.8	Maximas found in different time series while solving eqn. 3.4 with $A = 1.05$ and changing ω	57
3.9	Numerical solution of eqn. 3.4 for different values of A with their power spectra and phase space reconstructions.	58
4.1	Schematic diagram of the experimental setup	64
4.2	Schematic diagram(left) of magnetic field coils with the torus and the magnetic field produced by the coils at the torus for various values of current(right).	73
4.3	Floating potential fluctuations for different magnetic fields while increasing magnetic field	74
4.4	Floating potential fluctuations for different magnetic fields while decreasing magnetic field	75
4.5	Power spectra for different magnetic fields while increasing magnetic field	76
4.6	Power spectra for different magnetic fields while decreasing magnetic field	77

4.7	Dominant frequencies of the floating potential fluctuations with magnetic field. The blue and red dots are for increasing and decreasing magnetic fields respectively. The blue arrow is for inverse homoclinic transition and the red one is for homoclinic transition.	78
4.8	Pulsations of the glow recorded with a sampling time of 0.25 msec between consecutive frames for an applied magnetic field=2.5 G.	79
4.9	Photograph of the electrode with a time interval of $\frac{1}{1899}$ second between consecutive frames when magnetic field was 3.63G.	80
4.10	Photographs of the electrode for magnetic field $B \sim 2.5G$ (a.), with magnetic field $B \sim 3.5G$ (b.) and magnetic field $B \sim 4.5G$ (c.).	81
4.11	Kurtosis and skewness of the FPFs as a function of magnetic field where the blue points are for increasing field and the red ones are for decreasing field.	82
4.12	Entropy of the FPFs as a function of magnetic field where the blue points are for increasing field and the red ones are for decreasing field.	83

Chapter 1

Introduction

This thesis is an attempt to contribute to the knowledge of transitions among different kinds of nonlinear oscillations seen in low temperature discharge plasma system. An experimental study is done to understand how the floating potential fluctuation changes its type with change of control parameter. Observations done are mainly through Langmuir probe and high speed camera. A simple overview of the work done and its motivation is presented here before we get into the detailed descriptive elaborations.

1.1 Nonlinear Oscillation

Nonlinearity of a system is defined as a property which indicates a system response that is not directly proportional to the input. Our everyday perception tells us that in reality, linearity is a very rare and special case; whereas every system we deal in our common experience is nonlinear. From the stirring of sugar cube in a simple bowl of coffee [1] to the large scale phenomena like enormous tsunami waves [2, 3] are, in their very core, nonlinear oscillations. Human heartbeats[4, 5], biological networks [6], stock market index[7], migration of human[8] as well as other species on this planet[9] show different kind of oscillatory behaviors that are nonlinear in nature.

The sinusoidal oscillations are the rare linear waves, whereas any deviation from the sinusoidal pattern is a reflection of the presence of some kind of nonlinearity. Linear waves are described by linear equations, wherein the dependent variable and its derivatives are raised to the first power only. This allows application of superposition principle so that linear combination of simple solutions can be made to obtain complex solutions. Fourier techniques are available as data analysis tools for understanding such processes. The classical wave equation describing undamped linear waves has applications to numerous physical phenomena such as acoustic, electromagnetic , chemical, water waves and so on. When wave amplitude becomes larger, linear approximation makes down and nonlinear effects must be taken into account. Burgers, Kortweg-de Vries, Sine Gordon, cubic Shroedinger are well known examples of nonlinear equations that admit classic forms of analytical, closed form solutions such as solitary waves, shock waves, rogue waves and so on. Numerical investigation of nonlinear differential equations reveal nonlinear oscillations such as limit-cycles,

relaxation and chaotic oscillations, mixed-mode oscillations, periodic-chaotic sequences, to name but a few. In experimental observations there are examples galore of such phenomena whose occurrence is ubiquitous.

Very often these nonlinear waves are not attached to any specific system. Let us consider mixed mode oscillation for instance, it was first observed in halide ion concentration in chemical systems[10, 11] but later the same phenomenon was observed in other chemical systems[12, 13] as well as neuronal responses[14, 15] and electronic systems[16]. In daily experience, traffic jam of numerous cars is the most encountered manifestation of relaxation oscillations[17]; and that same kind of oscillation is observed in plasma system [18] too.

As we have just discussed that a particular kind of nonlinear oscillation can be observed in various systems but to find a system that can exhibit various kinds of nonlinear oscillations is not that trivial. For that kind of a system our consideration is that of a plasma system.

1.2 Nonlinear Oscillations in Plasma

Plasma can be very conducive for nonlinear wave exploration as it is highly nonlinear and it responds to very small variations in external parameters like magnetic field, electric field, pressure etc. An additional benefit of conducting nonlinear wave experiments in plasma system is that it can be perturbed by a small amount of energy.

Under various operating conditions the plasma system that can exhibit nice relaxation oscillations is capable of manifesting chaotic oscillations. Relaxation oscillation[18], triangular wave[19], different kind of intermittent oscillations[20], various types of chaos[21, 22] etc. are a few among many nonlinear oscillations observed in the plasma systems.

From the beginning of the study of plasma, waves and oscillations had always fascinated scientists with the profound diversity it possess. A plasma is inherently a nonlinear medium. The waves and oscillations that can propagate in a plasma become unstable due to various free energy sources present in the system. When the amplitude of the growing perturbation is small, linear approximation is used to study the instabilities. As the amplitude becomes sufficiently large, the linearization procedure breaks down. Nonlinear effects tend to limit the growth of instabilities through nonlinear saturation. Also, through mode coupling, energy transfer occurs toward modes which are linearly stable. Nonlinear effects also occur when a large amplitude plasma wave is excited by an external means. For example, the dispersion in the ion acoustic wave can be counter-balanced by nonlinearity and an ion acoustic soliton (pulse-like solitary perturbation) can propagate without appreciable deformation.

Nonlinear oscillations were found in plasma systems as electron plasma oscillations in Dawson's legendary work[23]. Contemporary to that work many theoretical works were done establishing the possibility of finding nonlinear oscillations in both hot and cold plasma[23–29]. Perturbative methods are most common analytical approximation methods in solving nonlinear equations in plasma. Nonlinearity in plasma systems can be broadly be categorized in two classes: coherent structures and chaotic oscillations.

Because of the intrinsic nonlinearity in the dynamical equations describing the plasma, many kinds of large scale coherent structures of different sizes can be formed. Examples of such coherent structures include solitary waves, sheaths, double layers, shock waves and so on and the interaction between them that lead to phenomena like relaxation oscillations,

intermittency and chaos [25, 26, 29–31].

Under conditional nonlinear influences the plasma system is capable of transitions from simple oscillations to dynamically rich and profound structures like turbulence, vortex or even shock wave.

A wide variety of experimental plasma systems have been used to observe these oscillations. High temperature systems like tokamaks[32–34] as well as systems operating under low temperature plasma situation[35] show various kinds of nonlinear oscillations[36].

In this way plasma offers an opportunity to experiment with all the nonlinear oscillations that have been previously observed in different other systems like chemical, fluid or biological systems in great details.

1.3 Path of transition among different nonlinear oscillations

A simple cohesion of these numerous structural richness and oscillatory dynamics opens the question of transition from one kind of oscillation to another. It is very often seen in plasma systems that one kind of nonlinear oscillation transforms into another kind of nonlinear oscillation. Sometimes a very small change in the system parameters can trigger this kind of a transition. In most of the occasions experimentalists see a transition taking place when the external parameters are changed. Phenomenons like period doubling[37, 38], relaxation oscillations and limit cycles[39, 40] were observed in the beginning phase of experimental study of nonlinear oscillations in glow discharge plasmas. Later the the attention shifted towards the paramount number of other nonlinear oscillations. For example intermittent oscillations were first observed in chemical systems. Later in glow discharge plasma systems

different types of intermittency[41, 42] was found. Not only that: the effect of different excitations inside the system during intermittency have been explored thoroughly. Use of the low temperature plasma systems to explore these transitions have some practical benefits as explained earlier. So, detailed analysis of nonlinear oscillations like period doubling, mixed mode oscillation, anti-periodic oscillations had also been explored using glow discharge plasma systems. It is rather impossible to cover all the aspects of nonlinear oscillations that glow discharge plasma has to offer but it can easily be said that these kind of oscillations can be explored properly using GDP as the working system.

Earlier we have talked about how a small change in parameters can change the type of oscillation in plasma system. But a journey in this transition is more fascinating than the destination itself. Say for instance, if a system is transiting between two different kinds of relaxation oscillations[39, 40] it can choose from many of the probable paths - period doubling[37, 38, 43], intermittent chaos [44–46], mixed mode oscillations[47, 48] etc. But the path it takes has a great impact on the nonlinear parameters and the frequency components of the oscillations during the transitions. Again when a plasma system is going to a chaotic state from another chaotic state it is very often observed to have very stable relaxation kind of oscillation in between; e.g., a point of stability or a stable fixed point is possible during the transition. Again there are scenarios like homoclinic and inverse homoclinic bifurcations where the transition is a gradual one and it gives a great deal of control over the system's frequency. So to speak, if a system is found to be in a homoclinic or inverse homoclinic transitory phase for a particular range of the parameter, that parameter window can be used as a control parameter of the governing frequency of the oscillations.

Sometimes it is seen that the path of transitions the system undergoes for the variation of a particular value of control parameter is different than the transitory path when the same parameter is reversed. This phenomena gives rise to the hysteresis in the nonlinear parameters associated with the oscillation concerned.

1.4 Motivation

In today's world plasma brings in the next phase of technological revolution. The applications range from plasma coating of various materials [49], for their enhancements, to plasma based particle accelerators [50–52]. Low temperature plasmas are now being used to disinfect medical tools as well as the wounds themselves[53]. In near future the possibility of having plasma jet propulsion system [54]is pretty high. For these applications, besides many more to be invented in the near future, to have full functionality, it is crucial that the nonlinearity of the system is explored as extensively as possible. Otherwise a highly nonlinear system like plasma can exhibit very unpredictable behaviour due a small change in the initial conditions.

It has always been a prominent point of interest to the community of plasma physicists to explore the different nonlinear oscillations possible inside a glow discharge plasma system. From the very beginning of the study of plasma physics it has been noticed that the focus point has always been fusion plasma due to its enormous application as future energy source. In fusion plasma systems many nonlinear waves have been observed. Apart from the saw tooth oscillations[55] it has exhibited complex phenomenon like intermittency[56, 57], homoclinic transitions[58] among many others to name.

Transitions like intermittency[41, 42, 59, 60] or homoclinic transitions[61] are very important ones while considering nonlinear oscillations in discharge plasma. Intermittency is a rich phenomenon describing oscillations of different type taking place in a simple time series where different types of oscillations occur with no temporal periodicity about the occurrence of the different type oscillation. While considering stability of the plasma in tokamak the intermittent occurrence of laminar phase and sawtooth waves had been observed under high temperature conditions. Similar to that the mixed mode oscillation is an oscillation[48] where the periodic block consists of some large and small amplitude oscillations, as the name suggests. The nonlinear parameters and exponents has a great deal of dependency on the type of oscillation the system has and accordingly the predictability of the system changes. During a homoclinic transition the frequency of the oscillation undergoes a smooth and monotonic transition and when the transition is over the time period of the oscillation becomes infinity. When the system undergoes a transition its randomness and chaoticity changes gradually; this is very important from application aspect as these routes can lead to a control over the amount of randomness in the system.

These phenomenons play an important role in the tokamaks. To clean the tokamak vacuum vessel, there are various options like use of radio frequency plasma, glow discharge plasma etc. for consideration. But before these low temperature plasmas can be used, their credibility must be tested. For example glow discharge plasma has high cleaning property but its non-uniformity is a big concern as it will damage the toroidal symmetry of the inner wall of a tokamak. The bursting that cleans the tokamak wall can also damage the same under various operating parameters specially when pulses of electrons and ions are emitted

from any sheath formed near the electrode. In turn these pulsations of the electrode sheaths can be directly related to the nonlinear oscillations that are present in the system. Or in other words- it is highly probable that the variation in the type of the floating potential fluctuations are connected to the sheath around the electrode and the quality of the cleaning.

Different types of nonlinear oscillations have been found in the glow discharge plasma in both toroidal and cylindrical symmetry. Each type of oscillation presents a different state of the electrode pulsation or sheath pulsation. On a different note these pulsations affect not only tokamak cleaning but also various material processing that are performed by plasma treatment. Some of these oscillations favor the purpose of cleaning and processing and some do not, depending upon the condition and need of the processing. But plasma being a highly nonlinear system, a very small change in the parametric condition of the discharge changes the type of the nonlinear oscillation the system has been exhibiting. Under the huge context of nonlinear oscillations in plasma it becomes very important that we also study the transitions among different kind of nonlinear oscillations to gather insight about the behavior of the system. High sensitivity to parametric conditions has even made glow discharge plasma an obsolete cleaning plasma system compared to its radio frequency counterpart. It is thus necessary to study the transitions of the nonlinear oscillations in order to explore the applicability of glow discharge plasma which is way more cheaper and hustle free plasma device.

1.5 Experimental Inventory

The beauty of experimental design is very much comprehended in its simplicity. For observing the various nonlinear oscillations we choose glow discharge plasma in two simple

geometries, namely cylindrical and toroidal. In the cylindrical geometry a hollow cylinder made of SS304 was used as cathode and an axial thin rod of the same material was used as anode. Generally the system was filled with argon gas after the vessel was brought down to a base pressure of 0.001 mBar. While observing a particular transition in the floating potential fluctuations, very often, the pressure was kept constant and the discharge voltage between the metallic hollow cylinder and its axis was varied. As our primary interest orbits around the type of nonlinearity in the oscillations focus was intensified on the oscillatory nature of the floating potential rather than its dc values; and the same was recorded using an unbiased Langmuir probe connected with a Digital Phosphorescence Oscilloscope (DPO).

In the toroidal system the vessel of SINP tokamak was used for the purpose of studying nonlinear oscillations in a glow discharge plasma. An SS electrode was inserted inside the vessel and the vessel itself was used as the ground. It was brought down to a base pressure of 0.001 mBar using a rotary pump before filling it up with hydrogen. A Langmuir probe made of SS was placed at diametrically opposite position to the electrode along the minor axis of the toroid to measure the FPFs. Here we kept both pressure and the discharge voltage constant and observed the change in nonlinear oscillations of floating potential fluctuations with the change of applied vertical magnetic field. In this experiment, using a slow motion high frame per second camera(Microtek), we recorded the photographs of the plasma around the electrode through a viewing port of the tokamak. The simultaneous data from the camera and the Langmuir probe revealed various aspects of the oscillations which would remain unseen otherwise. It was revealed that each of the different kind of

oscillations in glow discharge plasma corresponds to a different dynamics of the plasma itself.

Using these two types of setups our experiments were performed. Although intricate details of the various experimental parameters will be presented later, we can have a gross idea of the system from this discussion. With that familiarity of the system let us proceed to the methodology of how these data was interpreted using various analysis techniques in order to extract knowledge from these data.

1.6 Analysis Techniques

Interpreting the experimentally obtained data and gathering knowledge about its nonlinearity is always a challenge by itself. Although initial speculation about the time series data can always be done by simply plotting it against time. But qualitative and quantitative characterization of the data requires various analysis techniques. Although the full scope and spectrum of these methods are discussed later, a brief concept is provided below.

To begin with the data is plotted in phase space; by doing which one can have an idea about how the system is behaving around its center of attractions in phase space. This can be done mainly in two ways: a) by plotting the time derivative of the data against the data itself and b) by reconstructing the phase space. The first method is quite straight forward while the second requires construction of phase lagged time series. This lag is determined by the autocorrelation function of the data; the time taken by the autocorrelation function to decay into $1/e$ of its maximum value is taken as the lag(say T). Then the reconstructed time series would be $x(t), x(t + T), x(t + 2T)$... so on. When these are plotted against each other in reconstructed space it unveils a great amount of information about the dynamics

of the system.

Although phase space analysis gives an overview about how many periods are present in the system or the phase space paths are inter-twisted, it fails to quantify time period or frequency and power distributed in them. For that purpose we decompose the time series into sinusoidal oscillations using Fourier transformation and the power of a particular frequency is obtained by squaring the transformation coefficient for each frequency. This power spectra not only reveals the frequencies present in the time series but also how oscillation of one frequency interacts with all other frequencies during a transition of the floating potential fluctuations.

Very often it is hard to comprehend extracted information from the time series data if the visualization is not proper. Bifurcation diagrams provide us extensive tools to visualize the data. Within the context of the presented thesis we used mainly two kinds of bifurcation diagrams: a) amplitude bifurcation and b) frequency bifurcation. In amplitude bifurcation we plot the local extrema present in the floating potential fluctuations as a function of the external parameter. In these kinds of diagrams we can pin point the parameter values for which one oscillation branches into various oscillation or various oscillations merging into one. In frequency bifurcations we plot the frequencies which has a significant power contribution to the floating potential fluctuation as a function of the external parameter. The second kind of bifurcation diagram reveals branching and merging of the dominant frequencies in the parameter landscape.

Once we gathered this basic knowledge we venture into quantifying the nonlinearity and randomness of the system in terms of different exponents. For example the presence of

chaos can be readily be detected by observing the Lyapunov exponent. It is the measure of how fast two points in phase space diverge for a time series. Thus it is a direct measure of chaoticity of a system. If we consider l_0 is the initial separation between two points in a phase space diagram. Now if $l(t) \sim l_0 e^{\lambda t}$ then λ is the Lyapunov exponent. As it can be predicted easily that if $\lambda < 0$ the time series is obtained from an attractor; otherwise if $\lambda > 0$ there is chaos present in the system. Obviously higher value of this exponent tells that higher chaoticity is present in the floating potential fluctuations. Sometimes it is of paramount importance to know whether the FPFs possess memory or not. For example one can notice that a sinusoidal wave has a memory for a very long time whereas a sequence of random numbers has no memory at all. This property of a time series is measured by Hurst exponent. This exponent is named after Hurst who first used this technique to predict or quantify the probability of flood in the Nile river. If one high valued data point is followed by a low valued data point the data is said to be anti correlated and its Hurst exponent (H) has value $0 < H < 0.5$. If the data follows the trend smoothly as a result the data points are followed by similar kind of data points then the exponent has a value $0.5 < H < 1$. If for a time series $\langle \frac{R_n}{S_n} \rangle \sim n^H$ then H is the Hurst exponent for the limit $n \rightarrow \infty$; where R_n is the range and S_n is the standard deviation of n elements in the time series. Obviously the more chaotic behavior the time series have the more it's Hurst exponent is nearer to 0.5. These two exponents are great at measuring chaoticity of a time series but sometimes it is the correlation dimension(CD) of the time series that can give us the sense of complexity of the system. It actually tells us the dimension of the nonlinear interaction whose 1D projection is the time series. To find out the CD of the time series we first need to

define the dimension of space in which we are going to perform the calculation; or in other words we need to find out the embedding dimension of the system. Theoretically the CD should saturate with the increasing embedding dimension[62]. In this work we have taken the saturated values of CD for analysis.

$$C_{em}(\epsilon) = \frac{1}{N^2} \sum_{i,j=1i \neq j}^{\infty} \Theta(\epsilon - |x_i - x_j|^{em}) \quad (1.1)$$

$$CD_{em} = \lim_{\epsilon \epsilon' \rightarrow 0} \frac{\ln(\frac{C_{em}(\epsilon)}{C_{em}(\epsilon')})}{(\frac{\epsilon}{\epsilon'})} \quad (1.2)$$

Where Θ is the Heaviside step function, C_{em} is the correlation integral in a particular embedding dimension em , $|x_i - x_j|^{em}$ is the distance between the i th and j th point in that embedding space; and CD_{em} is the correlation dimension of the time series for that embedding dimension. ϵ and ϵ' are arbitrary smallness parameters.

These exponents might seem a bit exhaustive; and we don't always need to calculate these. On several occasions it is the various statistical parameters that does the job of obtaining information about the randomness of the time series. For example sometimes the skewness and kurtosis defined as the third and fourth moment of a time series does the job well. Specially when we are dealing with intermittent or volatile time series these two parameters do an excellent distinction between the presence and absence of these phenomena. A similar set of statistical parameters are different kind of information entropies; they also provide an eloquent method of quantifying randomness.

Once we are equipped with all these analysis techniques we can easily find out the nonlinearity, randomness, phase space configurations and frequencies and how they change

under the influence of external parameters.

1.7 Numerical Modeling

Often describing the transitions in terms of the data and their exponents is not enough for understanding the system behaviour. The capability of a low temperature plasma to exhibit nonlinear phenomenon was eloquently put forward by Keen and Fletcher [63–65]. In view of their work it is natural to model the ions to follow fluid equations while the electrons follow Boltzmann distribution under low temperature conditions.

$$n_e = n_0 \exp(e\phi/KT) \quad (1.3)$$

Where n_e/n_0 is the electron density, ϕ is the potential, K is the Boltzmann constant and T is the temperature. For an unmagnetized plasma, the momentum conservation equation for the ions can be written as:

$$n_i m_i \frac{dv_i}{dt} = n_i e E - m_i n_i \nu_i v_i \quad (1.4)$$

Where n_i is the ion density, m_i denotes the mass of the ions, v_i and E are the ion velocity and the electric field respectively. In this equation, E can be eliminated by using $E = -\nabla\phi$.

The ion continuity equation is given by

$$\frac{\partial n_i}{\partial t} + \nabla \cdot (n_i v_i) = S \quad (1.5)$$

where S is a source term which can be due to ionization, recombination etc. When it comes to the question of choice of the term S , the model proposed and implemented by Keen & Fletcher in studying Van der Pol plasma instability [63–65] is adapted and is given as follows $S = \alpha n_1 - \lambda n_1^2 - \mu n_1^3$ consisting of ionization term αn_1 , two body recombination

term $-\lambda n_1^2$ and three body recombination term $-\mu n_1^3$. Here the ion density n_i is assumed to be $n_i = n_1 + n_0$ and n_1 is the variation in n_i . In the study of nonlinear oscillations in plasma, such models have been extensively used in Kadji et al's works[66, 67].

So combining eq. 1.4 and eq. 1.5 we have

$$\frac{d^2 n_1}{dt^2} + (\alpha + 2\lambda n_1 + \nu_i + 3\mu n_1^2) \frac{dn_1}{dt} + \omega_0^2 n_1 + \nu_i(\alpha n_1 + \lambda n_1^2 + \mu n_1^3) = 0 \quad (1.6)$$

By considering the normalizations: $t \rightarrow \omega_0 t$; $x \rightarrow n_1/n_0$; $a = \nu_i/\omega_0$; $b = 2\lambda n_0/\omega_0$; $c = 3\mu n_0^2/\omega_0$; $e = \alpha/\omega_0$, eq. 1.6 turns out to be

$$\ddot{x} + (a + e + bx + cx^2)\dot{x} + x + a \left(ex + \frac{b}{2}x^2 + \frac{c}{3}x^3 \right) = 0 \quad (1.7)$$

Herein lies the crux of the fact that whenever we have encountered any transitions undergoing in the floating potential fluctuations we tried to find out the changes it brings to the parameters of eq. 1.7. In accordance with our perception, attempts to obtain changes similar to those observed in experiments were made by solving the above equation by using differential equation solver (Runge Kutta Fourth order methods) which will be discussed later along with the experimental results.

1.8 Brief Discussion On Different Plasma Oscillations

Plasma can support both electron and ion plasma oscillations. Ion plasma oscillations can be of two kinds, depending on the presence of magnetic field in the system namely ion acoustic waves and ion cyclotron waves. A third kind of oscillations also considering motions of ions inside the plasma, specially in partially ionized plasmas due to ionization

and recombination processes occur, called the ionization instability[68]. The latter leads to build up of ion acoustic waves in a plasma.

The basic nonlinear oscillations that have been obtained in this work have their characteristics rooted to the low frequency phenomena mentioned above. This is evident from the frequency domain in which such phenomena are observed. However, due to various kinds of nonlinear interactions, the oscillations take a wide variety of forms such as mixed mode oscillation, intermittent oscillations, relaxation oscillations etc. Before we venture into the transitions among different kinds of oscillations it is necessary to understand the oscillations themselves first. To begin with let us consider relaxation oscillations- a type of oscillation where the rising time of the wave and the time needed for the amplitude of the wave to fall are different from each other. This is very common in plasma systems as the system is a conducting medium but lacks absolute resistive properties. Most of the phenomenon observed and modeled in this work are basically relaxation oscillations of different kinds but their amplitude, temporal periodicity, gives them certain characteristic distinguishing features.

When an oscillation has both large and small amplitude oscillations occurring in various sequences, then the patterns obtained are called mixed mode oscillations. When m number of large oscillations are followed by n number of small oscillations, the mixed mode oscillation is said to be a m^n kind of mixed mode oscillation. These oscillations were first observed in chemical system where halide ions were observed to exhibit mixed mode oscillations in the famous Belusov-Zhabotonski reaction[11]. In recent experiments it was seen in the context of complex plasma instabilities also. An important parameter in mixed mode

oscillations is Farey number[69] which is the ratio $\frac{n}{(n+m)}$ for a n^m mixed mode oscillation. Under parametric circumstances if a system showing mixed mode oscillation changes the number of large or small oscillation it should follow Farey algebra and the corresponding Farey number is often seen showing a staircase like behavior under parametric variation.

As stated above, when two kinds of oscillations manifest themselves separately in a single time series and toggling between these two kinds oscillations has no temporal periodicity, such oscillations are known as intermittent oscillations[70–72].

Chapter 2

Experimental evidence of intermittent chaos in a glow discharge plasma without external forcing and its numerical modelling.

Intermittent chaos was observed in a glow discharge plasma as the system evolved from regular type of relaxation oscillations (of larger amplitude) to an irregular type of oscillations (of smaller amplitude) as the discharge voltage was increased. Floating potential fluctuations were analyzed by different statistical and spectral methods. Features like a gradual change in the normal variance of the interpeak time intervals, a dip in the skewness and a hump in the kurtosis with variation in the control parameter have been seen which are strongly indicative of intermittent behavior in the system. Detailed analysis also suggest that the intrinsic noise level in the experiment increases with the increasing discharge voltage.

An attempt has been made to model the experimental observations by a second order nonlinear ordinary differential equation derived from the fluid equations for an unmagnetized

plasma. Though the experiment had no external forcing , it was conjectured that the intrinsic noise in the experiment could be playing a vital role in the dynamics of the system. Hence a constant bias and noise as forcing terms were included in the model. Results from the theoretical model are in close qualitative agreement with the experimental results.

2.1 Introduction

As this thesis is about transitory paths among different kinds oscillations, let us focus on the intermittent path of transition. Intermittency is a well observed phenomena in many dynamical systems. Lorenz system [70] during transition to a strange attractor from a limit cycle shows intermittency. Rayleigh-Bernard convection [71] was reported to toggle between distinct laminar and turbulent phases. In some cases fully developed turbulence [72] also shows intermittency.

Experimental observations of intermittency have been reported in electronic systems [73], and in viscous media with the inclusion of two forcing terms of incommensurable frequencies [74]. In recent times this phenomena is claimed to be effective in slowing down the process of chaotic mixing [75]. The complex properties of biological systems have been modeled using deterministic dynamics with intermittency in the context of neuronal responses [76] and DNA sequencing [77] etc.

In plasma systems intermittency has been observed in externally forced glow discharge plasma [41, 42, 59, 60] and in tokamaks [56, 57], the existence of coherent structures in strongly turbulent plasmas in the edge region has been considered to be responsible for the intermittent nature of particle transport.

In the present work, intermittent chaos has been observed in an argon gas discharge plasma without any external forcing. We analysed the time series data of the floating potential fluctuations (FPFs) by estimating the normal variance (NV) of the interpeak time intervals, besides power spectra, phase space plots etc. These analyses help to observe how the system and its statistical behavior vary in the route to chaos via intermittency.

In addition to the usual quantification of intermittency, we have also shown perhaps for the first time that the normal variance of the interpeak time interval exhibits a gradual transition from a lower to a higher value which would have been very sharp if there was no intermittency. In addition the skewness exhibits a dip and kurtosis shows a hump, which would not have been observed in the absence of intermittency. We have also estimated that the intrinsic noise level increases with the discharge voltage and hence we conjecture that it plays a vital role in the route to chaos.

An attempt has been made to understand the experimental observations using the standard numerical model[63–66] starting from two fluid equations leading to a nonlinear ordinary differential equation. In general it has been shown that noise plays an important role in intermittency [78, 79]. Since our analysis reveal that the intrinsic noise level increases with discharge voltage, we included a forcing term consisting of a bias and a Gaussian noise. The latter signifies the intrinsic noise inherently present in an experiment. An extensive analysis on the time series data obtained from the numerical solutions have been carried out. Interestingly these results are in close qualitative agreement with the experimental observations.

The outline of the chapter is as follows: Section 2.2 describes the experimental setup. The experimental results, followed by their analysis and the discussions are in section 2.3. Section 2.4 contains the numerical modelling, and the different kinds of analysis of the solutions. section 2.5 has conclusions drawn from section 2.3 and 2.4.

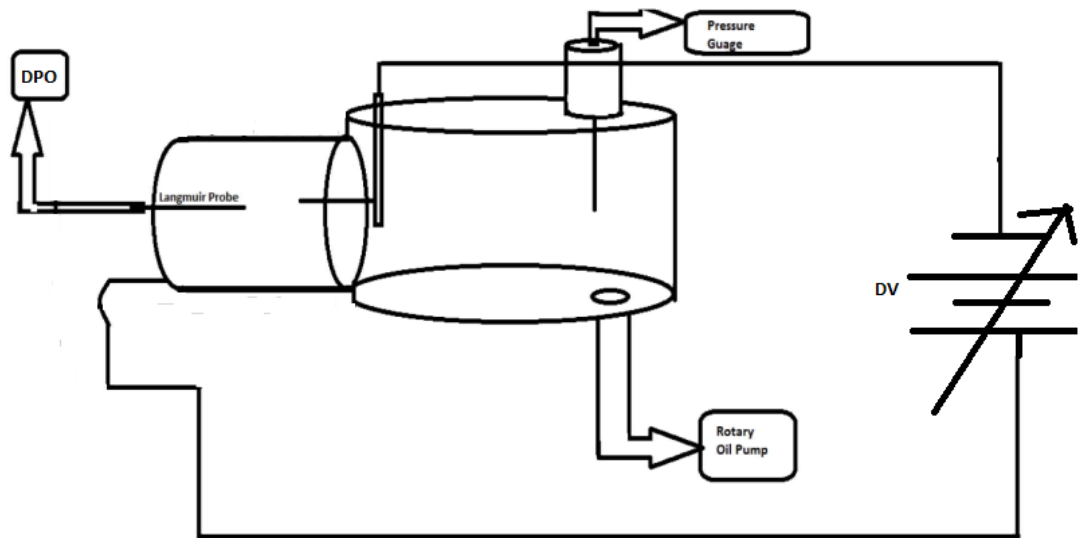


Figure 2.1: Schematic diagram of the experimental setup(DV- Discharge Voltage, DPO- Digital Phosphorescence Oscilloscope)

2.2 Experimental setup

Fig. 2.1. shows a schematic diagram of the experimental setup [80, 81], in which we used a hollow stainless steel cylinder (of length 10 cm and radius 5.5 cm) as cathode and an stainless steel rod of radius 0.5 cm as anode. This assembly was mounted inside a vacuum chamber connected to a rotary pump. Plasma was produced by a dc power supply whose voltage could be varied from 0 to 1000 volts, but for the present experiments it was operated in the range of 628 to 674 volts. After evacuating the chamber to a base pressure of 0.001 mbar, it was filled with Ar gas to 0.028 mbar. An unbiased Langmuir probe was used to acquire the floating potential fluctuation(FPF) data of length of about 10000 points acquired at a sampling frequency of 100 kHz.

2.3 Experimental results

2.3.1 Raw Data

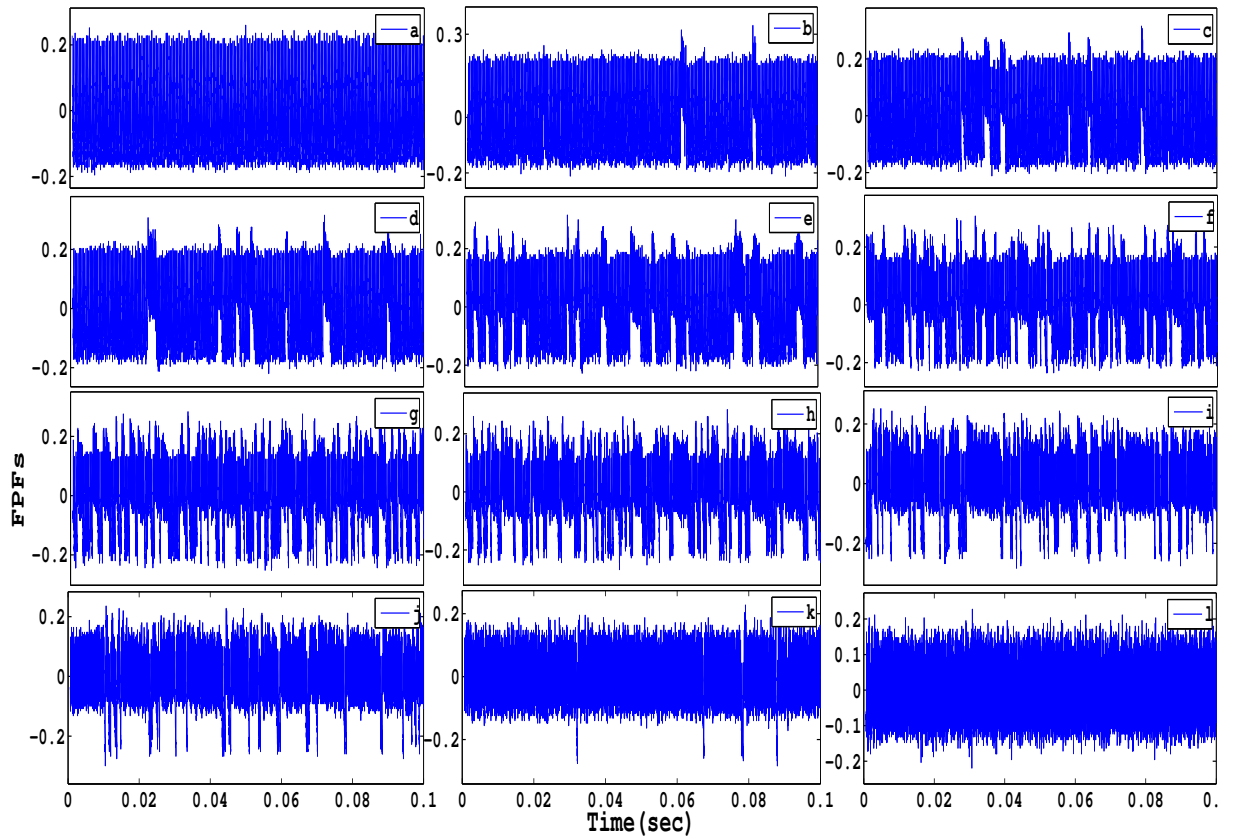
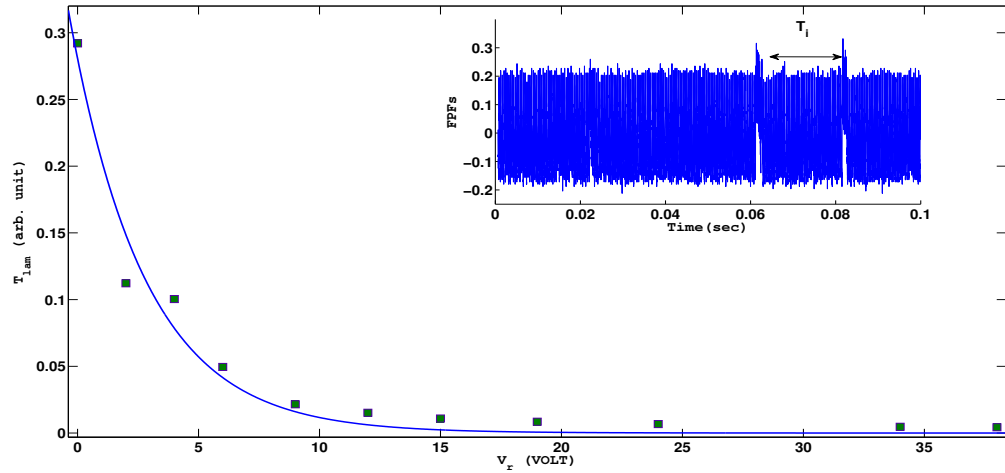


Figure 2.2: Floating potential fluctuations for various DV: a) 628 V b) 636 V c) 638 V d) 640 V e) 642 V f) 645 V g) 648 V h) 651 V i) 655 V j) 660 V k) 670 V l) 674 V

Plasma discharge is usually obtained at a voltage between 250-300 volts, and depending on the pressure, different types of behavior in the FPF are observed-sometimes chaotic to order and sometimes order to chaos in the fluctuations. Fig. 2.2(a-l) show the raw data of the intermittent chaos that was observed at voltages ranging from 628-674 volts. In the time series data two kinds of oscillations were observed; type I and type II. Type I oscillations

Figure 2.3: T_{lam} vs V_r

are relaxation oscillations with a rising time 7×10^{-5} sec and decaying time 3.3×10^{-4} sec; where as type II oscillations have a lower amplitude, more chaotic nature and have an upshifted mean level compared to type I oscillations. Fig. 2.2a is a type I relaxation oscillation obtained at 628 volts. On further increase of the DV, type II oscillations begin to appear at irregular intervals of time (fig.2.2(b-k)). As the DV was further increased, these oscillations occurred more frequently than type I and finally around 674 volts and beyond only type II oscillations were observed.

As in this experiment, the amplitude and the frequency of type I oscillations are quite regular, these oscillation have been considered analogous to laminar phase in other experiments [41, 60]. The intermittent behavior of the oscillations was quantified by estimating the normalised mean uninterrupted time-length T_{lam} of type I oscillations. T_{lam} is given by the equation

$$T_{lam} = \frac{\sum_{i=1}^n T_i}{nN} \quad (2.1)$$

where n is the number of occurrences and N is the total time length and T_i is the time-length of i th type I oscillation. Fig 2.3 shows a plot of T_{lam} Vs rescaled DV V_r where $V_r = V - V_c$, and V_c is the DV at which intermittency is first observed and in our experiment it was about 636 volts. T_{lam} exhibits a more or less an exponential fall with a functional dependence given by

$$T_{lam} = 0.2807 * exp(-0.3184V_r) \quad (2.2)$$

2.3.2 Normal Variance of Interpeak Time-Interval

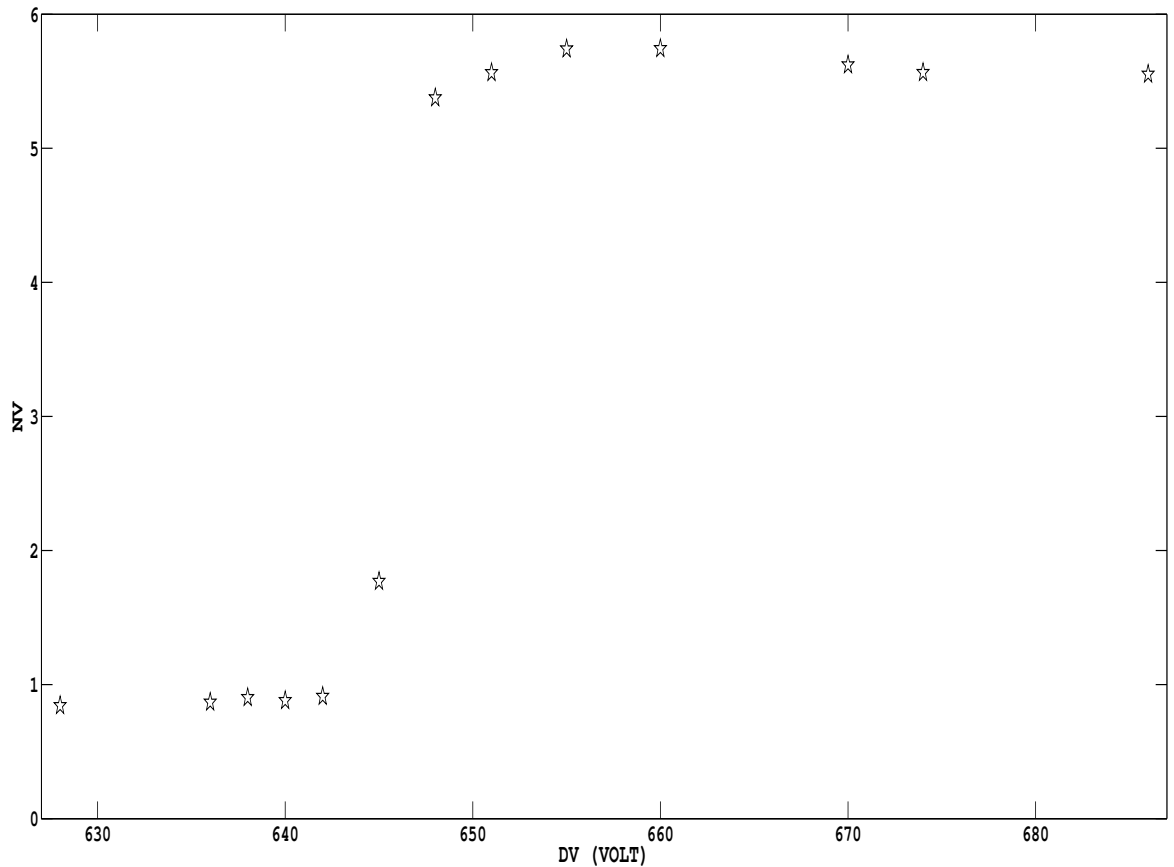


Figure 2.4: Normal Variance of inter-peak time-interval vs Discharge Voltage

The regularity of the oscillations have been estimated using normal variance(NV) of interpeak time-interval. NV is defined as

$$NV = \frac{1}{\bar{\tau}} \left(\frac{1}{n} \sum_{i=1}^n (\tau_i - \bar{\tau})^2 \right)^{\frac{1}{2}} \quad (2.3)$$

where τ_i is the time interval between two consecutive peaks. Fig.2.4 shows a lower NV, between Discharge Voltage (DV) of 628 - 640 volts, when the type I oscillations were more in number. But as DV is increased, type II oscillations begin to dominate, and the regularity decreases as seen by the increase in the NV from 642-652 volts. Around 670 volts the time series is predominantly type II oscillations and since it is also chaotic the NV saturates at a higher value indicating increased irregularity. This can be considered as a good measure of intermittent chaos in addition to fig 2.3. If the transition was a direct one from regular to chaotic oscillations it would have been much more sharper whereas in intermittent systems this will be a gradual one.

2.3.3 Power Spectrum

Fig. 2.5 shows the power spectrum of the FPFs . Fig 2.5(628V) shows that when type I oscillations are present only 2.6 kHz is a dominant mode, whereas when type II oscillations are present as in fig 2.5(674V), the dominant mode is 5.2 kHz. It is also clearly seen from fig. 2.5(674V) that the 5.2 khz peak is accompanied by smaller peaks on both sides indicating chaotic nature of the type II oscillation.

Fig. 2.6 shows the significant frequencies obtained from the power spectrum as a function of DV. Here a peak with 1% height of the maximum peak for a particular power spectrum is considered to be significant. For low DVs, when only type I oscillations were present, distinct frequency peaks were observed. For DVs between 642-660 volts, there is an

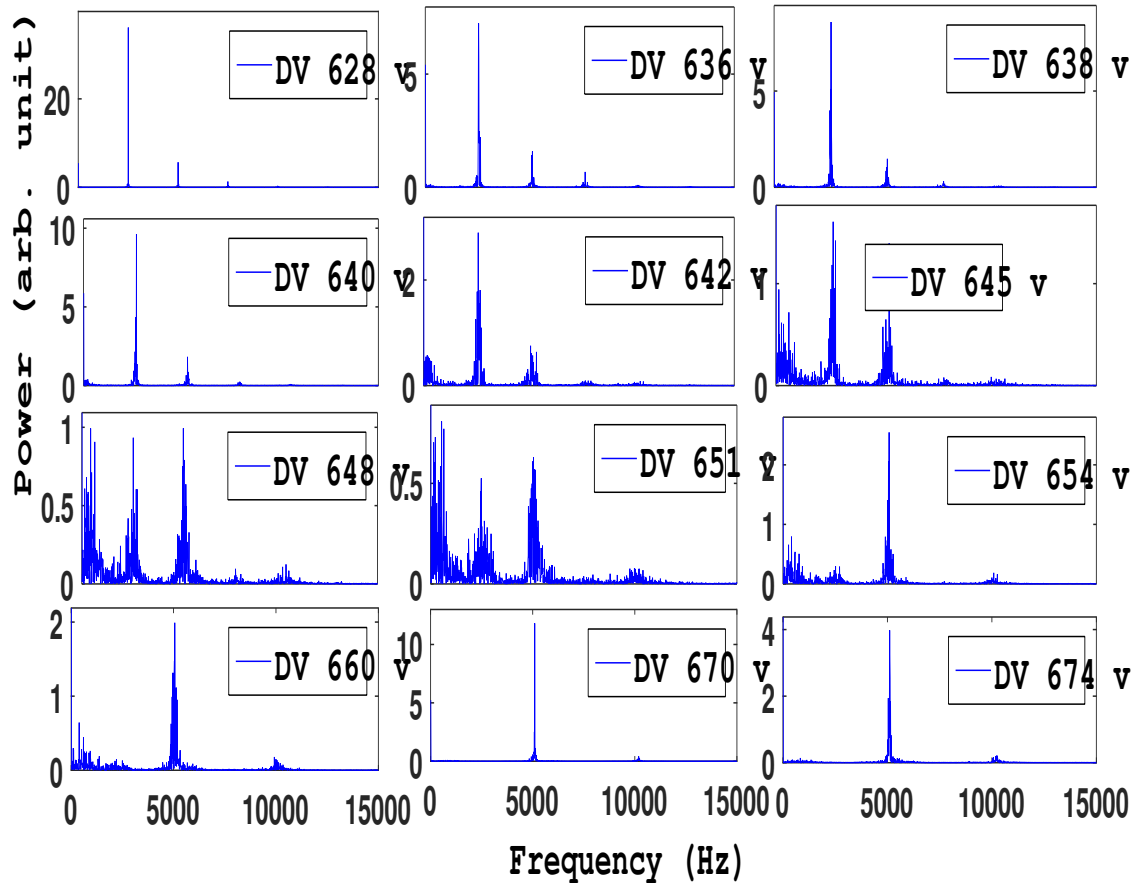


Figure 2.5: Power spectra of FPF of the raw data shown in fig.2.2

increase of type II oscillations and the peaks tend to broaden into a chaotic band which corroborates with the NV that also shows an increase of irregularity; When type II oscillations dominate at $DV > 660$ volts, only the frequency peaks around 5.2 kHz are observed. The experimental conditions are quite favourable to ion acoustic instabilities which can be excited in the range of 3-10 kHz. So initially it is quite likely that the low frequency oscillations were triggered followed by the higher ones at higher DV. These two modes can nonlinearly interact to give rise to lower frequency components which are observed in the 500 Hz regime. Such low frequency components can also originate from ionization instabilities [68].

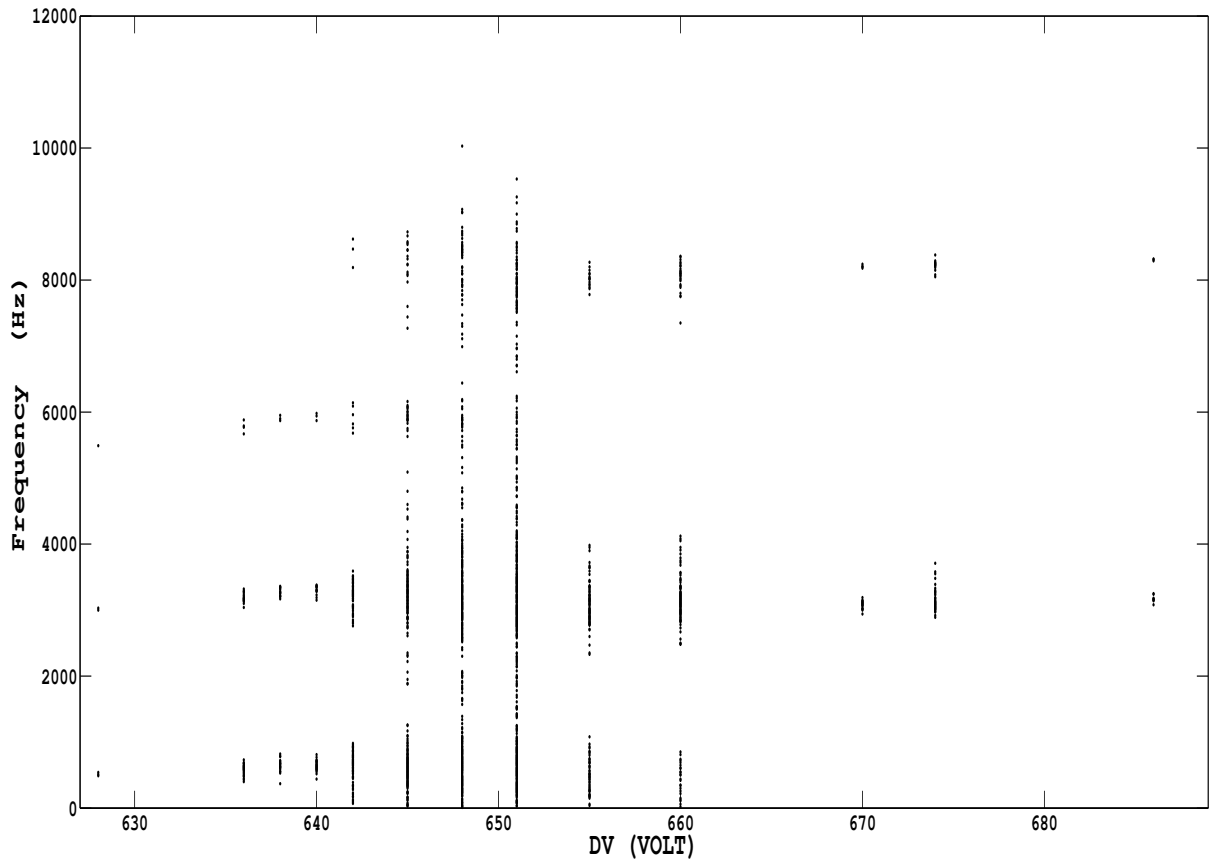


Figure 2.6: Significant frequencies for different DVs

2.3.4 Phase Space Plots

Fig. 2.7 shows the phase space plots of the FPFs for different DVs. For type I relaxation oscillations we get a single lobe as seen in fig 2.7(a).

As the intermittent oscillations set in, there is an appearance of another lobe within the first lobe as in figs. 2.7(f-j). Around 660 volts, one of the lobes disappear leaving only one lobe corresponding to the type II oscillations.

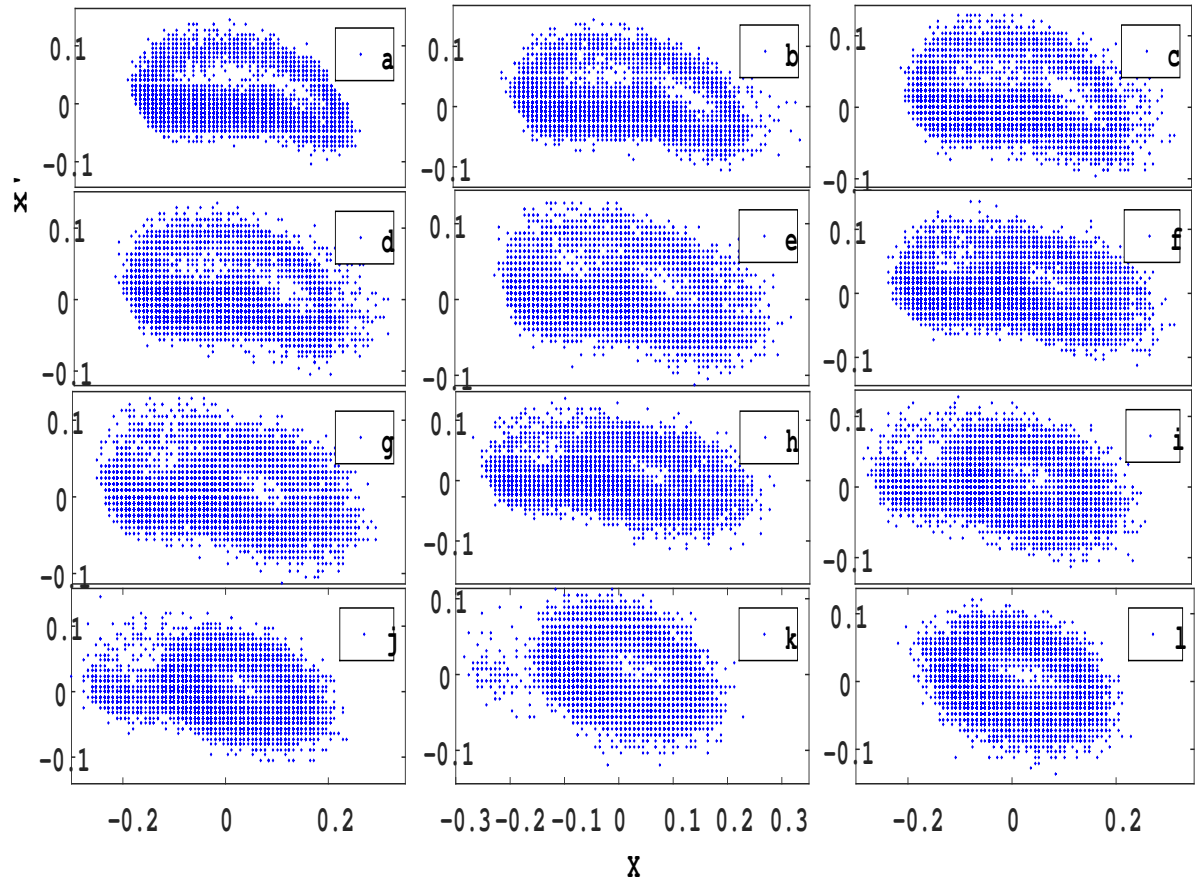


Figure 2.7: Phase space plots for various floating potential fluctuations shown in figure 2.2

2.3.5 Skewness and Kurtosis

We estimated the skewness and kurtosis of the floating potential fluctuations as a function of the DV, as shown in figs. 2.8(a) and 2.8(b) respectively. Skewness decreases from 0.6 when only type I relaxation oscillations were present to 0.15 indicating maximum intermittency when both type I and II oscillations are simultaneously observed. It then again tends to increase to around 0.6 when only type II oscillations are present. Kurtosis increases from about 2.3 to 2.7 indicating a more flat distribution and maximum intermittency followed

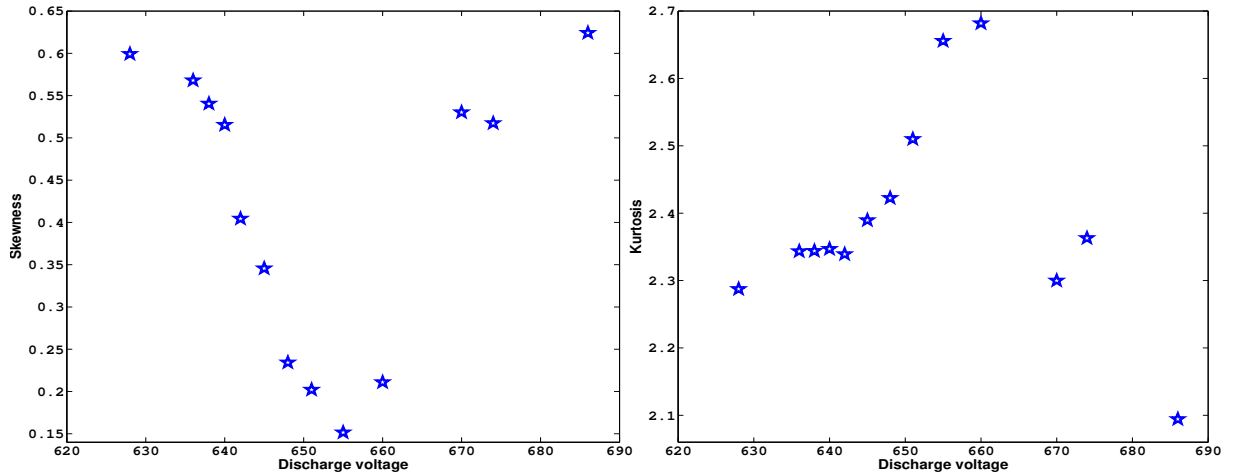


Figure 2.8: Skewness and Kurtosis of FPFs for various DVs

by a decrease to about 2.1 when only type II oscillations are present.

2.4 Numerical Modelling

In order to understand the experimental observations we used the analytical model developed by Kadji et al [66] in presence of both ionization and recombination terms [63].

After a Fourier decomposition in space, the temporal dynamics is governed by the following second order nonlinear ode given by

$$\ddot{x} + (a + e + bx + cx^2)\dot{x} + x + a\left(ex + \frac{b}{2}x^2 + \frac{c}{3}x^3\right) = 0 \quad (2.4)$$

where x denotes the floating potential fluctuations, \dot{x} represents the differentiation with respect to time normalized by ω where $\omega^2 = kc_s$, c_s denoting the ion acoustic speed. Here a denotes the collisional, e the ionization term, b and c represent the recombination effects respectively. In the limit a, b, c and $e \rightarrow 0$, we recover the usual ion acoustic oscillations from the eqn 3.4. Since noise has been shown[78][79] to play an important role in driving

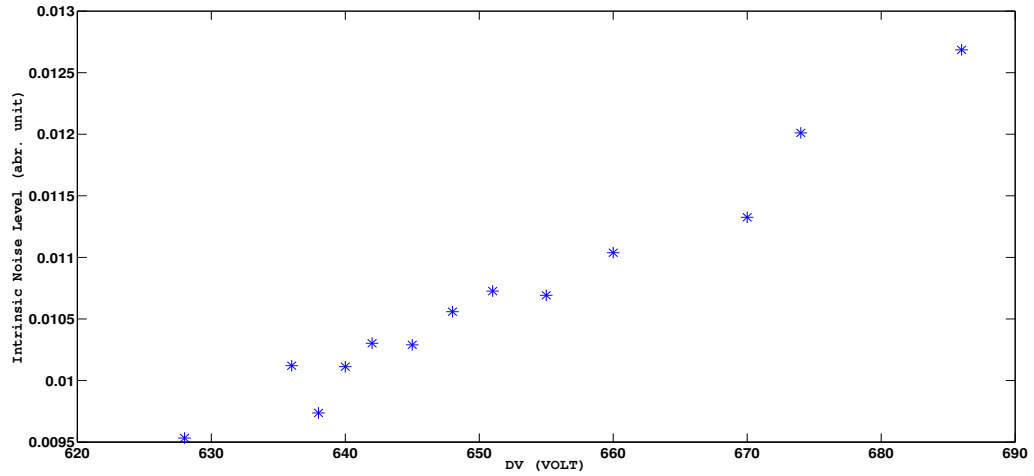


Figure 2.9: Noise level for various floating potential fluctuations shown in figure 2.2 intermittency, it was felt that the intrinsic noise could be responsible for the intermittent chaos in the present experiments. This was verified by estimating the noise level in our experiments as shown in fig. 2.9 which exhibits an increase with DV. Hence Gaussian noise was used as a forcing term in the rhs of eqn. 3.4 as shown in eqn.2.5.

In order to investigate the behavior of the nonlinear oscillations in the presence of an external discharge voltage, we included an additional term $A(1 + randn(1))$ on the right hand side of eqn. 3.4.

$$\ddot{x} + (a + e + bx + cx^2)\dot{x} + x + a\left(ex + \frac{b}{2}x^2 + \frac{c}{3}x^3\right) = A(1 + randn(1)) \quad (2.5)$$

Where A mimics discharge voltage and $A \times randn(1)$ is represents the intrinsic noise level of the system; $randn(1)$ is a Gaussian distributed random number with variance= 1 and mean = 0.

Eqn. 2.5 is solved numerically with initial conditions of $x_0 = 1$ and $\dot{x}_0 = 1$ at $t=0$. The parameters a,b,c and e are assumed the following values i.e 0.12, 0.931, 0.88, -1.9

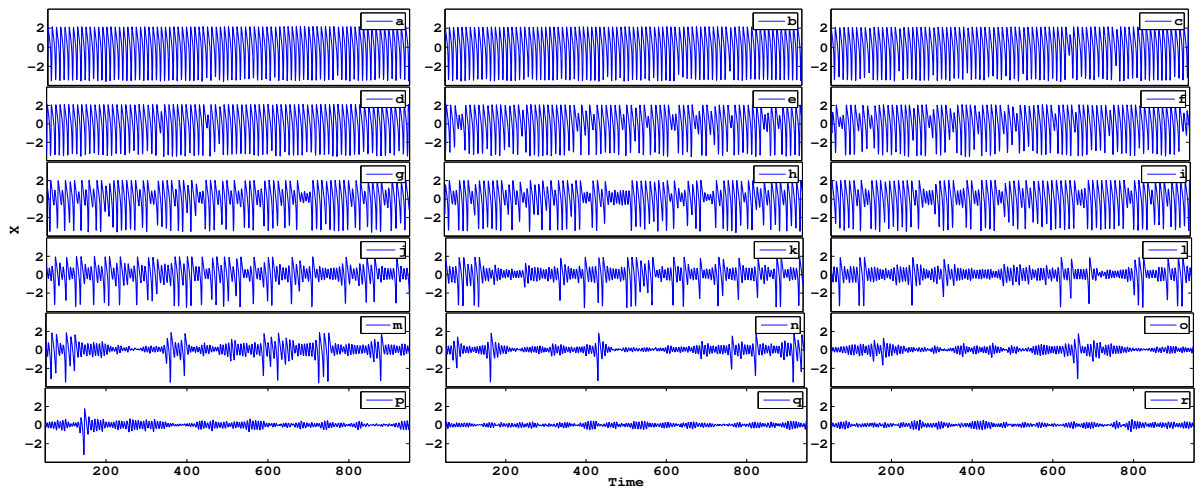


Figure 2.10: Solutions of theoretical modelling for various A : a) 0.78, b) 0.79, c) 0.80, d) 0.805, e) 0.81, f) 0.815, g) 0.82, h) 0.825, i) 0.83, j) 0.835, k) 0.84, l) 0.845, m) 0.85, n) 0.855, o) 0.86, p) 0.865, q) 0.87, r) 0.875

respectively.

The time series obtained by solving the above equation for various values of A are shown in Fig. 2.10. At $A = 0.78$ we observe two intermittent bursts in the midst of relaxation oscillations which increases in number at higher values. The oscillations appearing between the relaxation oscillations also exhibit a chaotic behavior. On increasing A beyond 0.87 the relaxation oscillations totally disappear leaving behind only the chaotic oscillations. Interestingly, we see that the numerical results have a close resemblance with the experimental observations.

From the time series data obtained by solving eqn 2.5, we estimated the normal variance of the interpeak time interval of the peaks which is shown in fig. 2.11, which also exhibit a similar trend.

Fig 2.12 is the plot of the power spectrum which also shows a close similarity to the

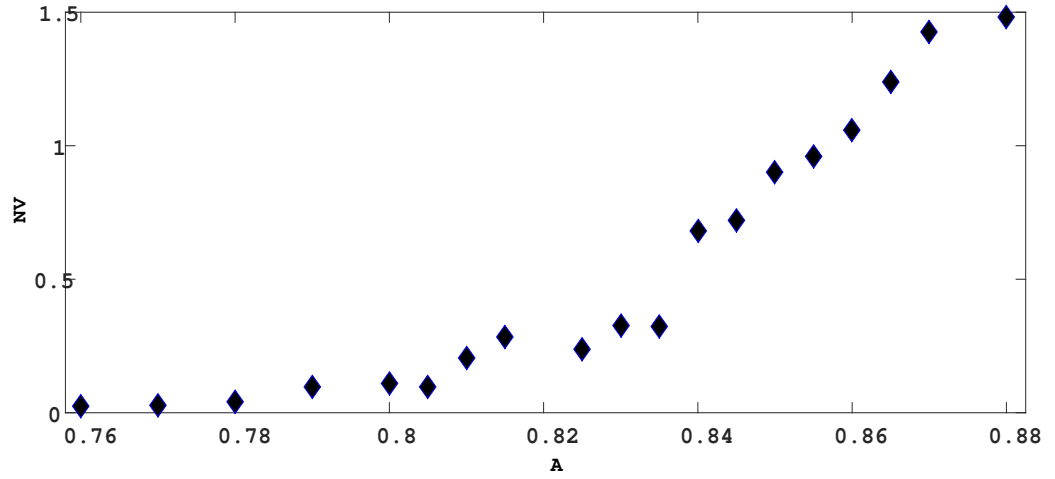


Figure 2.11: Normal variance of interpeak time interval of numerical solutions vs A

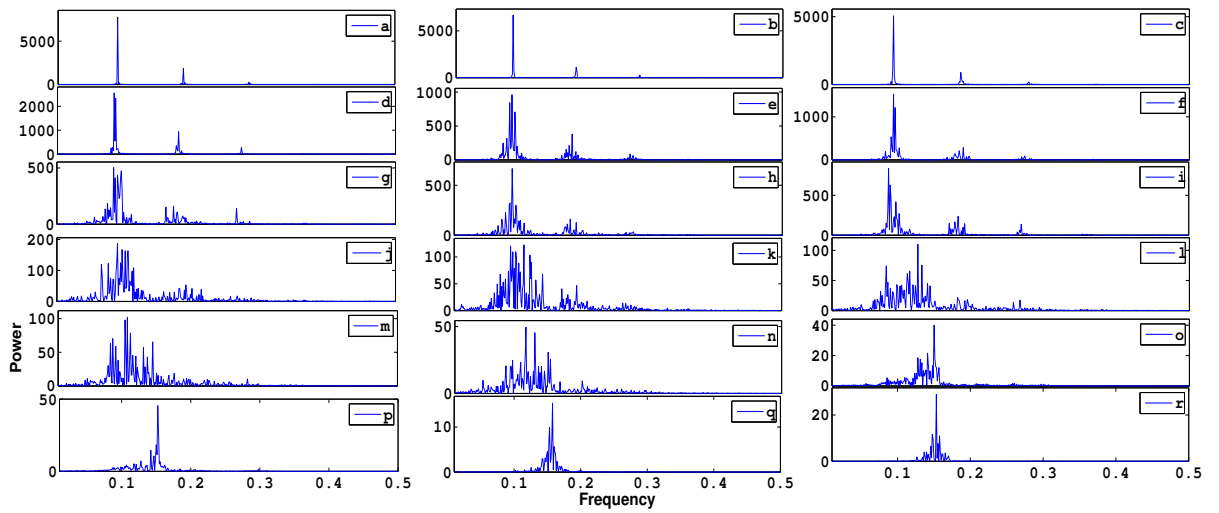


Figure 2.12: Power spectra of numerical solutions shown in fig.2.10

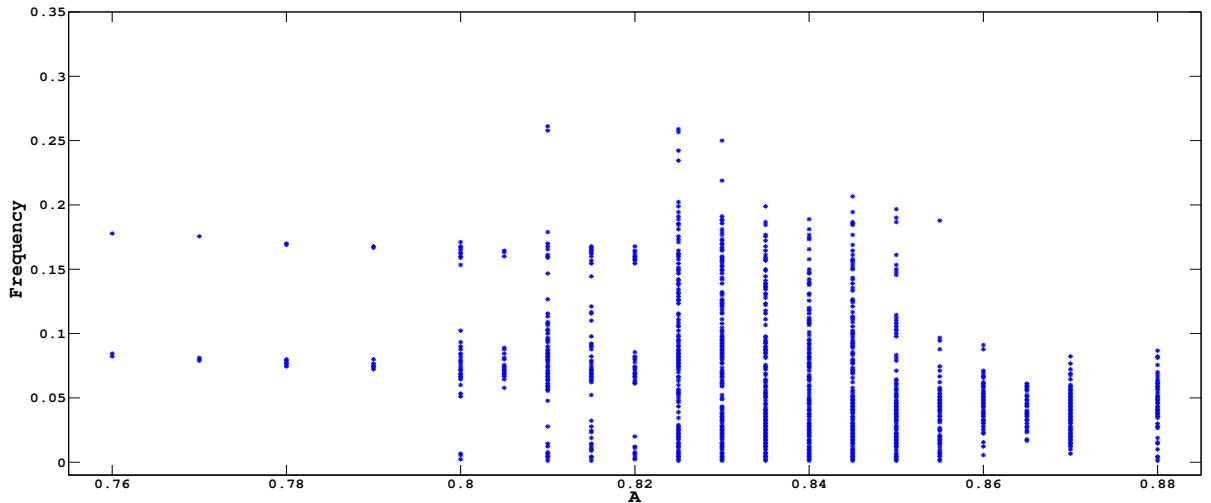


Figure 2.13: Frequencies of Power spectra peaks plotted against A

experimental results. Initially there are sharp peaks when only the relaxation oscillation is present, but as the chaotic oscillations have started appearing the peaks have a spread over a range of frequencies (fig. 2.13) and when the relaxation oscillations disappear the spread around the peaks also disappears which is similar to the experimental observations.

The behavior of phase space trajectories is identical to that obtained in the experimental observations as seen in fig. 2.14. We start with a closed orbit for the relaxation oscillations, and as we go on increasing A another smaller scroll representing the chaotic oscillations appear and finally only the smaller one remains.

The skewness and kurtosis shown in fig. 2.15 are also observed to closely resemble those obtained from the experiment.

In the above modelling, the system was forced with a noise term along with a constant bias on the right hand side of equation. To show the effects of noise as a forcing term it was varied independent of the constant bias and the solutions for each of the set of values

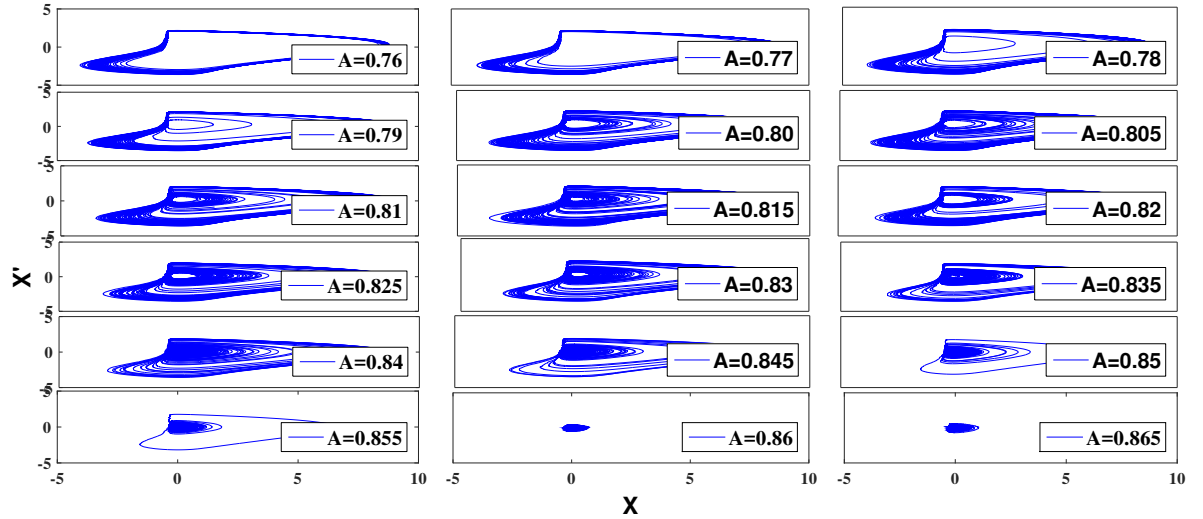
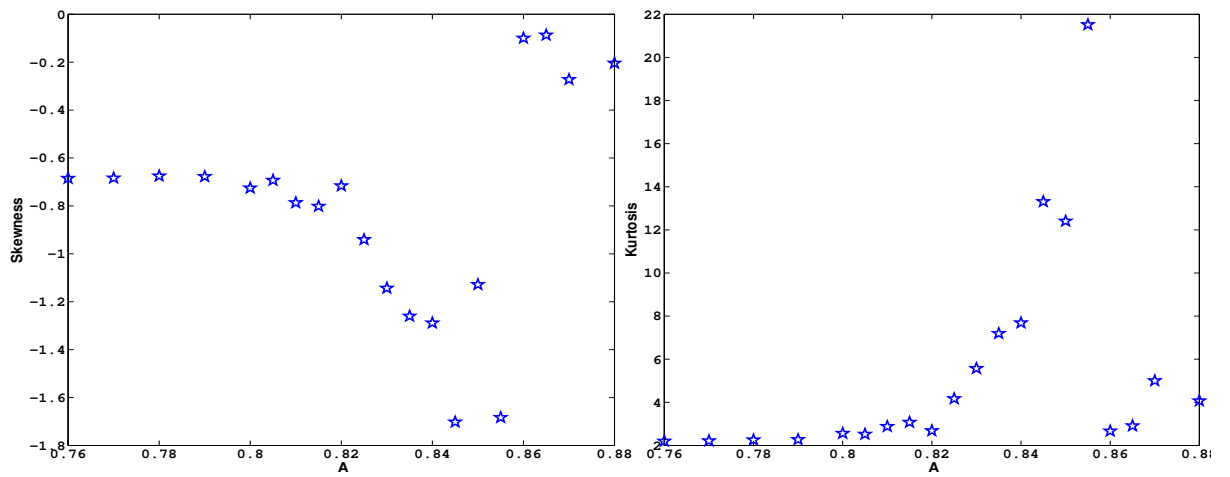


Figure 2.14: Phase space plot of numerical solutions

Figure 2.15: Skewness and Kurtosis of solutions for different values of A

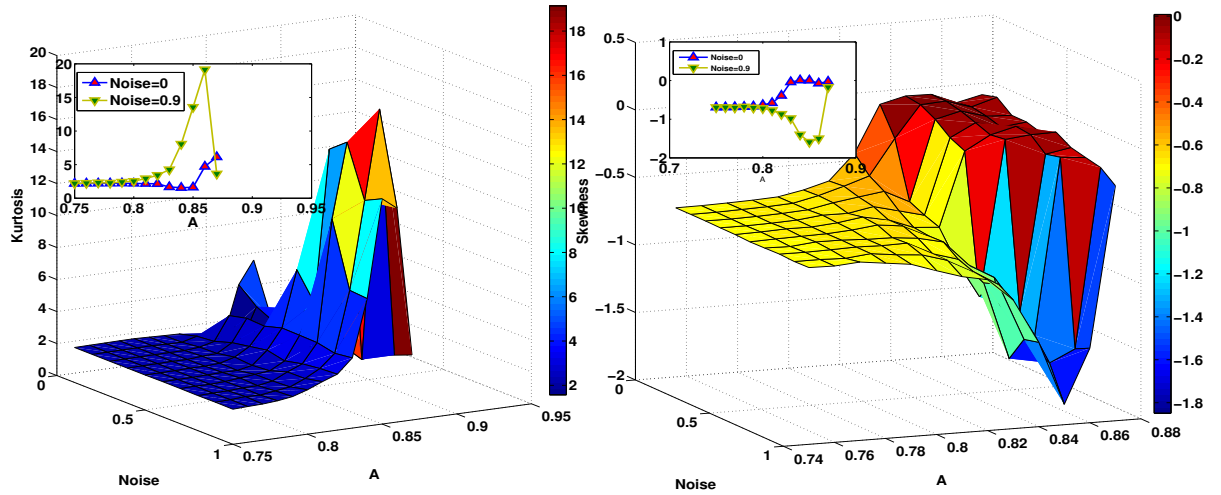


Figure 2.16: Kurtosis and Skewness of solutions plotted as a function of constant bias and noise amplitude

of *Noise* and *Bias* were taken as the time series.

$$\ddot{x} + (a + e + bx + cx^2)\dot{x} + x + a(ex + \frac{b}{2}x^2 + \frac{c}{3}x^3) = Bias + Noise \times rand(1) \quad (2.6)$$

By varying only bias, keeping zero noise a sudden transition from relaxation oscillations to a chaotic state was observed without any intermittent behavior. But when noise is included a clear route to chaos is seen via intermittency. It has been shown that the presence of intermittency left shifts and broadens a probability distribution function of a time series; that is it increases kurtosis and reduces skewness. To visualise the occurrence of intermittency when *Noise* and *Bias* are varied separately, their skewness and kurtosis are observed (fig. 2.16). Here when for *Noise* = 0 the kurtosis and skewness undergoes a sudden transition between *Bias* = 0.84 to *Bias* = 0.86; and it is not through intermittency. With increase of *Noise* the skewness have a transition from -0.7 to -0.1 via a value of -1.8 . The kurtosis also shows a transition from 2.2 to 3.7 through 15.9 when *Noise* is

increased. It is a clear indication that Noise plays a role in intermittency to occur. With $Noise = 0$, we varied bias and observed that there was no dip in the skewness when there was no intermittency, but with noise a clear dip was observed when there was intermittency. Similarly the kurtosis also shows a hump in the presence of noise which can be considered as a verification for intermittency.

2.5 Conclusions

Intermittent chaos has been observed in a glow discharge plasma, by increasing the DV wherein initial relaxation oscillations are interrupted by bursts of chaotic oscillations. The intermittent behavior has been quantified showing T_{lam} to have an exponential scaling. In addition the estimation of normal variance, skewness and kurtosis can also be effectively used to detect intermittency. The NV should exhibit a gradual transition when intermittency is present. Skewness and kurtosis should show a dip and a hump respectively while transiting via intermittency.

The power spectrum shows at least two frequencies, 2.6 and 5.2 kHz and with the increase of DV it appears that the nonlinear interaction between these two modes leads to bands of frequencies around the main ones. The intermittent behavior can be explained as due to the following reason: Since in the intermittent cases, the system does not have sufficient energy to sustain type II oscillations but have more than enough energy needed for type I oscillations, it toggles between these two modes. Since it is a nonlinear system it probably shows up as an intermittent chaos.

Chapter 3

Irregular - regular - irregular mixed mode oscillations in a glow discharge plasma

Floating potential fluctuations of a glow discharge plasma are found to exhibit different kinds of mixed mode oscillations. Power spectrum analysis reveals that with change in the nature of the mixed mode oscillation (MMO), there occurs a transfer of power between the different harmonics and subharmonics. Estimates of correlation dimension and the Hurst exponent suggest that these MMOs are of low dimensional nature with an anti persistent character. Numerical modeling also reflects the experimentally found transitions between the different MMOs.

3.1 Introduction

Periodic phenomena that are commonly observed in plasmas display oscillatory responses with a unique distinct amplitude. Another not so well explored and understood complex nonlinear phenomena in the context of plasmas are periodic oscillations exhibiting sequences of multi-peaked patterns known as mixed mode oscillations. Generally oscillations with

clearly distinct amplitudes displaying a temporal cycle or pattern can be considered as mixed mode oscillations[48]. A pattern made of two kind of oscillations repeating itself over time gives rise to this kind of behavior. The cycle or pattern mentioned above can be a simple or regular one where only one pattern is occurring again and again over time. It may also be a series of patterns with or without a particular order to follow. These MMOs can be described by the nomenclature m^n where the pattern construing the MMO consists of m number of large amplitude oscillations and n number of small amplitude oscillations. Regular MMOs can be of m^n form, i.e, only one pattern is repeating itself over time. A series of patterns following an order repeating over time following the sequence $m_1^{n_1}m_2^{n_2}...$ constitute a compound mmo. The series of patterns that follow no order can be named irregular mmo, although no nomenclature like the other two kinds of mmos is applicable here but one can still read a segment of the oscillation following the same convention.

Occurrence of mmos was reported for the first time in 1964 by Zhabotinskii[10] in the study of a chemical reaction that became famous as the Belusov-Zhabotinskii (Z) reaction[11] Subsequently such phenomena were observed in many chemical reactions[82], neuronal responses[14, 15] as well as electronic circuits[16]. The sequence of periodic states occurring in the chemical reactions has a complex bifurcation structure as a function of control parameters and a compact organization for these sequences is provided by Farey arithmetic. Mmos have been extensively studied through numerical modeling [83]-[84] of coupled oscillators in presence of separate time scales leading to an understanding of mmo dynamics found in various applications.

Not many results have been reported on mmos in plasmas. Braun et al. [61] had shown

for the first time in a glow discharge plasma, a mixed sequence of mmos and chaotic behavior following Shilnikov homoclinic chaos. Numerical simulations of mmos in a glow discharge plasma was reported by Hayashi[85] using one-dimensional fluid equations. Recently mmos were also reported[47] in dusty plasmas with structures exhibiting an incomplete devil's staircase stimulating interest in the development of new dynamical system theories as well as new theoretical approaches for the study of dusty plasma dynamics.

Plasma, being a highly nonlinear medium, is capable of exhibiting different kind of nonlinear oscillations that are sometimes triggered by external forcing or just spontaneous response of the system[86]. Typically interesting phenomena like intermittency or mmos can emerge from nonlinear interaction of different kinds of ionization waves. In the present work mmos in a glow discharge plasma are being reported as the discharge voltage (DV) is varied keeping the pressure of the system fixed. As we gradually increase the discharge voltage: at first we notice irregular mixed mode oscillations. On further increasing the DV the oscillations evolve as: irregular mmo \rightarrow compound mmo \rightarrow regular mmo \rightarrow irregular mmos. Distinction between irregular and ordered mmos is visualized using power spectrum and phase space plots. A qualitative knowledge of nonlinearity of the system can be obtained from the relative powers of sub harmonics and harmonics present in the power spectrum. But for a quantitative understanding we look at the change in Lyapunov exponent as the system goes through different kinds of mmos. More ordered the floating potential fluctuations become the less is its Lyapunov exponents. This fact is again reflected in the changes Hurst exponent of the system which suggests that the system has different types of memory while exhibiting different types of mmos; meanwhile the correlation dimension shows a

gradual change in the complexity of the system.

A simple model capable of describing the nonlinear phenomena occurring in ion sound instabilities has been developed by Keen and Fletcher[87] based on the two-fluid equations and subsequently extended to include external excitation to investigate chaos and intermittency[88]- [67] In order to study mmos, we employ similar model and assume that one of the modes present in the experiment to be the driving term in the equation. The nature of the mmo is seen to change either by changing the frequency or the amplitude of the driving term. Thus transition between regular and compound mmo is reproduced numerically.

3.2 Experimental setup

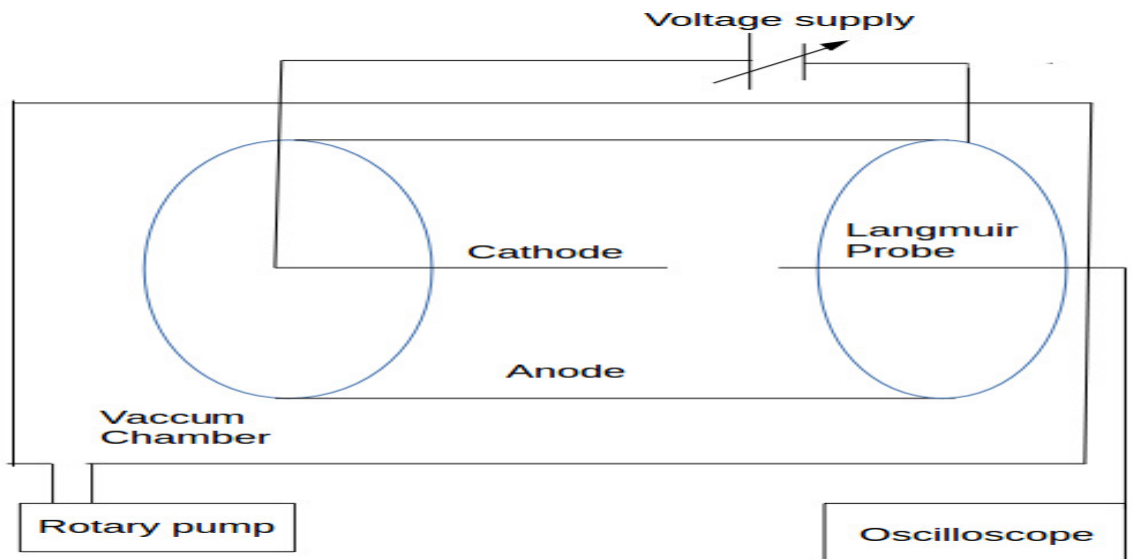


Figure 3.1: Schematic diagram of the experimental setup

The experiment was performed in a setup, similar to the setup of the previous experiment, shown in fig. 3.1 where a hollow cylinder of diameter of 4.2 cm and length 6.9 cm is used as anode and a solid cylindrical wire of diameter 1.5 mm and length 3.5 cm is used as cathode. The plasma was created inside the hollow anode by applying DC discharge voltage between the electrodes that can be varied over the range 0 to 1000 Volts. The entire setup was mounted inside a vacuum chamber which was evacuated using a rotary oil pump and the pressure was monitored using a Pirani gauge. The setup and the chamber were separated by teflon coating. A Langmuir probe with cylindrical tip was inserted inside the hollow anode without any bias to measure the floating potential fluctuations of the plasma. The anode, cathode, probe-tip, vacuum chamber were made of stainless steel. Data acquisition was done by connecting the probe to an oscilloscope.

After evacuating the chamber to a base pressure of 0.001 mBar the chamber was filled with Ar gas up to 0.320 mBar pressure. Floating potential fluctuations were observed by using the discharge voltage as a control parameter and over the range of values from 736 to 800 volts, interesting phenomena related to MMO's were observed. While recording the floating potential fluctuation data we kept the recorded data length fixed at 10000 points and the frequency of sampling the data points have been 25 kHz.

3.3 Results and discussions

The present work attempts to study mixed mode oscillations in a glow discharge plasma, but to understand the dynamics properly we need to know the plasma parameters of the system so that a basic knowledge about the operating situation of the plasma system is gathered. Different plasma parameters were measured using the Langmuir probe. The

electron temperature is found to be $T_e = 4\text{eV}$. Ion density of the current system was $10^7/\text{cm}^3$. As we know $C_s = \sqrt{\frac{\gamma z K_b T_e}{M_i}}$. For our experiment with $Z = 1$ and $\gamma = 1$, for Argon $M_i = 40$ we have $C_s = 3.095 \times 10^5 \text{cm/sec}$. For these parameters we can have ion acoustic frequency as: $\nu_s = \frac{C_s}{2\pi(d/2)}$. Numerically this frequency comes close to 25KHz .

3.3.1 Floating Potential Fluctuations

Depending on the experimental conditions provided, the floating potential fluctuations(FPFs), taken at a fixed position within the hollow anode can exhibit different types of oscillations. In this experiment discharge voltage was taken as the control parameter that was varied gradually and the pressure was kept constant at $P = 0.340 \text{mBar}$. At various lower discharge voltages relaxation oscillations were seen (fig. 3.2)at lower discharge voltages, while oscillations with distinctly separable amplitudes made their appearance from $DV = 736$ Volts. The occurrence of small and large oscillations followed no temporal recurrence at 736Volts; so this mixed mode oscillation can be termed as irregular mmos due to lack of periodicity. The FPF at $DV = 742$ Volts is also an irregular mmo like the FPF at $DV = 736$ Volts but a few new oscillation blocks have been observed here like 1^7 and 1^8 along with the oscillation blocks 1^3 and 1^4 that have been already present from 736 Volts. At about 754 Volts a sequence of blocks as $1^1 1^2 1^4$ constitute the FPF; this is the compound mixed mode oscillation that stays there for upto 760Volts. This periodicity of $1^1 1^2 1^4$ oscillation is partially broken by repetitive 1^4 blocks at 766 Volts. On further increasing DV, mmos of 1^4 appear in the entire time series and the oscillation transforms into a regular mmo from a compound one. At 779 volts this 1^4 mmo transforms into a 2^2 mmo. On increasing DV even further to 788 volts or 800 volts we see mmos with a random pattern of oscillation

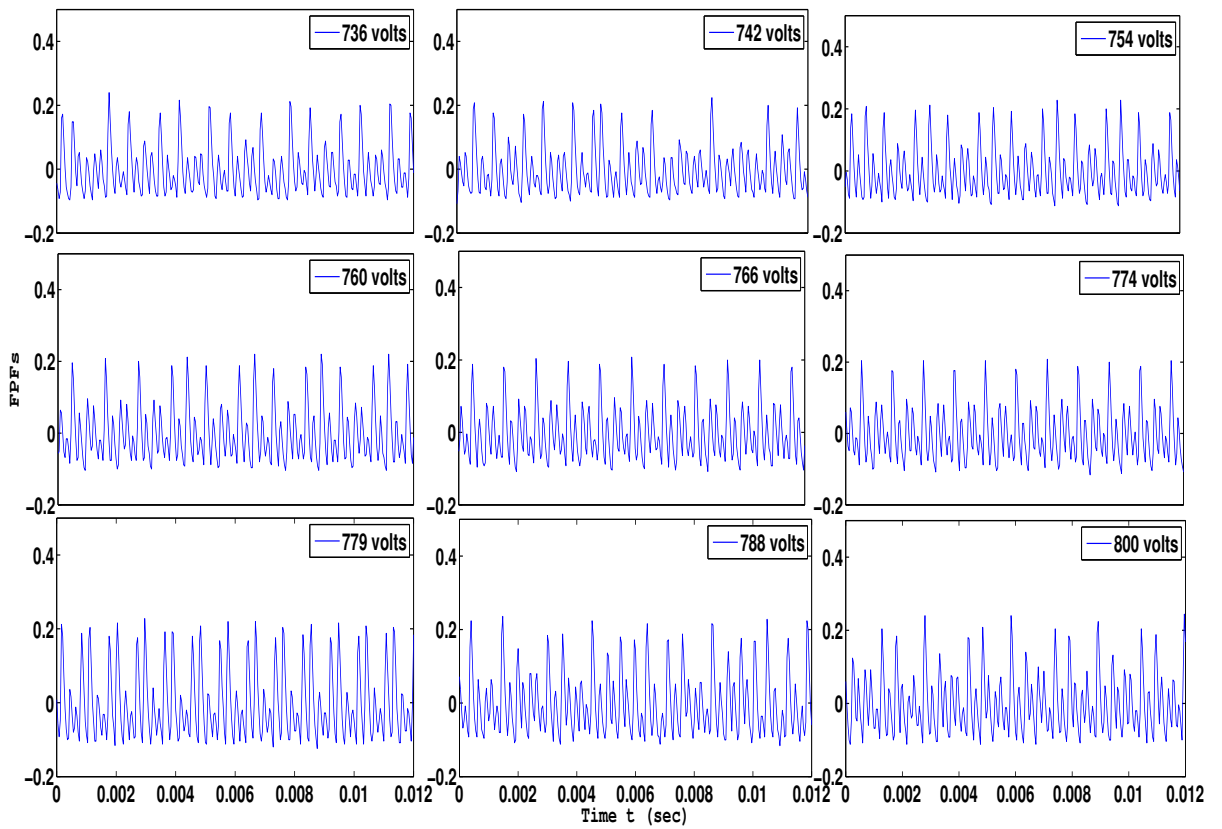


Figure 3.2: Floating potential fluctuations for different voltages

blocks $1^1, 1^2, 1^4, 1^7$ and 1^8 . But in these final irregular mmos the relative abundance of 1^4 is higher compared to others. So the mmos are observed in the following manner: irregular \rightarrow compound \rightarrow regular \rightarrow irregular; as DV is increased, which is observed to be a robust phenomenon.

3.3.2 Power Spectra

To gain an initial idea in any nonlinear phenomenon a look into the power spectrum analysis is needed. The information about how different frequency components of a floating potential

fluctuation contributed to the resultant mmo is explored here. Fig 3.3 shows the power spectrum wherein we see that during irregular mmos there are some distinct peaks with a spread around each of them for DVs of 736 and 742. On further increasing DV the spread of frequencies reduces leaving only the sharp peaks at distinct frequencies up to 779 volts.

At about 788 volts the spread of frequencies around the distinct peaks are seen and at 800 volts this broadening increases. The frequencies of the regular mmos correspond to ionization wave frequency and its harmonics. The frequencies seen in the compound mmos may be a result of the nonlinear interaction of different modes in the system.

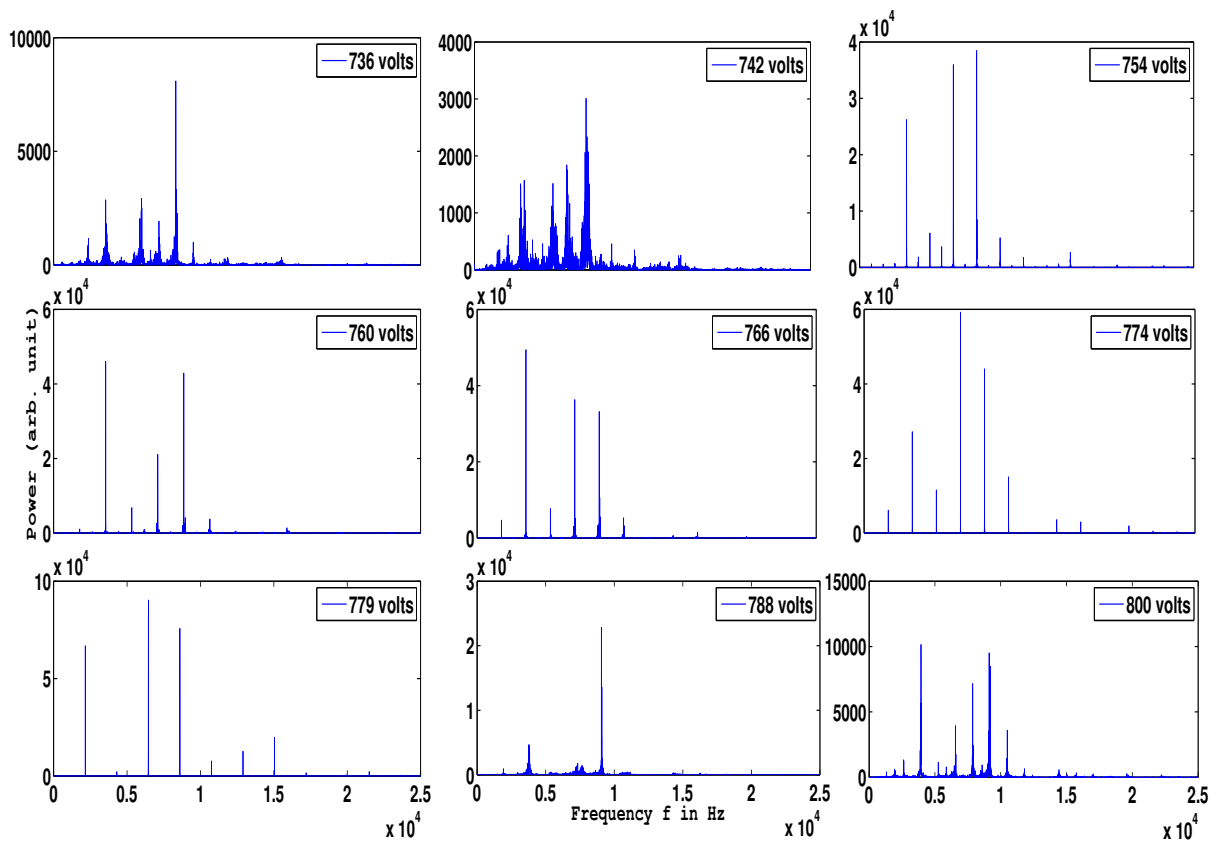


Figure 3.3: Power spectrum of FPFs obtained at different discharge voltages

Initially the power spectra is showing wide bands for irregular mmos but in this scenario also one can find that the system has broad band subharmonics of the largest peak. At 754 volts when $1^1 1^2 1^4$ compound mmo is present one of the lower side band frequencies gains more power and becomes comparable to the fundamental one. This low frequency peak causes a modulation amongst the low amplitude oscillations in the mmo. In the regime of this compound mmo at 760 volts we see a previous subharmonic becomes fundamental, and the fundamental itself becomes its harmonic although their power is comparable.

In this case the modulation is so strong that it dominates the power spectra. At the beginning of the regular 1^4 mmos again there is a swapping of harmonics, fundamental and subharmonics. This inter-shifting goes on until the irregular mmos reappear and only a fundamental and one of its subharmonics survive. After that the broadening takes over and many subharmonics tend to appear. From this exchange of power amongst the different frequencies one can conclude that strong nonlinear interactions are present [89] in the system. But to quantify these properties we have to carry out non-linear time series analyses.

3.3.3 Phase Space Reconstruction

In a rich dynamics like mmo it is expected to have many points of attraction around which the phase space points would revolve. Phase space is reconstructed from the time series obtained as FPFs by using lag-delay method. The time lag τ is chosen to be the time needed after which the autocorrelation function of the time series drops to $1/e$ of its maximum value.

In the current experiment, the phase space reconstruction have a numerous closed paths as shown in fig. 3.4. These paths can be grossly categorized in two groups: the big ones corresponding to the large oscillations and the cornered interwoven smaller ones corresponding

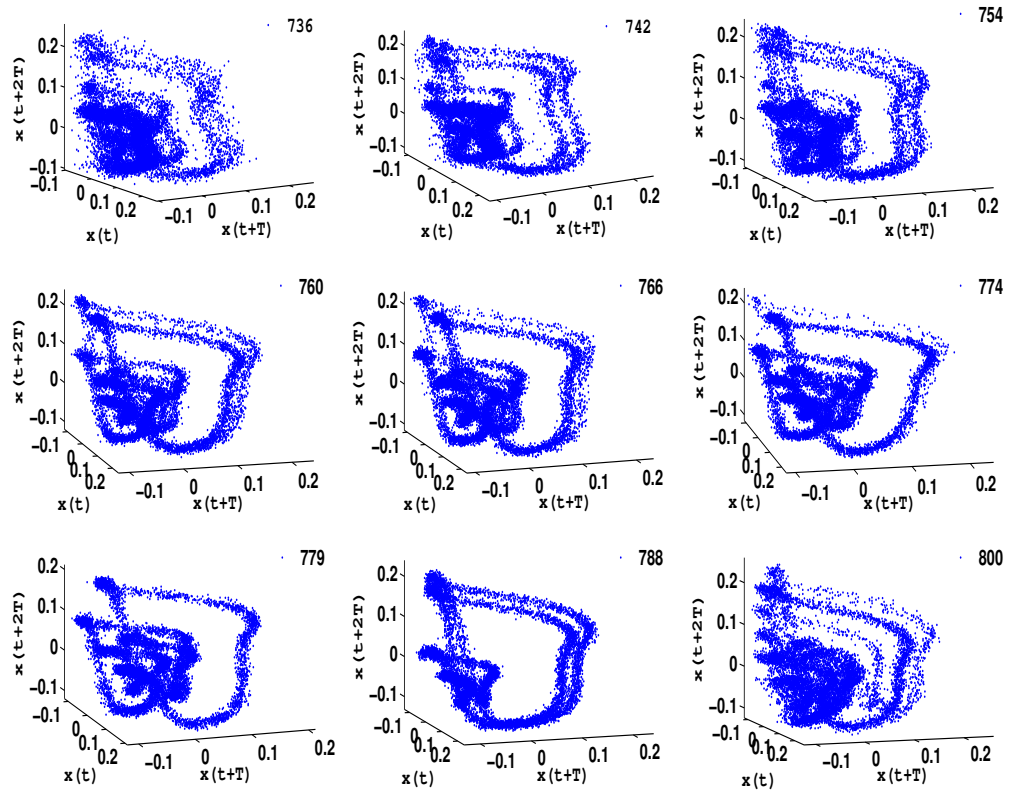


Figure 3.4: 3D reconstructed phase space diagram for various discharge voltage to the small oscillations. Irregular mmos observed at the lower discharge voltages correspond to a seemingly clustered phase space reconstruction. In these cases very faint or almost no defined phase space path is seen, and the data points are diffused out of the path in a random fashion. Mixed mode oscillations tend to become regular from 754 volts and the spread of data points around the phase space path is seen to decrease. For regular mmos appearing at 766 Volts and 779 volts the reconstructed paths are sharper. After that when again irregular mmos appear, the points in phase space have a scattered occurrence.

It is evident from the above figure (3.4) that the irregular mixed mode oscillations

have diffused phase space paths indicating randomness; which will be later explored using Lyapunov exponents. The interwoven paths clearly state that the embedding dimensions for all the time series in the current experiment are greater than three. As a matter of fact it turned out to be seven and was used a crucial parameter while calculating correlation dimensions for various FPFs.

3.3.4 Nonlinear analyses

How the nonlinearity of the system evolves with variation in the control parameter can be understood by studying three properties of the system: Lyapunov exponent, Hurst exponent and correlation dimension. All these parameters are obtained from measurable statistical properties of the time series; as each of the statistical properties reflect different aspects of nonlinearity, we find it necessary to evaluate all three of Lyapunov exponent, Hurst exponent and correlation dimension to find out chaoticity, persistence and complexity respectively.

Lyapunov exponent is the measure of how fast two points in phase space diverges for a time series so it is a direct measure of chaoticity of a system. Let's assume l_0 is the initial separation between two points in a phase space diagram. Now if $l(t) \sim l_0 e^{\lambda t}$ then λ is the Lyapunov exponent.

In fig. 3.5 we see the Lyapunov exponents for various discharge voltages. For initial two irregular mmos the lyapunov exponent is high, near 0.14. For the next three DVs we have seen compound mmos which shows a decreasing trend in LE(Lyapunov Exponent). This trend is a clear indication that the chaoticity of the system is decreasing. For the next two time series the regular mmos show very low and almost constant LE at 0.04. The last two irregular mmos we see increasing LE. So the plasma as a dynamic system goes chaos to

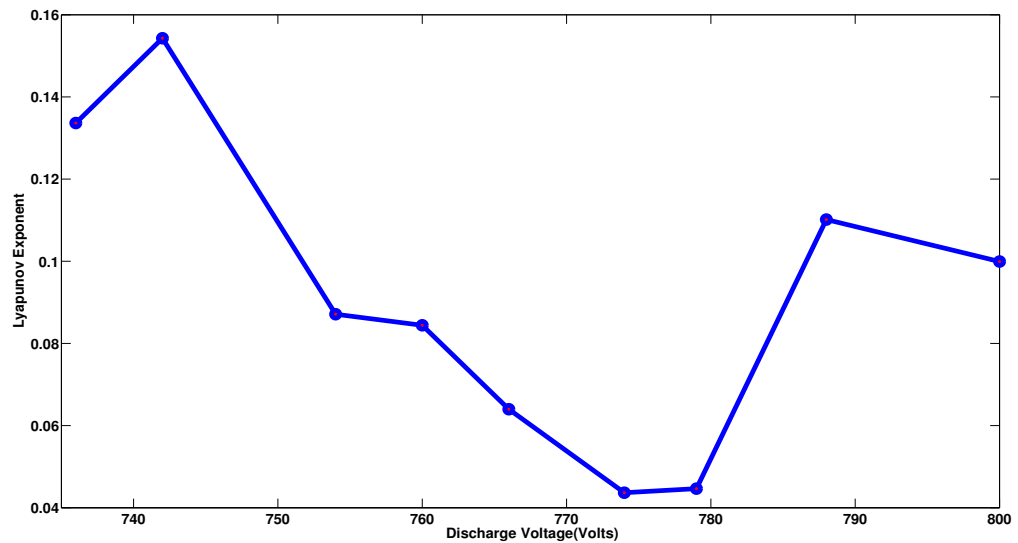


Figure 3.5: Luapunov Exponent for various floating potential fluctuations

order to chaos transition.

The characteristics of memory of the system can be understood by analyzing the sequence at which the oscillations of a time series appear. If there is no recurrence in the sequence it is a chaotic one with Hurst exponent 0.5. But if the sequence follows a trend it is said to be persistent with $0.5 < H < 1.0$. On the other hand if the sequence changes its trend alternatively and very often then it is an anti persistent oscillation with the Hurst exponent lying below 0.5. If for a time series $\langle \frac{R_n}{S_n} \rangle \sim n^H$ then H is the Hurst exponent for the limit $n \rightarrow \infty$; where R_n is the range and S_n is the standard deviation of n elements in the time series.

The irregular and compound mmos that are observed at lower discharge voltages exhibit a Hurst exponent that varies around 0.2(fig. 3.6). But for discharge voltages around 766 volts the exponent decreases to a very small value as long as regular mmos are seen. So

regular mmos can be recognized as very anti persistent oscillations. Beyond 779 volts, when the mmos are again irregular a gradual increase in the exponent is seen although the system response remains anti persistent. This indicates that the two types of oscillations present together induces long term memory about switching between amplitudes in the system.

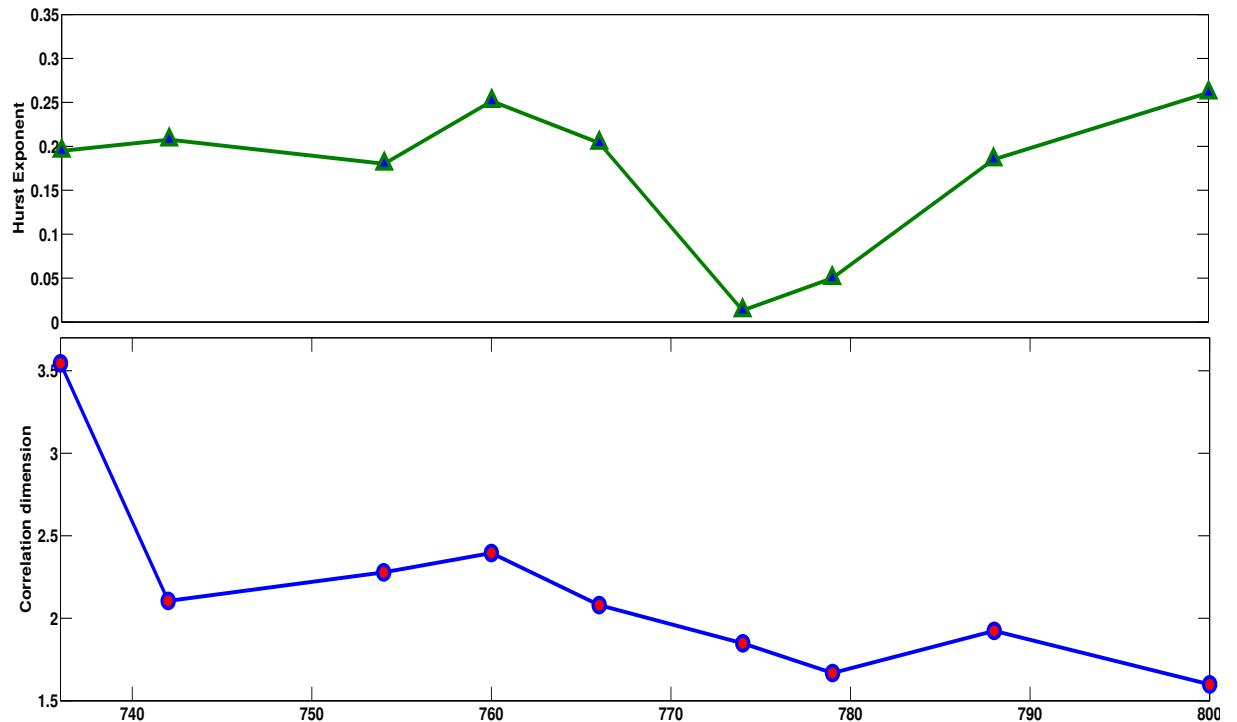


Figure 3.6: Hurst exponent and Correlation dimension for various floating potential fluctuations

Dimension of a system is defined as the power of the radius of the hypersphere (ϵ) with which the volume of the system within the hypersphere changes. Correlation dimension[90] (CD) is a measurable parameter similar to the dimension of a system; the only difference is that here we count data points of the system as we increase the volume of the hypersphere. It actually tells us what is the dimension of the nonlinear interaction whose 1D projection

is obtained in the time series. But to calculate the CD of the time series we first need to define the dimension of space in which we are going to perform the calculation; or in other words we need to find out the embedding dimension of the system. Theoretically the CD should saturate with the increasing embedding dimension[62]. In this work we have taken the saturated values of CD for analysis.

$$C_{em}(\epsilon) = \frac{1}{N^2} \sum_{i,j=1}^{\infty} \Theta(\epsilon - |x_i - x_j|^{em}) \quad (3.1)$$

$$CD_{em} = \lim_{\epsilon \epsilon' \rightarrow 0} \frac{\ln\left(\frac{C_{em}(\epsilon)}{C_{em}(\epsilon')}\right)}{\left(\frac{\epsilon}{\epsilon'}\right)} \quad (3.2)$$

Where Θ is the Heaviside step function, C_{em} is the correlation integral in a particular embedding dimension em , $|x_i - x_j|^{em}$ is the distance between the i th and j th point in that embedding space; and CD_{em} is the correlation dimension of the time series for that embedding dimension. ϵ and ϵ' are arbitrary smallness parameters.

At lower discharge voltages, when the time series reveals that irregular mmos are present in the system, the irregularity contributes to the high value of correlation dimension(fig. 3.6). When compound mmos are observed at higher values of discharge voltage, we see a gradual decrease in CD with the decrease continuing for regular mmos also. After CD reaches a minima for regular mmos it remains low for irregular oscillations. So high value of correlation dimension can not be associated with less ordered mixed mode oscillations, neither it is meant to. Rather it is straight forward to think that the system is going through a transition from a higher CD situation to lower CD situation as the current experiment is performed. There is a gradual decrease in the complexity of the system as clearly indicated

by the power spectra where it is evident that the broadening of peaks in final irregular mmos is not so prominent compared to the initial ones.

3.4 Numerical Modeling

Mathematical modeling of real physical systems has always been a challenging task, and more so for a complex system such as plasma that exhibits different kinds of oscillatory and chaotic responses through various types of attractors and bifurcation phenomena with variation in control parameters. In order to model the different nonlinear oscillations exhibited by a glow discharge plasma during ionization instabilities, a nonlinear equation has been developed by Keen and Fletcher[87] by considering the ion sound instabilities using two fluid equations with the inclusion of ionization and recombination effects. In order to gain insight into chaotic dynamics, a similar nonlinear equation has been proposed by Kadji et al[67] and phenomenon like homoclinic bifurcation[91] and intermittency[88] have been successfully studied utilizing this type of model. Theoretical modeling of mmos has recently been done[92] using a third order scalar equation known as the jerk equation.

While trying to reproduce mmo as the solution of an equation depicting a discharge plasma system we followed Kadji et al's work where the system is considered to be consisting of two fluids with both two and three body recombinations have been taken into account. Density fluctuations in an unmagnetized low temperature plasma arising due to ion acoustic perturbations follow the equation:

$$\ddot{x} + (a + e + bx + cx^2)\dot{x} + x + a\left(ex + \frac{b}{2}x^2 + \frac{c}{3}x^3\right) = 0 \quad (3.3)$$

where a, b and c are ionization, two and three body recombination terms, e and x represent

the ion neutral collision rate and the density fluctuations respectively. The time scale in the above equation is normalized with respect to the ion acoustic frequency that lies around 25 kHz.

Many theoretical works reporting [85] mixed mode oscillations in a two dimensional system have shown that external forcing is necessary to generate these oscillations. But though there were no external forcing in the present experiment, it is likely that some self-generated plasma mode inside the system can act as a forcing and the system can be considered as a self-driven one. This is an assumption that has been made and a forcing term $A \cos(\omega t)$ is introduced in the model.

$$\ddot{x} + (a + e + bx + cx^2)\dot{x} + x + a\left(ex + \frac{b}{2}x^2 + \frac{c}{3}x^3\right) = A \cos(\omega t) \quad (3.4)$$

While solving this equation(eqn. 3.4) we have chosen the constants as $a = 0.12$, $b = 0.931$, $c = 0.525$, $e = -1.7$; the choice of the constants was done by successive trials . Various values of the parameters w and A produce mmo as solution. In the experimental scenario, the control parameter was discharge voltage which can trigger either a change in the frequency of the excited mode, ω or its amplitude A . Both are considered as possibilities:

Case *I*:

Numerical investigations of eqn. 3.4 have been carried out keeping ω fixed at $\omega = 0.19$; which if scaled up to the ion acoustic frequency becomes close to an observed frequency (near 5.0kHz) in the power spectra, and the amplitude A varied. The time series for different values of A reveals different sequences of mixed mode oscillations. The characteristics of the different mmo sequences can be better understood by considering the variation of the maximum value of the oscillation at the peak with respect to the control parameter. The

maxima obtained in the solution of eqn. 3.4 is shown in figure (8) as a function of the amplitude A .

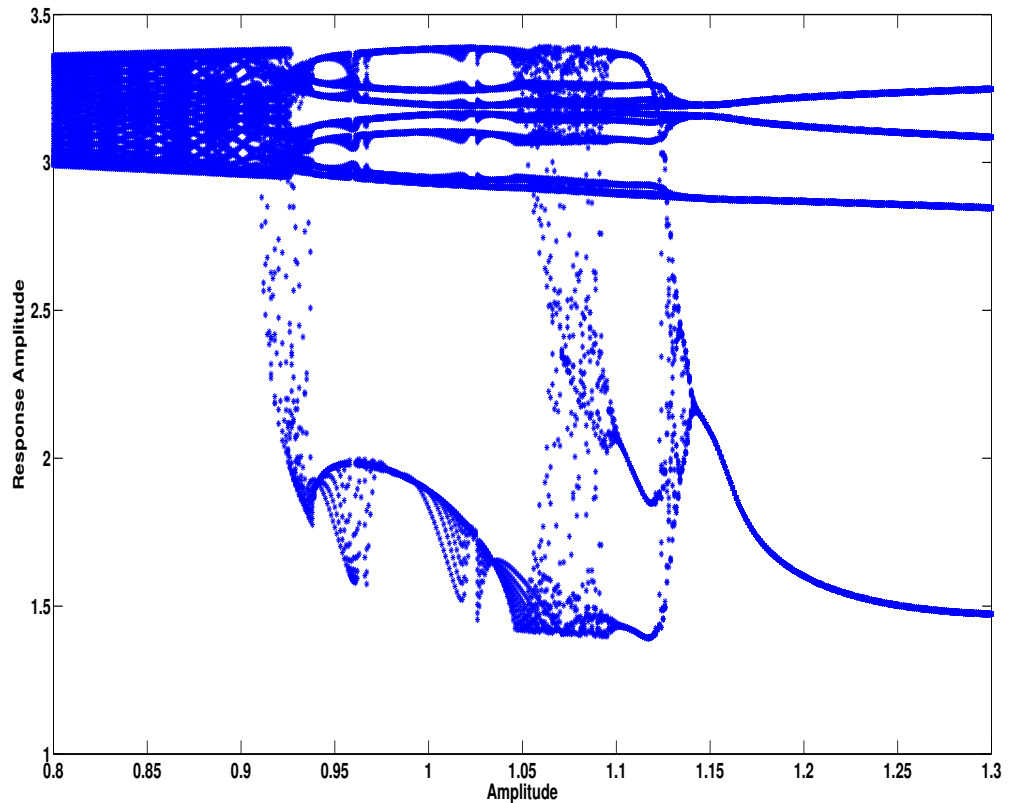


Figure 3.7: Maximas found in different time series while solving eqn. 3.4 with $\omega = 0.19$ and changing A .

Fig. 3.7 shows that for low values of A , there exist several closely spaced peaks with values lying between 3 to 3.4. Depending upon the values of A , the different maxima come very close to each other, merge together or diverge. For instance near $A = 0.9$ a branch of diffused points begins to descend and converges near $A = 0.94$ to a value 1.9. The closely packed high valued points resolve into seven distinct trails; but these trails are also close

enough to be noticed separately in a time series. The lower trails, corresponding to the small amplitude oscillations in the time series, keeps on converging and diverging again and again. At some values of A like 1.102 and 1.145 we see scattered streams of points are descending from the high valued trails and converging into a single curve. The closely packed trails of maxima may not be prominently different while considering the possibility that the response oscillations are behaving as mmos. But the descending trails may give the solutions some rich dynamics.

Case II: In the second case, the amplitude A is kept fixed at 1.05 and the frequency ω is varied. We see the top most trails of the peaks gathered around 3.0 as shown in fig. 3.8.

Also in this case, the lower branch is present right from the beginning; for some values of ω there are more than one lower branch of maxima present. Here also, like Case I, merging and diverging of branches are seen, however, these changes are very rapid with respect to the changing ω .

Both the cases are rich in dynamics and can exhibit a wide range of mmos. The presence of closely packed maxima trails in both pictures indicate that one can even find slowly varying amplitude in typical solution of the equation that can give rise to the famous crown like[93] 3D reconstructed phase space. So for choosing which way we should vary our parameters we looked back at the power spectra of the experimentally found data. In the experimental data we find that the amplitude of the peaks change and the harmonics, principle mode and sub harmonics toggle among themselves. So there is a transfer of power among the modes as the discharge voltage changes. But the peaks themselves do not change much in frequency. That gives a clear indication that changing A while keeping ω constant

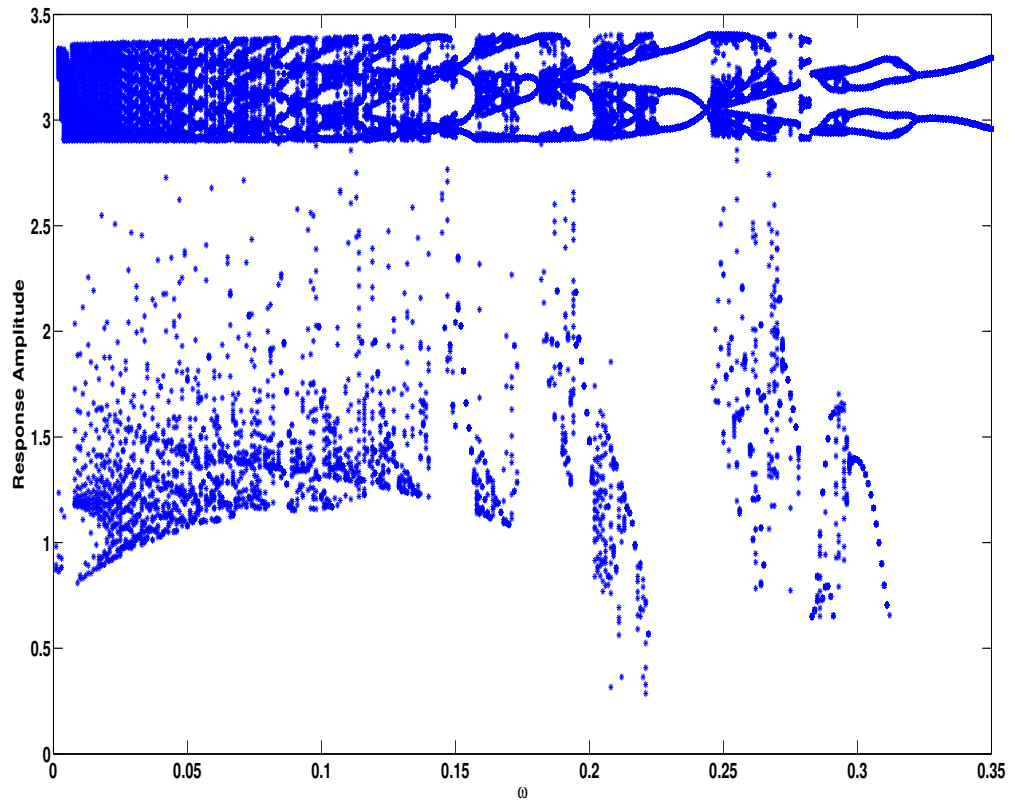


Figure 3.8: Maximas found in different time series while solving eqn. 3.4 with $A = 1.05$ and changing ω .

can be a good representation of the experimental scenario in numerical modeling.

Experimental observations show that a variation in DV can lead to change in A resulting in modifications of mmos. From fig. 3.9 we can see that when $A = 0.85$, the solution was just periodic oscillations with a sharp peak in the power spectra and a single scroll in the reconstructed phase space. But increasing A to 0.95 results in a regular mmo of 7^1 . This regular mmo has a sharp peak and an extra point of attraction in the reconstructed space. When $A = 1.10$, the solution is a compound mmo of $7^1 3^1$. This new attractor shows a

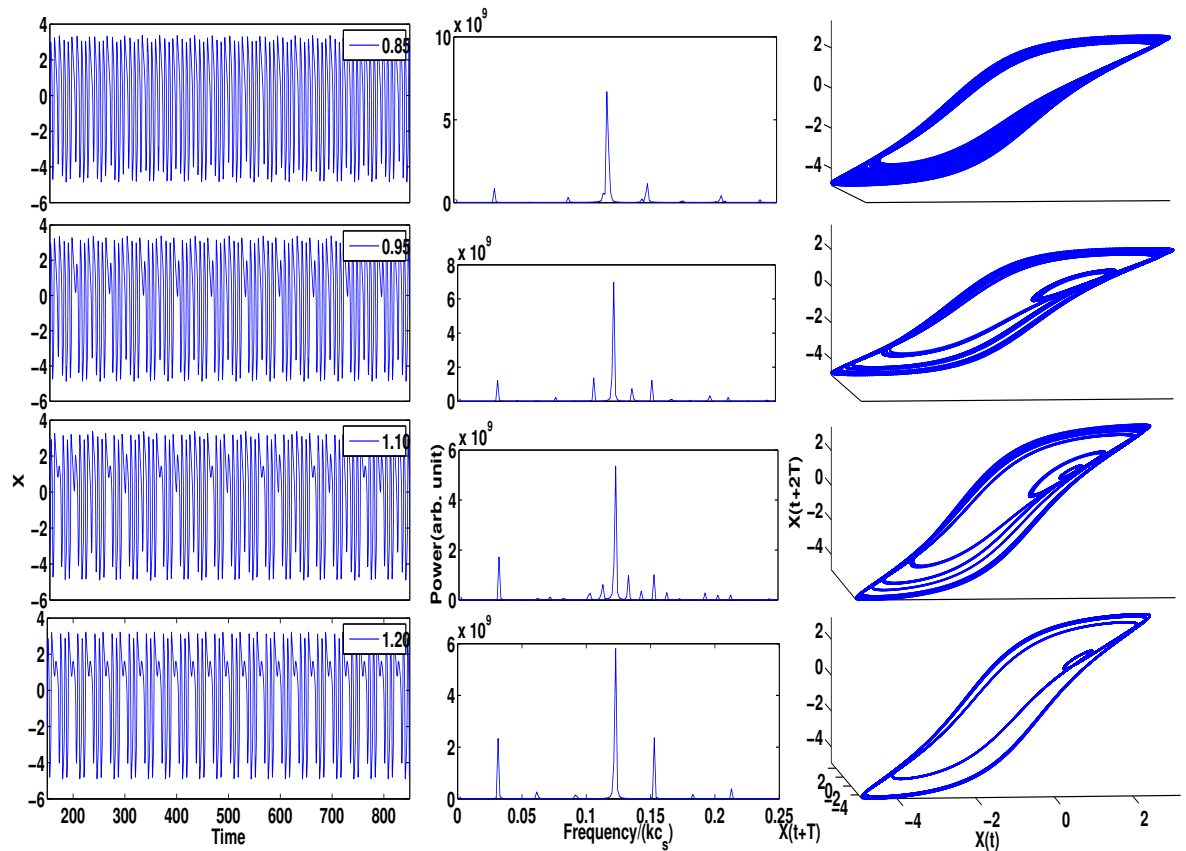


Figure 3.9: Numerical solution of eqn. 3.4 for different values of A with their power spectra and phase space reconstructions.

substructure in this compound mmo. On further increasing A to 1.20 we see that the system has returned to a regular mmo of 3^1 nature. So we can say that a self generated mode driving the system can be the reason behind the different types of mmos.

Here the oscillations found as solutions belong to a small range of parameters as all the constants in the equations other than A are kept unchanged. So the statistical parameters are not expected to show much variation. Also the oscillations in the modeling are mainly

dominated by large oscillations, they are found to be persistent in contrast to the anti-persistence of the experimental floating potential fluctuations. So although the statistical parameters of the experimentally found data and numerical solutions are not expected to match exactly, the understanding of those parameters are consistent with the nature of mmos.

3.5 conclusions

Mixed mode oscillations are rich dynamics that have been found in the current experiment as the only control parameter DV is varied in the experiment. The transitions goes as Irregular mmo \rightarrow compound mmo \rightarrow regular mmo \rightarrow irregular mmo. This sequential variation is a robust phenomenon and can be retraced by reducing discharge voltage. The system has shown that its correlation dimension under goes a fall while the discharge voltage is increased. So as the discharge voltage is increased the system response is settling down to a reduced complexity. This fact is further backed by the fact that the final irregular mmos have very less spread in power spectra compared to the initial one. A similar fact is also associated with the diffusion of data points out of the defined path in phase space between the two kinds of irregular mmos. Apart from the comparison between the two kinds of irregular mmos, we can see a gradual decrease in Hurst exponents as the system goes from compound mmo to regular mmo. As the Hurst exponents lie bellow 0.5 it indicated that more ordered state indicates a more strong memory related to the alternate occurrence of high and low value in the time series. The variation of chaoticity among the FPFs is well behaved and predictable in nature, and it clearly states although the two irregular mmos have different complexity their chaoticity remains higher compared to other kinds of mmos.

There are various indications that the nonlinearity seen in the present experimentally found is originally coming from a mode generated inside the system itself. In power spectra we have seen power transfer among different frequencies indicating that one or more mode is predominantly influencing the system dynamics. This concept has been adapted in the numerical modeling section where a sinusoidal forcing, mimicking external forcing, is applied to the system; and the frequency of that forcing is kept equal to an experimentally found frequency. On varying the amplitude of the forcing the solutions of the governing equation show transitions between different kinds of mixed mode oscillations.

So one can conclude that a plasma system can undergo transition where its FPFs have a transition in the values of correlation dimension and system memory. All these can be blamed on a simple situation where a mode from the system itself is exciting the system.

Chapter 4

Hysteresis of fluctuation dynamics associated with a fireball in a magnetized glow discharge plasma in a currentless toroidal assembly

Floating potential fluctuations associated with an anode fireball in a glow discharge plasma in the toroidal vacuum vessel of the SINP tokamak are found to exhibit different kinds of oscillations under the action of vertical magnetic field of different strength. While increasing the vertical magnetic field the fluctuations have shown transitions as: chaotic oscillation \rightarrow inverse homoclinic transition \rightarrow intermittency \rightarrow chaotic oscillation. However on decreasing the magnetic field the fluctuations are seen to follow: chaotic oscillations \rightarrow homoclinic transition \rightarrow chaotic oscillation; that is the intermittent feature is not observed. Fireball dynamics is found to be closely related to the magnetic field applied; results of visual inspection with a high speed camera are in close agreement with the fluctuations and the fireball dynamics is found to be closely related to the transitions. The statistical properties like skewness, kurtosis and entropy of the fluctuations are also found to exhibit this hysteresis behaviour.

4.1 Introduction

Physicists are observing the phenomenon of hysteresis for a long time, it was historically found in the response of magnetic material to magnetic field. Later this phenomenon was found in physical systems like nano material[94], biological culture[95], brain activity[96], electrical circuits[97] etc. which behave nonlinearly to many external control parameters. Even in human society, systems like unemployment and wages[98] relation are also been found to exhibit hysteresis. On the other hand plasma is a versatile crucible of experiments on complex dynamics depending on the experimental conditions imposed. Previously reported works show many exciting phenomena like intermittency [99, 100], homoclinic[101] bifurcations, mixed mode oscillations, spiking and bursting[102] among many others.

In plasma systems hysteresis has been theoretically predicted and verified experimentally[103] in cylindrical[103, 104] glow discharge plasmas. Hysteresis in discharge current was observed[105] in an unmagnetized plasma by varying the discharge voltage and attributed to a negative differential resistance in the current voltage characteristic. Nonlinear damped, driven drift waves are also shown[106] to exhibit hysteresis with respect to the forcing amplitude with the choice of initial conditions affecting the width of the hysteresis. Experimental observations in Inductively coupled plasmas reveal huge hysteresis with respect to plasma power and attributed to the effects of electron energy distribution function[107]. However, such observations on hysteresis have not been reported so far in toroidal systems. The present work is an attempt to explore hysteresis behaviour in floating potential fluctuations by estimating the statistical parameters. Fireball dynamics were observed in the glow discharge plasma produced in the toroidal vacuum vessel of the SINP tokamak in presence of a vertical

magnetic field. By increasing the vertical magnetic field, transitions like: Chaotic Oscillations \rightarrow inverse homoclinic transition \rightarrow intermittency \rightarrow chaotic oscillations were observed while on decreasing the field the system does not follow the previous path but goes like: Chaotic oscillations \rightarrow homoclinic transition \rightarrow chaotic oscillation.

The effects of sheath near the cathode on an arc like high pressure discharge plasma has been emphasized in various works[108, 109]. Visual inspection reveals existence of bright sheaths or fireballs[110] near the electrode. The electrode collects electrons from the plasma as a result of which the anode is encapsulated, partially or fully, by ions and quasi-neutrality of plasma leads to formation of double layers. Recent experiments report observation of multiple double layers associated with anode glows in a toroidal geometry[111]. A high frame per second camera was used to keep track of the fireball oscillations at the electrode and it was found that the blob exhibits different types of pulsations. The sharp edges of this double layer are clearly visible in the photographs; reduction of the inter-frame time makes the pulsation of the blob visible. The time period of these pulsation are in good agreement with the power spectra peaks of the Langmuir probe data. It has also been seen that the blob around the anode, in response to the magnetic field, undergo different transitions for increasing and decreasing field conditions. These pulsations of the blob result in the floating potential fluctuations. The effect of magnetic field on this blob in the form of $\vec{E} \times \vec{B}$ has been found to be related to the homoclinic and inverse homoclinic transitions of the system while decreasing and increasing the magnetic field respectively. Spectral and statistical analysis of the FPFs reveal how the fireball dynamics changes with increasing and decreasing magnetic fields and also gives an idea about the nature of the distribution

that could be prevailing in the system.

4.2 Experimental setup

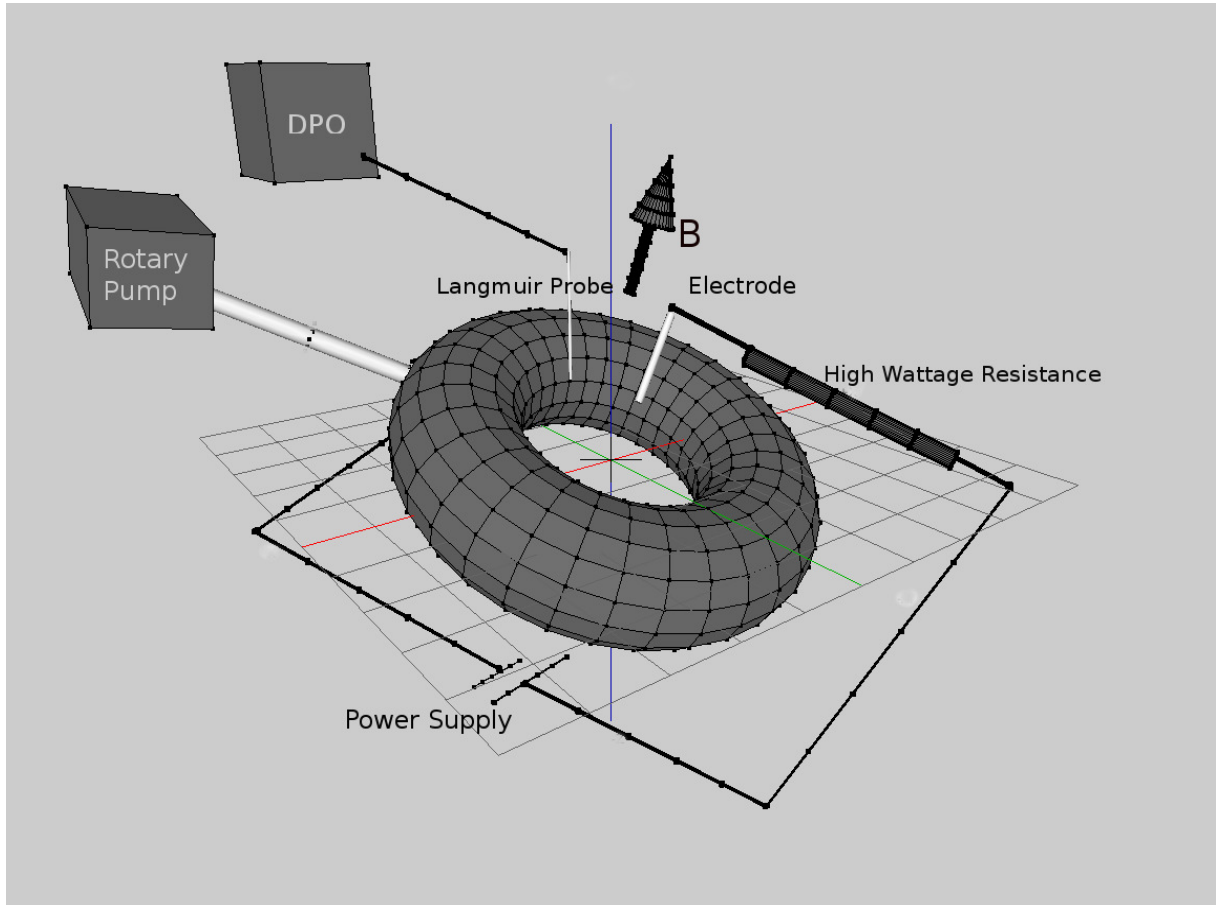


Figure 4.1: Schematic diagram of the experimental setup

The typical experimental set up is shown in fig. 4.1, in which a Langmuir probe without any biasing was used to measure floating potential fluctuations (FPFs). The toroidal vessel of SINP tokamak with major radius 30 cm and minor radius 7.5 cm has been used as the discharge chamber. The vessel was evacuated to a base pressure of 0.01 mbar using a rotary oil pump.

An electrode of length 3 cm and mean radius 0.7 cm was used as the anode while the vacuum vessel was grounded as shown in the figure. The distance between the two top ports through which the electrode and the probe was inserted was 10 cm. The vessel was filled with hydrogen upto a pressure of 0.23mbar and a discharge voltage of 0.45kV to sustain the discharge plasma. The system has a provision to generate both toroidal and vertical magnetic fields. The present experiment, were carried out using only vertical magnetic field. Four coils, two above the torus and two below the torus(fig. 4.2) having 24 turns each were used to create the vertical magnetic field in the vessel. The magnetic field produced by the current flowing in the coils is shown in the fig. 4.2. During this experiment the current through the magnetic coils was varied so as to increase the magnetic field from 0 to 4.65G. A Langmuir probe was inserted to measure the floating potential fluctuations in the system through which the floating potential fluctuations were recorded for various magnetic field using an oscilloscope. The typical data length was about 10000 for all the time series.

A high frame per second Mikrotron (V1 .6.3.0) camera was used to capture photographs of the electrode which helped us to visualize dynamics of the sheath formed near the electrode. For capturing the response of the sheathe for unmagnetized situation frames were taken at a rate of 4000 per second; while that speed was reduced to 1899 frames per second for capturing the rotation of the sheath in magnetized condition.

The photographs taken show the fireball dynamics near the electrode. If ΔT is the time difference between two consecutive frames taken and the photographs resembled themselves after n^{th} frames then the frequency of the observed phenomena is estimated as $f = \frac{1}{n\Delta T}$. Frequencies from visual diagnostics through camera and Langmuir probe diagnostics via

oscilloscope were tallied for same condition(magnetic field) of the experiment.

4.3 Results and discussions

The plasma floating potential fluctuations were found to show oscillatory features of different type depending on intensity of the vertical magnetic field applied on it(fig. 4.3 and fig. 4.4). The FPFs exhibit a chaotic oscillation for very low magnitude of B_v as shown in fig. 4.3 (a). This feature persisted up to 3.33G after which relaxation type oscillations appeared (fig. 4.3 (b)); this oscillation becomes more periodic and its time period decreases with increase in magnetic field intensity (fig. 4.3 (c)) . So the transition the FPFs have been undergoing was a inverse homoclinic one, and modifies to a intermittent bursting like behaviour at 3.89G. On further increase of B_v the transition to chaos via intermittency is completed near 4.59G.

While the magnetic field was reduced(fig. 4.4), the system starts with a chaotic behaviour, which directly undergoes homoclinic transition bypassing the intermittent phase present in the increasing magnetic field scenario. The time period between two consecutive crests increase with decreasing magnetic field showing an exact reverse phenomenon that was observed while increasing the field. At B=3.17G the FPFs oscillations again become chaotic.

Power spectra(fig. 4.5 and fig. 4.6) clarifies the type of transitions that we are seeing here. It is notable that the frequency components present in the power spectra varies over a wide range depending on the type of oscillations the FPFs are exhibiting and the type of transitions they are going through.

The initial and the final oscillations both were with low magnetic field and the nature

of oscillations were almost similar for both, hence the power spectra also show similar feature(fig. 4.5(a) and fig. 4.5(i)). In these types of oscillations, various sharp peaks are present ranging from a few hundred Hz to 6 kHz; but the peaks are not broadened to form bands. While increasing the magnetic field, the homoclinic transition shows a single prominent peak with decreasing frequency(fig. 4.5(c)). This peak suddenly disappears as soon as intermittency sets in, giving rise to a very low frequency band(fig. 4.5(f)) which probably corresponds to the toggling between the bursts of low frequency large amplitude oscillations and the chaotic oscillations. On further increase of magnetic field, the chaotic oscillations begin to fill up the entire time series and when the transition is complete the system is left with high frequency peaks as in fig. 4.5(i). While decreasing the magnetic field the system stays in the final state for $B = 4.52G$ to $4.30G$ after which a low frequency band appears which continues to shift towards 200 Hz as seen in fig. 4.6 (d) indicative of inverse homoclinic transition. Once this transition is complete the system is left with chaotic broad range of peaks(fig. 4.6(h), 4.6(i)).

To view the effects of increasing and decreasing magnetic field on the power spectra, the dominant frequencies are plotted against magnetic field (fig. 4.7). Here blue dots represent dominant frequencies while increasing the magnetic field and the red dots for decreasing field. The inverse homoclinic and the homoclinic transitions are visualized by the blue and red arrows respectively, which indicates a gradual change of frequency with respect to the magnetic field. It is clearly observed that while decreasing the magnetic field the low frequency($\sim 100Hz$) oscillations were not noticed indicating the absence of intermittency.

The sheath formation and its dynamics around the electrode is an important phenomenon in a glow discharge system since it contributes to the various frequency components. When the plasma was formed, a pulsating blob or fireball was found to be attached to the anode at a particular position. The pulsations were recorded with a high speed camera capturing every frame at a time interval of .25 msec (equivalent to 4000 frames per second). Fig. 4.8 shows the photographs of these pulsations wherein it is seen that the maximum brightness or darkness repeats after 4th or 5th photograph. However there are other intervals also after which the maximum (or minimum) glow of the system repeats itself. As the photographs were taken at an interval of 0.25 msec a time period less than twice of that (0.5 msec) is clearly not possible. For sake of minimizing the error we have focused on frequencies quite less than the Nyquist frequency. The sixth photograph (fig. 4.8(f)) shows a relatively large glow; the next large glow is the 10th photograph (fig. 4.8(j)), which implies a frequency of $\frac{1}{4000} \times 4 \sim 1000$. As a matter of fact the Langmuir probe data also shows peaks in the power spectra around 1000Hz for an unmagnetized plasma. The periodicity of increase and decrease in the glow size referred here is correspondent to one of the many possible frequencies present in the pulsation of the glow, some of which are captured at 4000 frame per second others are not, and hence there are other peaks also in fig. 4.5 (a). From this it can be concluded that the pulsation of the sheath is giving rise to the modes present in the unmagnetized plasma.

Fig. 4.9 shows the self rotation of the fireball around the electrode as the magnetic field is increased to 3.63 G. Fig. 4.9(a) shows its location on the right hand side of the electrode, coming to the front in fig. 4.9(b) and again going behind the electrode in fig. 4.9(d).

This motion continues as seen in the rest of the pictures that show a strong periodicity for every fifth photograph. From the blob's photograph that is taken at a rate of 1899 frames per second, the fireball's rotational frequency is estimated as $(\frac{1}{1899} \times 5 \sim) 370$ Hz. From the pixel count, the diameter of the blob is estimated to be 2.2 cm, using the electrode as reference dimension. Hence the path length per rotation and the speed of the blob are $2\pi \times (2.2 + \frac{0.7}{2})cm \sim 16cm$ and $59.25m/sec$ respectively. The rotation frequency of 370 Hz coincides with the peak in the power spectrum seen in fig. 4.5 (c) ($B = 3.63G$).

Fig. 4.10 shows that at low magnetic field a small fireball of anode sheath was formed at a particular location of the electrode which turned into a torus encircling the electrode with increasing magnetic field (fig. 4.10 (b)) and finally with higher magnetic field, the blob is seen to rest under the electrode and continues in that location for higher magnetic fields. The location of the blob toggles between fig. 4.10 (b) and fig. 4.10(c) giving rise to intermittent structures in the time series shown in fig. 4.3 (e)-(g). But while decreasing the magnetic field the blob jumps directly from the location in fig. 4.10 (c) to that of fig. 4.10 (b) without any intermittent oscillations.

The dynamics in fig. 4.9 and fig. 4.10 can be considered to be driven by the $\vec{E} \times \vec{B}$ force in the direction of the cylindrical symmetry of the electrode. For example, the direction of rotation of the blob is clockwise as seen from the top of the electrode. The rotation frequency of the blob directly corresponds to the frequency obtained from the time series data when homoclinic and inverse homoclinic transitions are taking place. During this phase, the frequency to magnetic field ratio is linear as indicated by arrows in fig. 4.7. The various frequencies observed in the power spectrum could be a resultant of a nonlinear

coupling between the pulsation of the fireball, rotation of the fireball which are also related to ion acoustic and ionization instabilities.

4.4 Statistical behaviour and chaoticity

In order to understand the fireball dynamics, time series analysis was carried on the floating potential fluctuations recorded by a Langmuir probe. Statistical parameters such as kurtosis, skewness and entropy were estimated and compared for both increasing and decreasing magnetic fields. Kurtosis and skewness are the fourth and third moments respectively, which for a Gaussian distribution are 3 and 0; skewness indicates how left or right shifted the distribution is and the spread of that distribution is measured in kurtosis. Hysteresis is very clearly evident in kurtosis (fig. 4.11(a)) and skewness (fig. 4.11(b)) When magnetic field is low, we observed a broadened and right handed distribution with kurtosis in the range $10 \sim 12$ and skewness in the range $0.6 \sim 1.2$. The beginning of the inverse-homoclinic transition is accompanied by a drastic transition of distribution functions. Kurtosis drops to ~ 3 and the skewness becomes negative indicating left shifted Gaussian-like distribution. While further increasing the field the kurtosis shoots up to 13 when intermittency is observed and the skewness is also increased to 1.5. This is followed by another drop in the kurtosis and skewness to 4 and 0 respectively indicating more or less a random behaviour in the signals..

Decreasing the magnetic field does not retrace the same path for the values of kurtosis and skewness as the oscillations are significantly different there. This implies hysteresis in the statistical parameters up to a magnetic field value of $3.6G$ beyond which it retraces the earlier values.

Entropy can be considered to be a measure of complexity of the system[112]. The variation of entropy, calculated using Shannon's algorithm, as a function of magnetic field current is shown in fig. 4.12. For low magnetic field a low entropy is observed(fig. 4.12) which exhibits a sudden increase to 19 at the commencement of inverse homoclinic transition followed by a sudden drop to 8 at the beginning of intermittency. Further increase of magnetic field, leads to another increase in complexity for the final chaotic oscillations. While decreasing the magnetic field, we see a shallow increase in the value of entropy which abruptly drops at the end of the homoclinic bifurcation without the intermittent phase. This signifies hysteresis in the complexity of the system as seen also by kurtosis and skewness. These observations suggest that the system's preference to remain in a state of higher entropy leads to hysteresis in the observations.

4.5 Conclusions

Study of fireball dynamics in a currentless toroidal assembly with a vertical magnetic field has been carried out in detail using floating potential fluctuations obtained from a Langmuir probe and visual diagnostics from a fast camera. The dynamics of the floating potential fluctuations exhibits the following route: chaotic oscillations \rightarrow inverse homoclinic transition \rightarrow Intermittency. \rightarrow chaotic oscillations with the increase of magnetic field whereas in the decreasing magnetic field regime, the above route is retraced but without the intermittency. The different regimes are clearly distinguished by the respective statistical parameters like entropy, kurtosis and skewness. It is interestingly seen that all the parameters exhibit a hysteresis with respect to the vertical magnetic field. Visual diagnostics with the high camera also corroborate the above results of hysteresis. Chaotic oscillations

are very correlated with pulsations of the fireball, oscillations during homoclinic transitions (regular and inverse) are due to physical rotation of the pulsating blob, intermittency is due to the toggling between the physical rotation of the pulsation, and finally settling down to the glow under the electrode representing the final state of chaotic oscillations. The frequencies of power spectra peaks agree very well with the quantitative estimates from the photographs.

Glow discharge plasma is traditionally used to remove oxygen and carbon impurities from tokamaks. The efficiency of glow discharge cleaning depends mainly on the nature of electron energy distribution function and highly on the uniformity of the spatial distribution of plasma[113]. Self consistent 2D glow discharge plasma model using Monte Carlo methods predicts that the high energy secondary electron beams from cathode can give rise to spatial uniformity in the accelerated plasma particles[114]. In order to acquire prior knowledge of the kind of cleaning to be adopted at such high pressures like that of ITER a hydrogen glow discharge cleaning has been carried out[115].

Our present work on hysteresis shows that the oscillations go through several bifurcations as a function of the vertical magnetic field values. The homoclinic bifurcation regime in the return path with decreasing magnetic field exhibits a rotation of the pulsating blob with some uniform velocity which can give rise to a good spatial symmetry. This regime is also observed for a wide range of magnetic field values as well. We believe that the choice of the right parameters through nonlinear dynamical characterization will be very beneficial for a variety of applications such as glow discharge cleaning in toroidal devices, plasma based material processing, particle accelerators and dusty plasmas.

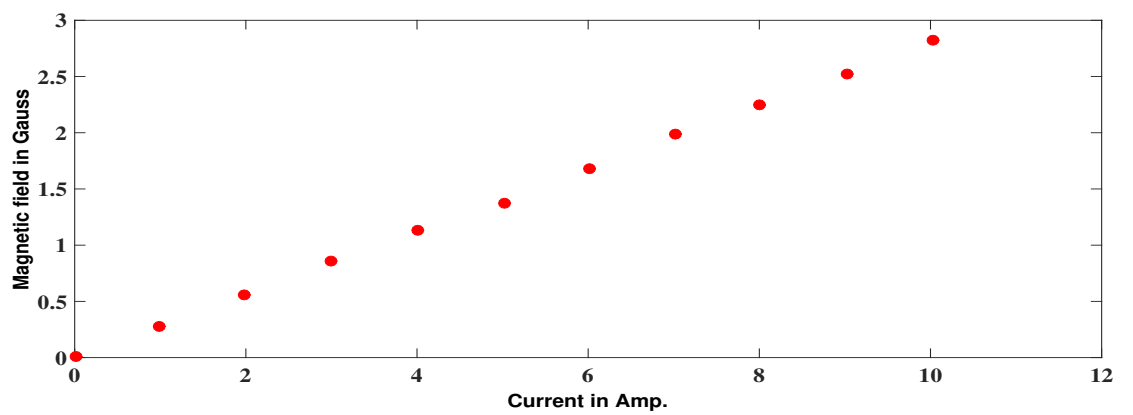
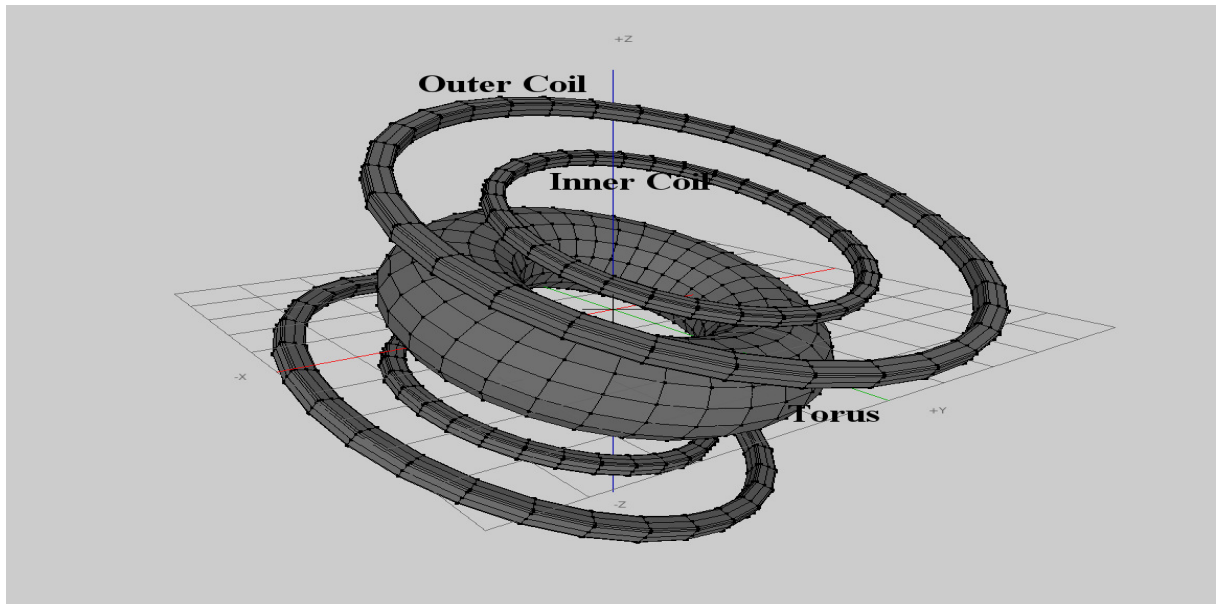


Figure 4.2: Schematic diagram(left) of magnetic field coils with the torus and the magnetic field produced by the coils at the torus for various values of current(right).

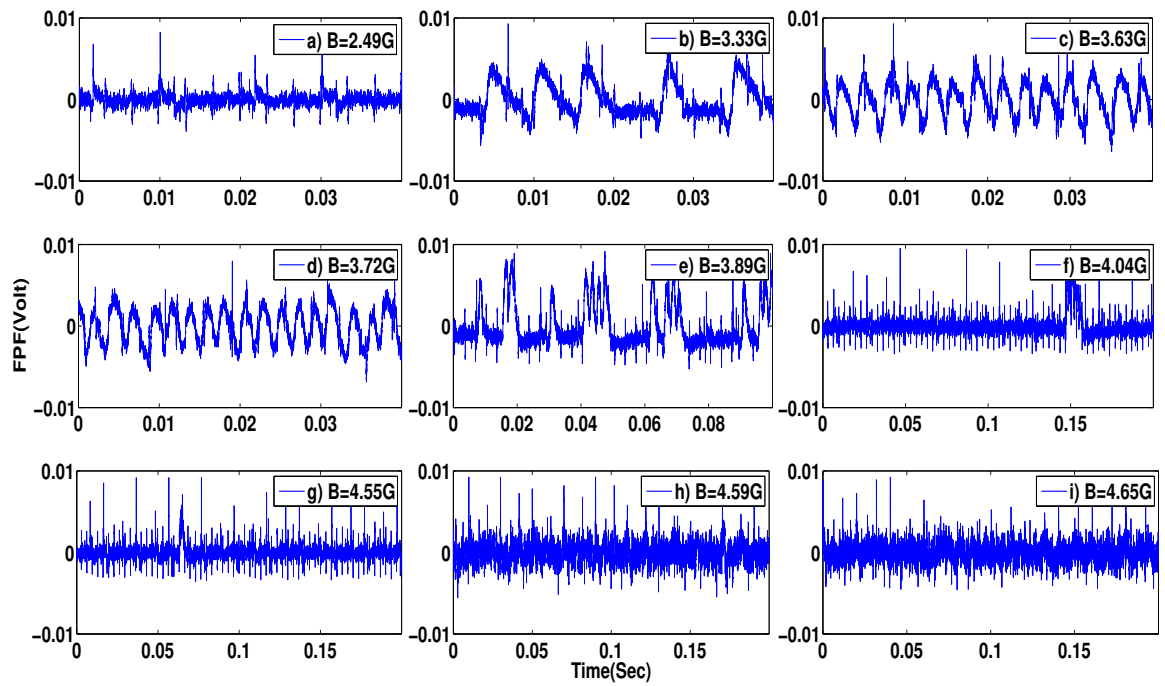


Figure 4.3: Floating potential fluctuations for different magnetic fields while increasing magnetic field

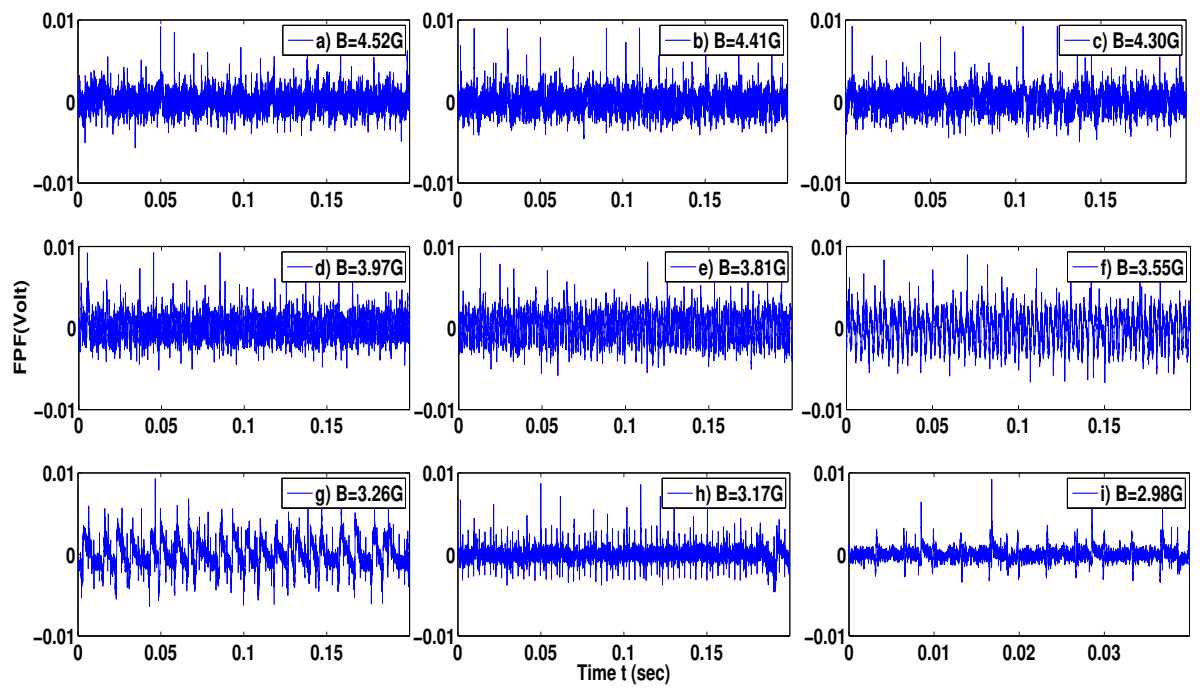


Figure 4.4: Floating potential fluctuations for different magnetic fields while decreasing magnetic field

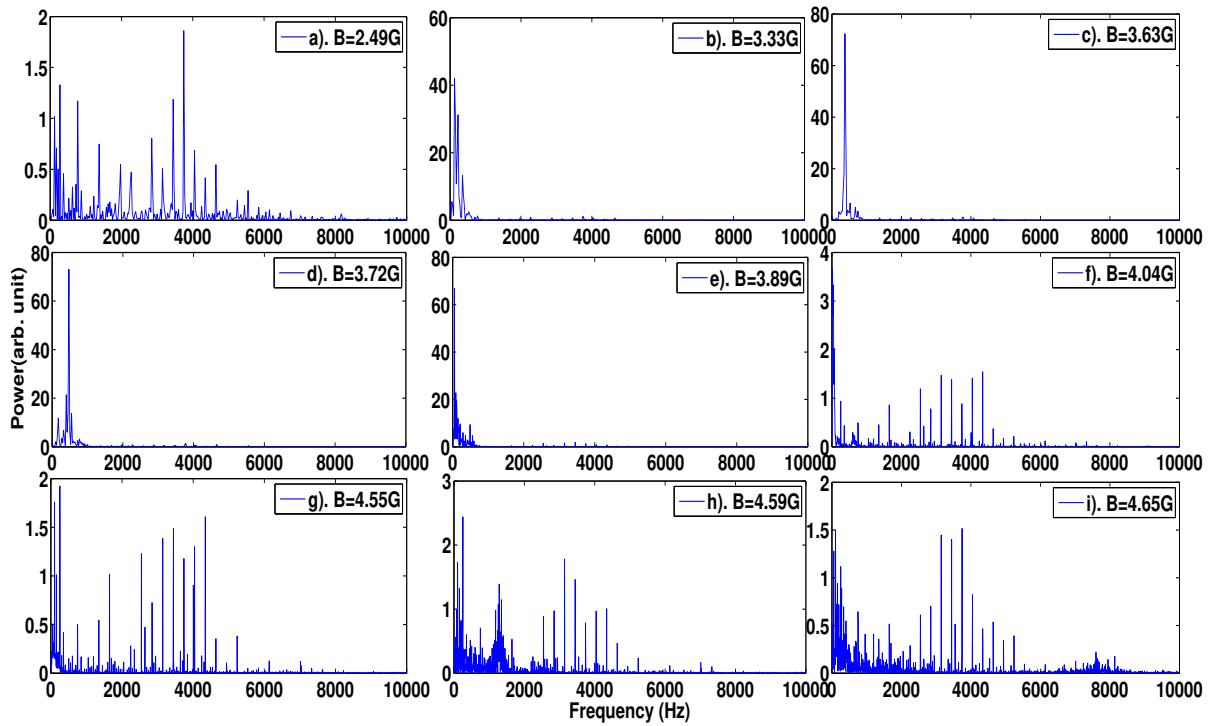


Figure 4.5: Power spectra for different magnetic fields while increasing magnetic field

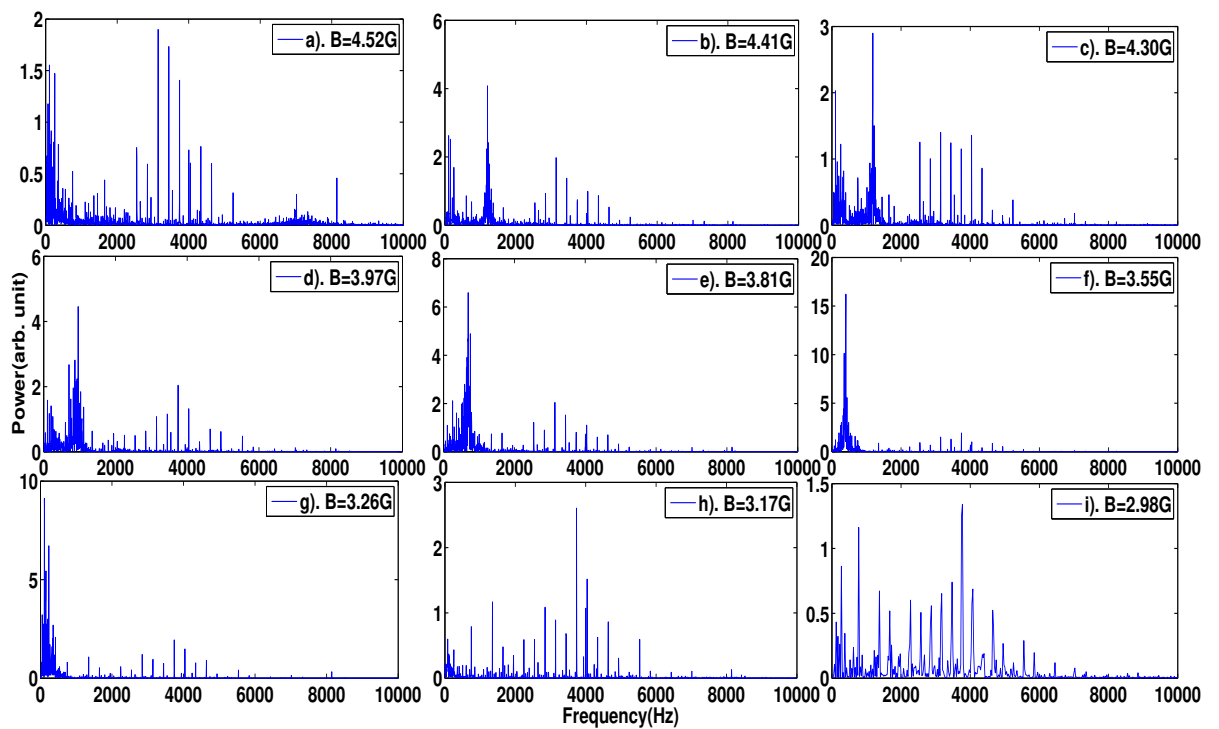


Figure 4.6: Power spectra for different magnetic fields while decreasing magnetic field

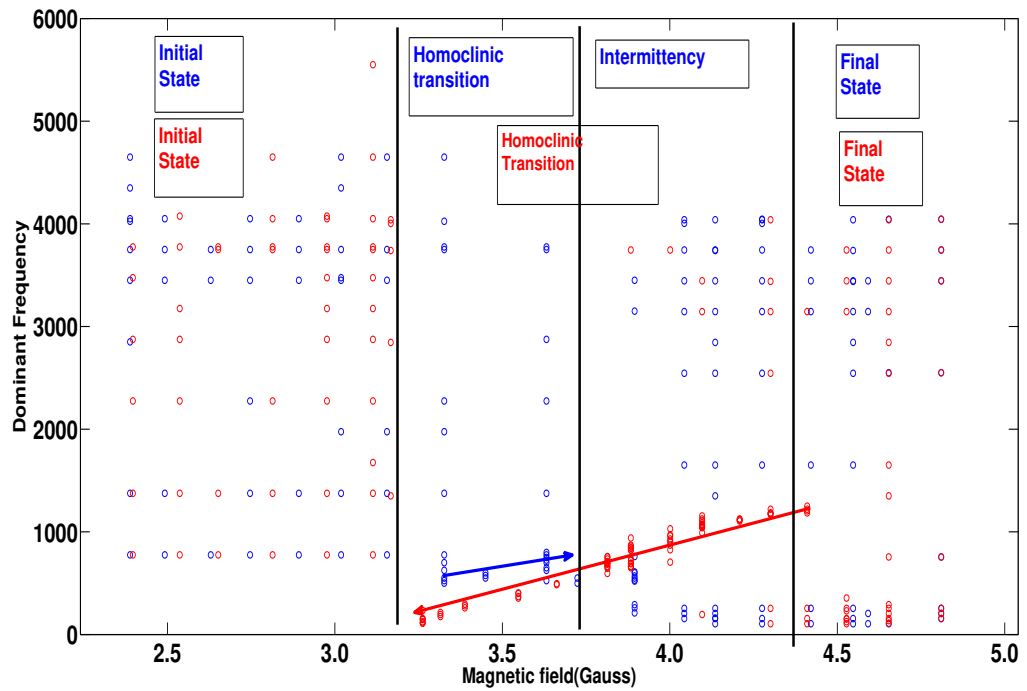


Figure 4.7: Dominant frequencies of the floating potential fluctuations with magnetic field. The blue and red dots are for increasing and decreasing magnetic fields respectively. The blue arrow is for inverse homoclinic transition and the red one is for homoclinic transition.

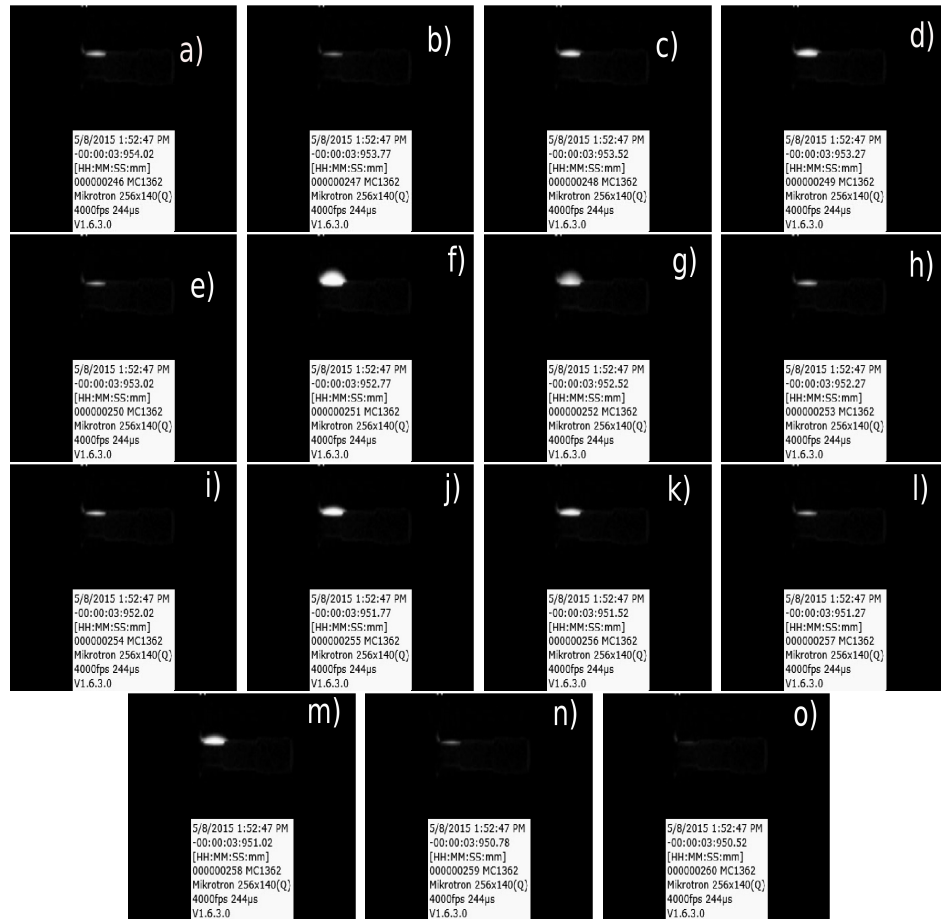


Figure 4.8: Pulsations of the glow recorded with a sampling time of 0.25 msec between consecutive frames for an applied magnetic field=2.5 G.

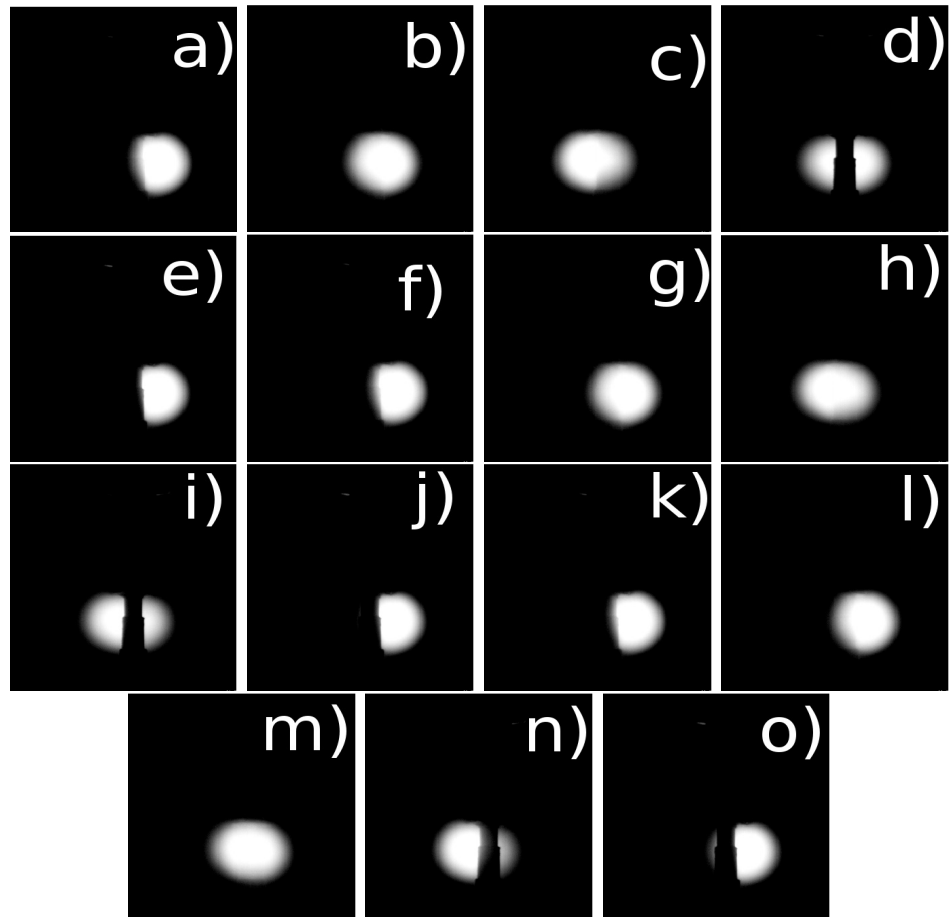


Figure 4.9: Photograph of the electrode with a time interval of $\frac{1}{1899}$ second between consecutive frames when magnetic field was 3.63G.

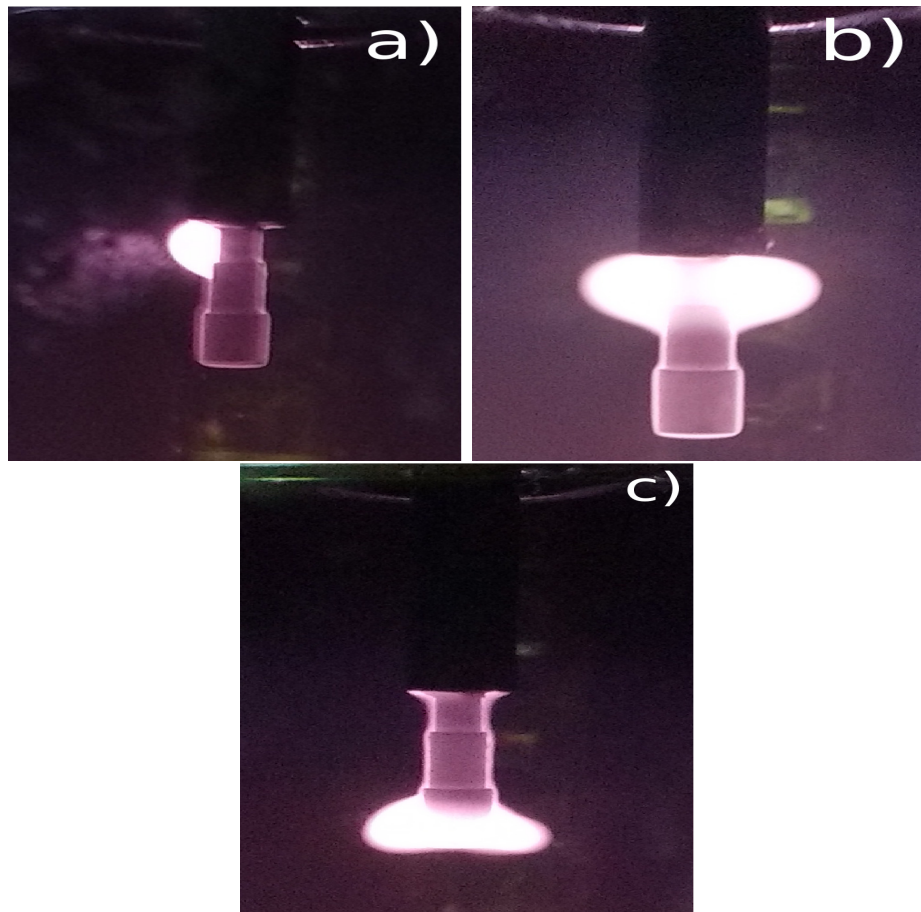


Figure 4.10: Photographs of the electrode for magnetic field $B \sim 2.5G$ (a.), with magnetic field $B \sim 3.5G$ (b.) and magnetic field $B \sim 4.5G$ (c.).

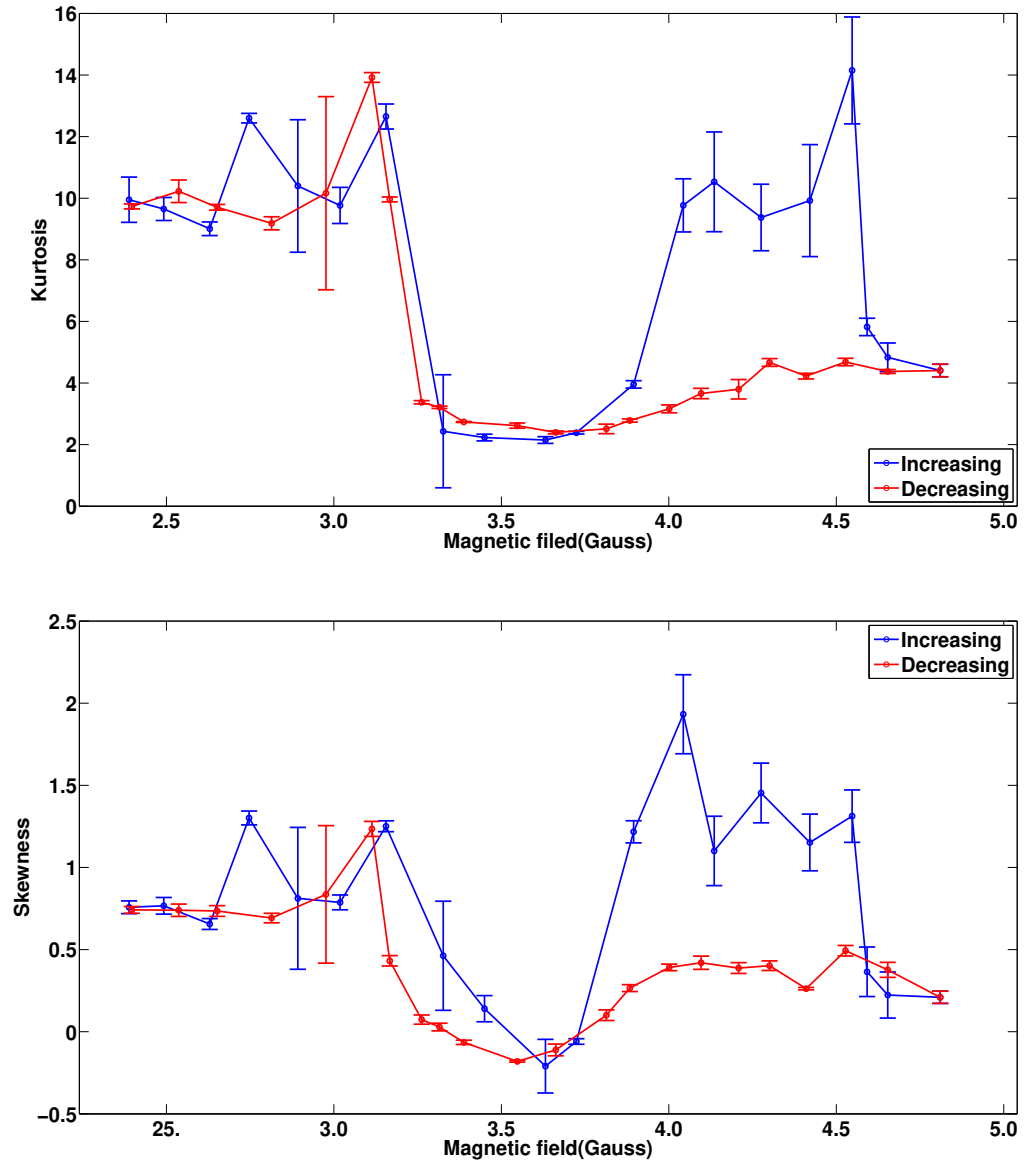


Figure 4.11: Kurtosis and skewness of the FPFs as a function of magnetic field where the blue points are for increasing field and the red ones are for decreasing field.

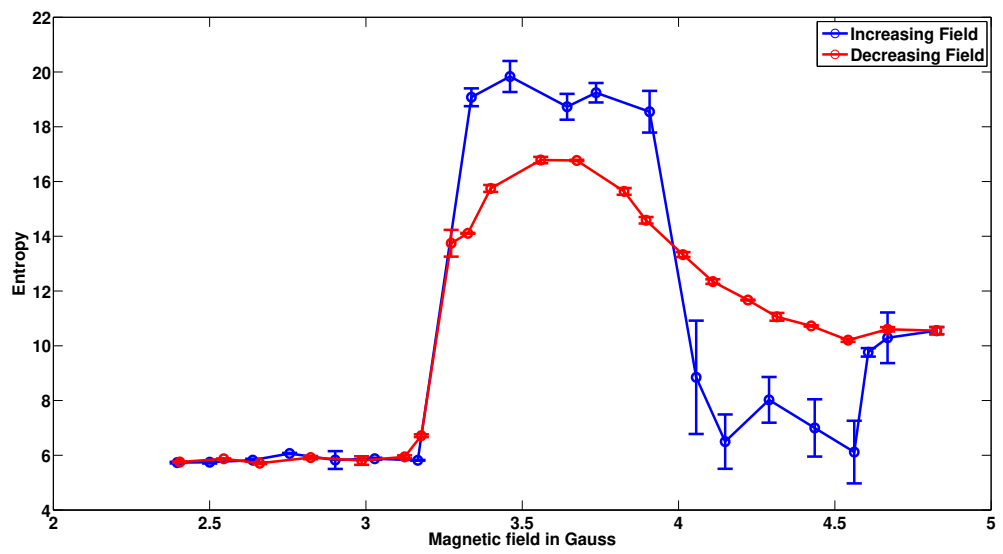


Figure 4.12: Entropy of the FPFs as a function of magnetic field where the blue points are for increasing field and the red ones are for decreasing field.

Chapter 5

Conclusions and Future Plans

This thesis have several conclusions regarding the nature and behaviour of floating potential fluctuations while the system undergoes various transitions. As proposed in the introduction section we have taken into consideration the floating potential fluctuations, their properties and statistical and nonlinear parameters while transitions were taking place. These transitions lead to various revelations about the system which can be further explored to continue future work.

5.1 Conclusions

Mainly there are three transitions that have been observed in the present work: intermittency, mixed mode oscillation and hysteresis of different non-linear oscillations. All of these deals with plasma floating potential fluctuations undergoing a transitions under the influence of external control parameters. These transitions give us opportunity to have a look into the occurrence of ordered and chaotic states as the system parameters compel the statistical and nonlinear parameters evolve.

Firstly glow discharge plasma as a nonlinear system is capable of showing various nonlinear features like mixed mode oscillations, intermittent chaos and homoclinic transitions. In these transitory routes lie the necessary information to characterize a system in terms of its nonlinear properties. Once the characterization is done one can use the nonlinear properties to detect the system state. The parameter space which gives change in nonlinearity with respect to external control parameters also indicates predictability of the system.

In the first chapter we have seen the floating potential fluctuation of the system is undergoing a transition from type I oscillation to type II oscillation through the intermittent path. The frequencies of these oscillations fall in ion acoustic and ionization instability regime which gives an indirect inference on the type of oscillations observed. In intermittency the experimental data, when projected into reconstructed phase space, tells that during this transition the system toggles between two distinct center of attractions. While the system goes around these center of attractions their path length of revolution is also different indicating a concrete reason behind the different amplitudes between type I and type II kind of oscillations. A particular deviation in statistical parameters has also been observed depending on the two types of oscillations. These behaviour of statistical parameters become handy when hysteresis was observed in glow discharge plasma in SINP tokamak. During the hysteresis one particular path of transition was intermittent chaos and characterization of the same was done using prior knowledge from previous experiment. This transition via intermittent path was modeled when external noise was used as a forcing.

In the second chapter, we have seen that the floating potential fluctuations were transiting among different kind of mixed mode oscillations. This work tells us that the type of

mixed mode oscillation present in a system can be altered using external parameters. The change in external discharge voltages reflected in the the change in the Hurst exponent and correlation dimension. Largest Lyapunov exponent also indicated observable increase in chaoticity when the system transited from regular mixed mode oscillation to irregular one and decrease in the same when it went from irregular MMO to compound or regular one. Thus knowledge about chaoticity, memory and dimension of the system while under going the transition is obtained from this experiment.

Both these experiments were mimicked to a simple numerical modeling. Then we came to know that a simple inherent noise level can act like an external forcing and can trigger the intermittency. Another assumption lead us to the finding that a spurious mode generated within the system itself can act as a forcing and cause the change in the type of mixed mode oscillation that was observed in the experiment performed. The time series obtained from these modeling also exhibited change in their nonlinear exponents which were qualitatively similar with the changes seen in experimental time series.

In the third work we have seen hysteresis in the nonlinear exponents and the type of floating potential fluctuations when the applied magnetic field is increased and then decreased. Here cylindrical symmetry is observed when the homoclinic or inverse homoclinic transitions were prominent in FPFs. During those phases a simultaneous photographic examination of the glow shows an uniform rotation of the blob around the electrode in cylindrically symmetric manner. This can be particularly useful in material processing. The fact that the system avoids intermittent path while the magnetic field is decreased gives an opportunity of operating the system in the symmetric state over a large parameter

span.

5.2 Future Plans

In this work we have explored various paths of transitions among the different nonlinear oscillations excited in a glow discharge plasma. There are scopes for further exploration on these transitions. In the first chapter we have seen the intermittent path of transition. As we have only varied discharge voltage, there remains an immense opportunity of future work by exploring pressure as a control parameter. We have argued about the crucial role of noise for intermittent route of transition. One can verify the role of noise by simply adding external forcing (as white noise) to the system.

Similarly in the transitions among mixed mode oscillations we have made use of only a small variation in the discharge voltage. We can explore the effect of other parameters, like pressure or externally applied magnetic field on these MMOs. In the numerical modeling of this transition we have proposed that a sinusoidal wave inside the system is exciting the system to undergo this transition. Again this proposal can be directly tested if the glow discharge plasma is subjected to an externally applied sinusoidal forcing when mixed mode oscillation is observed. Also in this kind of an experiment, one can directly relate the Farey sequence to the external control parameter and hence can check if the observed MMO is following Farey algebra or not.

In the third experiment we have seen how these transitions occur one after another in a glow discharge plasma produced in a toroidal device. The symmetry in fireball dynamics we observed here during homoclinic transition has the potential of industrial applications. For that purpose the present study should be extended to other geometries also. On the other

hand we have only explored the effect of change in vertical magnetic field on the nonlinear oscillations in a toroidal device. It is important to understand the response of floating potential fluctuations due to changes in other parameters like discharge voltage, pressure, toroidal magnetic field etc. The effectiveness of magnetized glow discharge plasma as a cleaning process for tokamaks depends on all these parameters. It will be interesting to relate the effectiveness of cleaning to the various operating regimes.

Bibliography

- [1] Mayer, H. C. & Krechetnikov, R. *Phys. Rev. E* **85**, 046117 (2012).
- [2] Madsen, P. A., Fuhrman, D. R. & Schffer, H. A. *Journal of Geophysical Research: Oceans* **113**, C12012 (2008).
- [3] Pelinovsky, E. N. & Mazova, R. K. *Natural Hazards* **6**, 227–249 (1992).
- [4] Ivanov, P. C. *et al. Nature* **399**, 461–465 (1999).
- [5] Glass, L., Goldberger, A. L., Courtemanche, M. & Shrier, A. *Proceedings of the Royal Society of London. Series A, Mathematical and Physical Sciences* **413**, 9–26 (1987).
- [6] Kaneko, K. *Physics D* **1**, 55–73 (1994).
- [7] Abhyankar, A., Copeland, L. S. & Wong, W. *The Economic Journal* **105**, 864–880 (1995).
- [8] Haag, G. *Evolving Geographical Structures* **15**, 24–61 (1983).
- [9] Costantino, R. F., Cushing, J. M., Brian, D., Desharnais & Robert, A. *Nature* **375**, 227 (1995).
- [10] Zhabotinskii, A. *Dokl. Acad. Nauk. SSSR* **157**, 392 (1964).

- [11] Turner, J., Roux, J., McCormick, W. & Swinney, H. *Phys. Lett.* **37**, 194 (1980).
- [12] Petrov, V., Scott, S. K. & Showalter, K. *The Journal of Chemical Physics* **97**, 6191 (1992).
- [13] Albahadily, F. N., Ringland, J. & Schell, M. *The Journal of Chemical Physics* **90**, 813 (1989).
- [14] Erchova, I. & McGonigle, D. J. *Chaos* **18**, 015115 (2008).
- [15] Krupa, M., Popovi, N., Kopell, N. & Rotstein, H. G. *Chaos* **18**, 015106 (2008).
- [16] S. Chakraborty, S. D. *Chaos* **20**, 023107 (2010).
- [17] Chowdhury, D. & Schadschneider, A. *Phys. Rev. E.* **59**, R1311:R1314 (1999).
- [18] Pietrzyka, Z. *et al. Nuclear Fusion* **39**, 587 (1999).
- [19] Nakamura, Y. & Sarma, A. *Physics of Plasmas* **8**, 3921 (2001).
- [20] P.Y.Cheung & A.Y.Wong, S. *Physical review letters* **61**, 1360 (1988).
- [21] Sun, H., Ma, L. & Wang, L. *Phys. Rev. E* **51**, 3475 (1995).
- [22] Ding, W. X., She, H. Q., Huang, W. & Yu, C. X. *Phys. Rev. Lett.* **72**, 96 (1994).
- [23] Dawson, J. M. *Phys. Rev.* **183**, 383 (1959).
- [24] Dawson, J. M. *Sci. Am.* **260**, 54 (1989).
- [25] Akhiezer, A. I. & Polovin, R. V. *Sov. Phys. JETP* **3**, 696 (1956).

- [26] Davidson, R. C. *Methods in Nonlinear Plasma Theory* (Academic, New York, 1972).
- [27] Coffey, T. P. *Phys. Fluids* **14**, 1402 (1971).
- [28] Katsouleas, T. & Mori, W. B. *Phys. Rev. E* **61**, 1 (1988).
- [29] Bernstein, I. B., Greene, J. M. & Kruskal, M. D. *Phys. Rev.* **108**, 546 (1957).
- [30] Tidman, D. A. & Krall, N. A. *Shock waves in collisionless plasma* (John Wiley & Sons, New York, 1971).
- [31] Moslem, W. M., Shukla, P. K. & Eliasson, B. *EPL* **96**, 25002 (2011).
- [32] Costley, A. E., Hastie, R. J., Paul, J. W. M. & Chamberlain, J. *Phys. Rev. Lett.* **33**, 758 (1974).
- [33] Matthews, G. F. *Journal of Physics D: Applied Physics* **17**, 2243 (1984).
- [34] Fonck, R. J., Darrow, D. S. & Jaehnig, K. P. *Phys. Rev. A* **29**, 3288 (1984).
- [35] Jackson, J. D. *Journal of Nuclear Energy. Part C, Plasma Physics, Accelerators, Thermonuclear Research* **1**, 171 (1959).
- [36] Lee, H. J. & Lee, J. K. *Physics of Plasmas* **5**, 2878 (1998).
- [37] Cheung, P. Y. & Wong, A. Y. *Phys. Rev. Lett.* **59**, 551 (1987).
- [38] F. Greiner, T. Klinger, H. K. & Piel, A. *Phys. Rev. Lett.* **70**, 3071 (1993).
- [39] Klinger, T., Greiner, F., Rohde, A., Piel, A. & Koepke, M. E. *Phys. Rev. E* **52**, 4316 (1995).

- [40] Tuszewski, M., White, R. R. & Wurden, G. A. *Plasma Sources Science and Technology* **12**, 396 (2003).
- [41] Chiriac, S., Dimitriu, D. G. & Sanduloviciu, M. *Phys. Of Plasmas* **14**, 072309 (2007).
- [42] Feng, D. L., Yu, C. X., Xie, J. L. & Ding, W. X. *Phys. Re. E* **58**, 3678 (1998).
- [43] D.Bora, V.N.Rai & P.K.Kaw. *Physics Letters A* **119**, 411–414 (1987).
- [44] Cheung, P. Y., Donovan, S. & Wong, A. Y. *Phys. Rev. Lett.* **61**, 1360 (1988).
- [45] J. Qin, L. Wang, D. P. Y. P. G. & Zhang, B. Z. *Phys. Rev. Lett.* **63**, 163 (1989).
- [46] Rempel, E. L. & C.-L.Chian, A. *Advances in Space Research* **35**, 951–960 (2005).
- [47] Mikikian, M., Cavvaroe, M., Couedel, L., Tessier, Y. & Boufendi, L. *Phys. Rev. Lett.* **100**, 225005 (2008).
- [48] Desroches, M. *et al. SIAM REVIEW* **54**, 211–288 (2010).
- [49] A.L.Yerokhin, X.Nie, A. A. & S.J.Dowey. *Surface and Coatings Technology* **122**, 73–93 (1999).
- [50] Joshi, C. & Katsouleas, T. *Phys. Today* **56**, 47 (2003).
- [51] Nakajima, K. *Nat. Phys.* **4**, 92 (2008).
- [52] Wang, X. *et al. Nat. Commun.* **4**, 1988 (2013).
- [53] Laroussi, M. *Plasma Process. Polym.* **2**, 391–400 (2005).

- [54] Martinez-Sanchez, M. & Pollard, J. E. *Journal of Propulsion and Power* **14**, 688–699 (1998).
- [55] Yamada, M. *et al.* *Physics of Plasmas* **1**, 3269 (1994).
- [56] Boedo, J. A. *et al.* *Phys. Of Plasmas* **10**, 1670 (2003).
- [57] Saha, S. K. & Chowdhury, S. *Phys. Of. Plasma.* **15**, 012305 (2008).
- [58] Roeder, R. K. W., Rapoport, B. I. & Evans, T. E. *Physics of Plasmas* **10**, 3796 (2003).
- [59] Feng, D. L., Zheng, J., Huang, W. & Yu, C. X. *Phys. Rev. E* **54**, 2839 (1996).
- [60] Stan, C., C.P.Cristescu & Dimitriu, D. *Phys. Of Plasmas* **17**, 042115 (2010).
- [61] T. Braun, J. A. L. & Gallas, J. A. C. *Phys. Rev. Lett.* **68**, 2770 (1992).
- [62] Hassouba, M. A., Al-Naggar, H. I. & Al-Naggar, N. M. *Phys. Plasmas* **13**, 073504 (2006).
- [63] Keen, B. E. & Fletcher, W. H. W. *J. Phys. D: Appl. Phys.* **3**, 1868 (1970).
- [64] Keen, B. E. & Fletcher, W. H. W. *Plasma Phys.* **13**, 419 (1971).
- [65] Keen, B. E. & Fletcher, W. H. W. *J. Phys. A: Gen. Phys.* **5**, 152 (1972).
- [66] Kadji, H. G. E., Nbandjo, B. R. N., Orou, J. B. C. & Talla, P. K. *Phys. Of Plasma* **15**, 032308 (2008).
- [67] Kadji, E., Benjou, N., Orou, C. & Talla, P. K. *Phys. Plasmas* **15**, 032308 (2008).

- [68] Lahiri, S., Roychowdhury, D. & Iyengar, A. N. S. *Phys. Of Plasmas* **19**, 082313 (2012).
- [69] Koper, M. T. M. & Gaspard, P. *J. Phys. Chem.* **95**, 4945–4947 (1991).
- [70] Manneville, P. & Pomeau, Y. *Phys. Lett.* **75A**, 1 (1979).
- [71] Ciliberto, S. & Bigazzi, P. *Phys. Rev. Lett.* **60**, 25 (1988).
- [72] P.Manneville & Y.Pomeau. *Physica D* **1**, 219 (1980).
- [73] Hammer, P. W., Platt, N., Hammel, S. M., Heagy, J. F. & Lee, B. D. *Phys. Rev. Lett.* **73**, 1095 (1994).
- [74] T.J.Price & T.Mullin. *Physica D* **48**, 29 (1991).
- [75] Wendell, D. M., Pigeonneau, F., Gouillart, E. & Jop, P. *Phys. Re. E* **88**, 023024 (2013).
- [76] Cabrera, J. L. & Milton, J. G. *Phys. Re. Lett* **89**, 158702 (2002).
- [77] Rybalko, S., Larionov, S., Poptsova, M. & Loskutov, A. *Phys. Rev. E* **84**, 042902 (2011).
- [78] Platt, N., Hammel, S. M. & Heagy, J. F. *Phys. Rev. Lett.* **72**, 3498 (1994).
- [79] Cisternas, J. & Descalzi, O. *Phys. Rev. E.* **88**, 022903 (2013).
- [80] Nurujjaman, M., Iyengar, A. N. S. & Parmananda, P. *Phys. Rev. E* **78**, 026406 (2008).

- [81] Nurujjaman, M. & Iyengar, A. S. *Phys. Lett. A* **360**, 717–721 (2007).
- [82] Chopin-Duman, J. *C.R. Acad. Sci. (Paris)* **C287**, 553 (1978).
- [83] Milik, A., Szmolyan, P., Loeffelmann, H. & Groeller, E. *Int. J. Bifur. Chaos* **8**, 505–519 (1998).
- [84] Krupa, M., Ambrosio, B. & Aziz-Alaoui, M. A. *Nonlinearity* **27**, 1555–1574 (2014).
- [85] Hayashi, T. *Phys. Rev. Lett.* **84**, 3334 (2000).
- [86] Flanagan, T. M. & Goree, J. *Phys. Plasmas* **17**, 123702 (2010).
- [87] Keen, B. E. & Fletcher, W. H. W. *Phys. Rev. Lett.* **23**, 760 (1969).
- [88] Ghosh, S. *et al. Phys. Plasmas* **21**, 032303 (2014).
- [89] Flanagan, T. M. & Goree, J. *Phys. Plasmas* **18**, 013705 (2011).
- [90] Grassberger & Procaccia. *Phys. Rev. Lett.* **50**, 346–349 (1983).
- [91] Saha, D. *et al. Phys Plasmas* **21**, 032301 (2014).
- [92] Wharton, A. M., Shaw, P. K., Janaki, M. S., Prasad, A. & Iyengar, A. N. S. *Phys Plasmas* **21**, 022311 (2014).
- [93] Sarmah, R. & Ananthakrishna, G. *Comm Nonlinear Sci Numer Simulat* **19**, 3880 (2014).
- [94] Pan, B., Lin, D., Mashayekhi, H. & Xing, B. *Environ. Sci. Technol.* **42**, 5480–5485 (2008).

- [95] Kramer, B. P. & Fussenegger, M. *PNAS* **102**, 9517–9522 (2005).
- [96] Kleinschmidt, A., Buchel, C., Hutton, C., Friston, K. J. & Frackowiak, R. S. *Neuron* **34**, 659–666 (2002).
- [97] Z.Wangand & Guggenbuhl, W. *Electronics Letters* **25**, 397–398 (1989).
- [98] Blanchard, O. J. & Summers, L. H. *NBER Macroeconomics Annual* **1** (1986).
- [99] Carter, T. A. *Phys. Plasmas* **13**, 010701 (2006).
- [100] Erico L. Rempel, W. M. S. & Chian, A. C.-L. *Phys. Plasmas* **13**, 032308 (2006).
- [101] Saha, D. *et al. Phys. Plasmas* **21**, 032301 (2014).
- [102] Basu, B. & Coppi, B. *Phys. Plasmas* **2**, 14 (1995).
- [103] Dinklage, A., Bruhn, B., Testrich, H. & Wilke, C. *Phys. Plasmas* **15**, 063502 (2008).
- [104] Kumar, R., Narayanan, R. & Prasad, A. *Phys. Plasmas* **21**, 123501 (2014).
- [105] Bosch, R. A. & Merlino, R. L. *Contrib. Plasma Phys.* **26**, 1–12 (1986).
- [106] Kaifen, H. & Salat, A. *Plasma Physics and Controlled Fusion* **31**, 123–141 (1989).
- [107] Lee, H.-C. & Chung, C.-W. *Scientific Reports* **5**, 15254 (2015).
- [108] Li, H.-P. & Benilov., M. S. *J. Phys. D: Appl. Phys.* **40** (2007).
- [109] Benilov, M. S. *et al. J. Phys. D: Appl. Phys.* **49**, 215201 (2016).

- [110] Stenzel, R. L., Ionita, C. & Schrittwieser, R. *Plasma Sources Sci. Technol.* **17**, 035006 (2008).
- [111] Manash Kumar Paul, P. K. Sharma, A. T. S. V. K. & Bora, D. *Phys. Plasmas* **21**, 062112 (2014).
- [112] Pincus, S. M. *Proc. Nati. Acad. Sci. USA* **88**, 2297–2301 (1991).
- [113] Pathak, H. & Saxena, Y. *Journal of Nuclear Materials* **220-222**, 708–711 (1995).
- [114] Hagelaar, G. J. M., Kogut, D., Douai, D. & Pitts, R. A. *Plasma Phys. Control. Fusion* **57**, 025008 (2015).
- [115] Kogut, D., Douai, D., Hagelaar, G. & Pitts, R. A. *Plasma Phys. Control. Fusion* **57**, 025009 (2015).